creative commons
COMMONS DEED

저작자표시-비영리-변경금지 2.0 대한민국

이용자는 아래의 조건을 따르는 경우에 한하여 자유롭게

- 이 저작물을 복제, 배포, 전송, 전시, 공연 및 방송할 수 있습니다.

다음과 같은 조건을 따라야 합니다:

저작자표시. 귀하는 원저작자를 표시하여야 합니다.

비영리. 귀하는 이 저작물을 영리 목적으로 이용할 수 없습니다.

변경금지. 귀하는 이 저작물을 개작, 변형 또는 가공할 수 없습니다.

- 귀하는, 이 저작물의 재이용이나 배포의 경우, 이 저작물에 적용된 이용허락조건을 명확하게 나타내어야 합니다.
- 저작권자로부터 별도의 허가를 받으면 이러한 조건들은 적용되지 않습니다.

저작권법에 따른 이용자의 권리는 위의 내용에 의하여 영향을 받지 않습니다.

이것은 이용허락규약(Legal Code)을 이해하기 쉽게 요약한 것입니다.

Disclaimer

dCollection

공학박사학위논문

Design, Modeling and Optimization of Modified MEA Scrubbing Process for Post Combustion CO_2 Capture

모노에탄올아민을 이용한 연소 후 이산화탄소 포집 공정 개선안의 설계, 모델링 및 최적화

2016 년 2 월

서울대학교 대학원

화학생물공학부

정 재 흠

Abstract

Design, Modeling and Optimization of Modified MEA Scrubbing Process for Post Combustion CO_2 Capture

Jaeheum Jung
School of Chemical & Biological Engineering
The Graduate School
Seoul National University

Post-combustion CO_2 capture with aqueous monoethanolamine (MEA) scrubbing is a promising and well-proven technique for reducing atmospheric CO_2 emissions. The MEA scrubbing process is suitable for treating flue gas from coal-fired power plants because of its high CO_2 capture capacity and its ability to be retrofitted into existing power plant facilities. However, the MEA scrubbing process is not cost effective in terms of CO_2 capture, in particular for the energy required for solvent regeneration. To overcome this issue, studies have been conducted to reduce the solvent regeneration energy through modifying the process configuration. However, the majority of these

modified processes call for additional capital costs due to the requirement for additional equipment.

The objective of this study is therefore to determine the optimal configuration for reducing the cost of CO_2 capture. The operating expenditure (OPEX) and capital expenditure (CAPEX) were considered together to reduce the total CO_2 capture cost. Firstly, analysis of the conventional MEA scrubbing process energy system was carried out to determine the key variables for reducing the solvent regeneration energy. These key variables were the temperature at the stripper top, and the temperature approach at the cross heat exchanger. Analysis of the existing modified MEA scrubbing process was then carried out. The modified MEA scrubbing processes can be classified into three groups based on their energy reduction mechanism. The energy reduction mechanism of group I involves an increasing in the lean loading at the stripper bottom, while that of group II involves decreasing the solvent inlet temperature at the stripper top, and that of group III involves increasing the heat recovery. Combination of the multiple modified MEA scrubbing processes exhibiting positive interactions was then investigated. Absorber intercooling, cold solvent split, and rich vapor compression were selected as the optimal combination based on quantitative studies. For the combined configuration, the equivalent energy decreased 5.7%, from 1.22 GJ_e/ton CO_2 to 1.15 GJ_e/ton CO_2. Following energy consumption minimization, the additional CAPEX was calculated as a penalty term.

Subsequently, the superstructure model of the modified configurations was prepared, involving six different modified configurations and various split flow configurations. As the cost model was built into the superstructure, the superstructure model calculated the OPEX and CAPEX terms simultaneously. Finally, optimization of the superstructure model of the modified MEA scrubbing configurations was carried out, simultaneously solving the process variables for six different modified configurations. The objective of scenario I was to minimize the equivalent energy without considering the CAPEX term. As a result, the equivalent energy for CO_2 capture and compression decreased 22.1%, from 1.30 GJ_e/ton CO_2 to 1.02 GJ_e/ton CO_2. The objective of scenario II was to minimize the total cost, i.e., the sum of the OPEX and CAPEX terms. As a result, the total cost of CO_2 capture and compression decreased 10.2%, from €54.7/ton CO_2 to €51.0/ton CO_2. The annualized cost reduction was therefore €25.7 M/yr for a 630 MW_e power plant.

Keywords: Post-combustion CO_2 Capture, MEA Scrubbing, Superstructure Optimization

Student ID: 2010-21014123123

Contents

List of Figures

List of Tables

Chapter 1: Introduction

1.1 Research motivation

In terms of post-combustion CO_2 capture, the monoethanolamine (MEA) scrubbing process is one of the most commercially available and well-proven techniques for reducing atmospheric CO_2 emissions. The MEA process is suitable for treating large amounts of CO_2 from power plants and can be retrofitted into existing power plant facilities. However, solvent regeneration in the MEA scrubbing process is not cost effective. A number of studies have therefore been conducted to attempt to reduce the required solvent regeneration energy through modification of the process configuration. Numerous studies have reported the energy reduction effect for various modified configurations. Furthermore, recent studies report a significant energy reduction effect by combining multiple modified configurations. However, combining multiple modified configuration is a complex issue because the various process variables are highly interact with one another. Although parametric studies or qualitative analysis can provide insight into the combining configuration, determination of the optimal combination for a modified MEA scrubbing process is difficult. Additional energy reduction is expected when a flowsheet optimization is conducted for multiple different modified configurations.

Furthermore, the majority of modified processes result in additional capital costs due to their requirement for additional equipment. As the capital expenditure (CAPEX) term accounts for 30–45% of the total CO_2 capture and compression costs, both the operating expenditure (OPEX) and the CAPEX should be considered together for reducing the overall final cost [1, 2]. Although the CAPEX term is important, the majority of previous studies have ignored the additional CAPEX term or considered it as penalty term for minimizing the OPEX term. When the multiple different modified configuration model involves the cost model, the OPEX and CAPEX terms are simultaneously considered to reduce the actual cost.

1.2 Research objectives

The objective of this study is to determine the optimal configuration for reducing the CO_2 capture cost, i.e., the sum of the OPEX and CAPEX terms. A series of process configuration analyses were thus conducted in a regular sequence.

Initially, the energy system of the conventional MEA scrubbing process will be analyzed for indicating the key variables in determining energy requirements. Subsequently, analysis of the energy reduction effect of the modified MEA scrubbing processes will be examined. Through the parametric

study of each modified configuration, this study classifies the modified configurations into three groups according to the energy reduction mechanism. In addition, the combination of modified configurations that interact positively with each other will be determined based on the qualitative analysis. The author will then analyze the energy reduction effect and capital cost penalty for the combined configuration. Furthermore, the superstructure model will be built, considering multiple modified configurations. The superstructure model consists of six different modified configurations and various split flow configurations. In addition, the superstructure model involves the cost model consisting of the sum of the OPEX and CAPEX terms. Finally, optimization of the superstructure model to minimize energy consumption and total cost will be carried out, with the equivalent energy reduction effect and total cost effect defined.

1.3 Outline of the thesis

Chapter 1: Introduction of the research motivation and objective of the thesis

Chapter 2: Analysis of the conventional MEA scrubbing process

Chapter 3: Analysis of the modified MEA scrubbing process

Chapter 4: Combination of the modified MEA scrubbing process

Chapter 5: Modeling of the superstructure for the modified MEA scrubbing process

Chapter 6: Optimization of the superstructure for the modified MEA scrubbing process

Chapter 7: Conclusions and remarks

Chapter 2: Conventional MEA Scrubbing Process*

2.1 Overview

When a CCS facility is installed at an existing fossil fuel power plant, the power generation efficiency decreases by 15–30% [3-5] and the cost of electricity (COE) increases by 45–80% [6]. The sum of the CO_2 capture and compression costs comprise over 75% of the total carbon capture and storage (CCS) costs [7], and the CO_2 capture operating costs comprise over 80% of the total operating costs for capture and compression [3]. Thus, the capture process is the most important part of CCS and consequently, a number of studies have focused on reducing the CO_2 capture costs. The various capture techniques developed to date, along with their advantages and challenges, are summarized in Table 2-1.

Among these capture techniques, the CO_2 capture process employing aqueous MEA scrubbing is a promising and well-proven technology for reducing CO_2 emissions from fossil fuel power plants. The MEA process is

*Part of this chapter is taken from the author's published paper: Jung, J.; Jeong, Y. S.; Lee, U.; Lim, Y.; Han, C., New Configuration of the CO_2 Capture Process Using Aqueous Monoethanolamine for Coal-Fired Power Plants. *Industrial & Engineering Chemistry Research* **2015,** 54, (15), 3865-3878. http://pubs.acs.org/doi/abs/10.1021/ie504784p

suitable for treating flue gas from coal-fired power plants because of its high CO_2 capture capacity and its ability to be retrofitted into existing power plant facilities. For this reason, various pilot-to-commercial scale demonstrations and parametric studies employing the MEA scrubbing CO_2 capture process have been undertaken [4, 8-14]. However, this MEA process has one significant issue, namely its high consumption of reboiler heat energy for solvent regeneration in the stripper. This constitutes approximately 80% of the capture process OPEX, which is ~50% of the total CCS OPEX, as shown in Fig. 2-1. A number of studies have therefore focused on reducing the reboiler heat energy consumption.

Table 2-1. Advantages and challenges for various post-combustion CO_2 capture techniques [15]

Capture Technique	Advantages	Challenges
Absorption I Aqueous Solvent (Chemical)	-High suitability for dilute CO_2 flue gas -Mild operating conditions -Commercially available and well-proven technology	-High solvent regeneration energy -Significant solvent loss due to acidic impurities in the gas stream
Absorption II Dry Solvent (Physical)	-Lower energy requirement -Less susceptible to impurities in the gas	-High operating pressure -Low suitability for dilute CO_2 flue gas
Adsorption	-Very high CO_2 recovery -Easy operation	-Very high operating pressure -Costly
Membrane	-High space efficiency -Lower energy requirement -Easy operation	-Very high operating pressure -Low product purity -High cost
Cryogenic	-Proven technology	-High operating energy -Not suitable for large amounts of flue gas

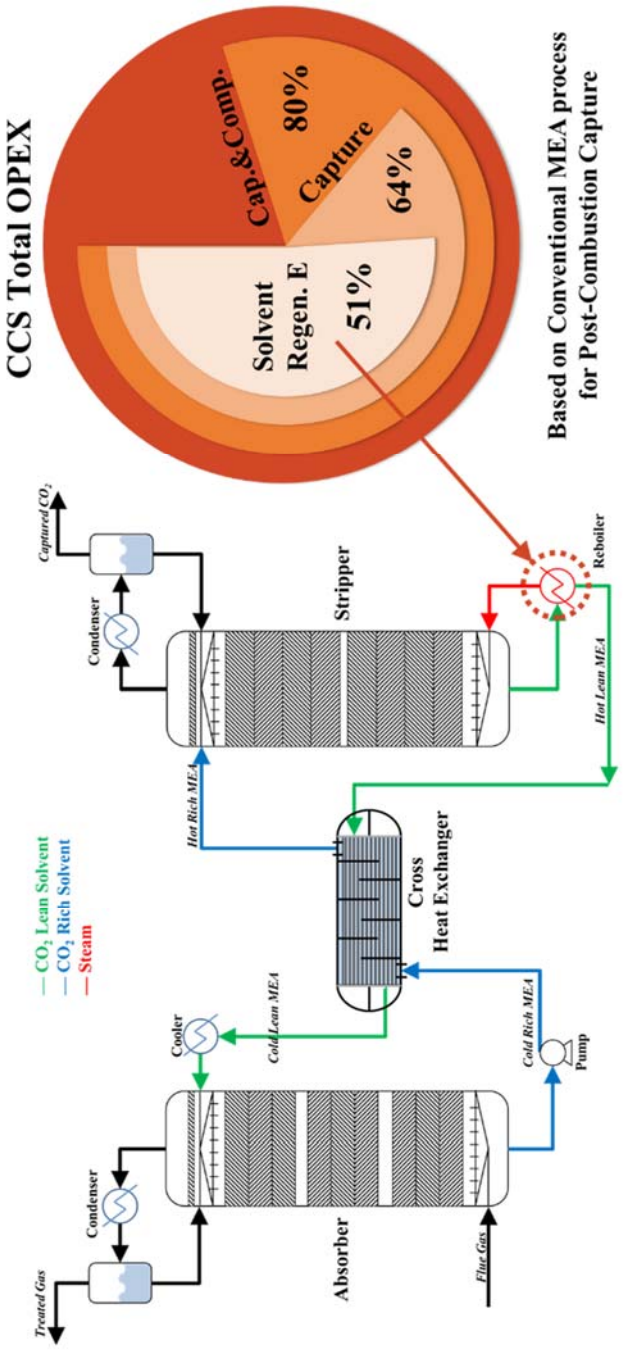

Fig. 2-1. The most energy-intensive unit of the conventional MEA scrubbing process

2.2 Process description

The conventional CO_2 capture process with MEA scrubbing is composed of an absorber, a cross heat exchanger, and a stripper, as indicated in Fig. 2-2. The SO_x-free flue gas (Flue Gas) enters the absorber bottom, and the cold lean solvent (Cold Lean MEA) enters the absorber. In the absorber, the MEA solvent selectively absorbs CO_2 by an exothermic reaction and then drains out at the absorber bottom (Cold Rich MEA). The remaining flue gas is purged out at the absorber top (Treated Gas). The cold rich solvent is preheated through the cross-heat exchanger and enters the stripper top (Hot Rich MEA). In the stripper, the hot rich solvent desorbs CO_2 by an endothermic reaction at high temperature and drains at the stripper bottom (Hot Lean MEA). The gaseous CO_2 is cooled by passing through a condenser and captured at the stripper top (Captured CO_2). After the hot lean solvent is cooled through the heat exchanger and the cooler, the lean solvent is recycled to the absorber top to absorb CO_2 in the flue gas again.

In the MEA scrubbing process, the solvent regeneration energy can be classified by the sensible heat term, H_S, the desorption reaction heat term, H_R, and the latent heat term, H_L, as indicated in Fig. 2-3. Sensible heat represents the energy required to convert the cold solvent to hot solvent, while the desorption reaction heat represents the energy required to desorb CO_2 from the solvent, and the latent heat represents the energy required to vaporize

water. The energy required for solvent regeneration is supplied by the cross heat exchanger and the reboiler. In the cross heat exchanger, the majority of the required sensible heat is supplied from the hot solvent to the cold solvent. As a result, the reboiler mainly supplies energy for CO_2 desorption and water vaporization. As MEA is an aqueous solvent, this process requires a significant amount of heat energy for water vaporization, corresponding to 20–35% of the total reboiler heat energy [8]. By improving the process configuration, the latent and sensible heat requirements can be reduced, while the desorption reaction heat requirement can be reduced by improving the physical property of the solvent.

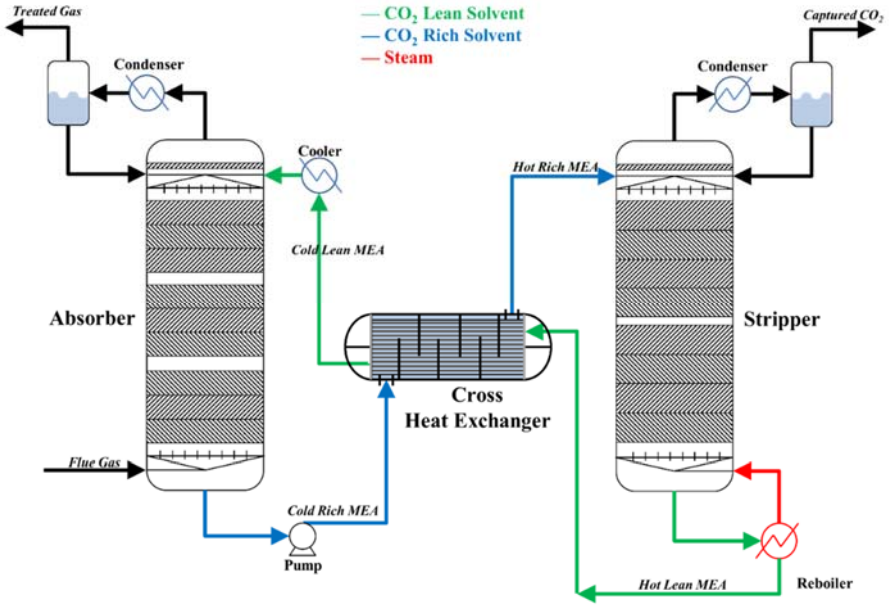

Fig. 2-2. Simplified process flow diagram of conventional CO_2 capture process using aqueous MEA

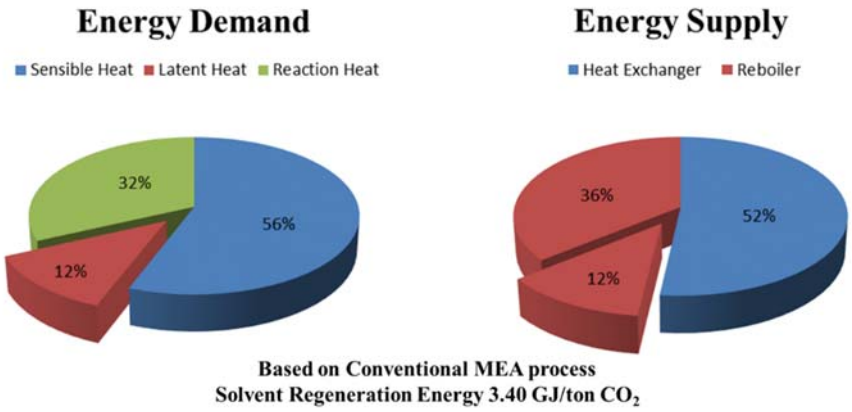

Fig. 2-3. Distribution of the energy demand and energy supply of the conventional MEA process

2.1 Energy system analysis

The reboiler is the most energy intensive unit for solvent regeneration in the conventional CO_2 capture with MEA scrubbing. To analyze the reboiler heat requirement, the stripper system was simplified as indicated in Fig. 2-4. The enthalpy change between the outlet stream (D, B) and the inlet stream (F) is equal to the sum of the reboiler duty and condenser duty as indicated in Eq. (2-1). The h_B, h_D, and h_F values represent the molar enthalpies for the bottom stream, distillate stream, and feed stream, respectively.

$$B \times h_B + D \times h_D - F \times h_F \cong |Q_{Reb}| - |Q_{Cond}| \qquad (2\text{-}1)$$

As indicated in Eq. (2-2), the reboiler heat duty (Q_{Reb}) is determined by the condenser cooling duty (Q_{Cond}) and enthalpy change between the stripper inlet and the outlet streams (ΔH).

$$|Q_{Reb}| = |Q_{Cond}| + |\Delta H| \qquad (2\text{-}2)$$

The condenser cooling duty (Q_{Cond}) is a function of the stripper top temperature. From the mass balance equations, the D_{CO2}, D_{H2O}, V_{CO2}, and V_{H2O} values can be calculated according to Eqs. (2-3) to (2-6):

$$D_{CO_2} = \mathrm{D} \times y_{CO_2}\big|_{T=T_{Cond}} \qquad (2\text{-}3)$$

$$V_{CO_2} = \mathrm{V} \times y_{CO_2}\big|_{T=T_{Top}} \qquad (2\text{-}4)$$

$$D_{H_2O} = D_{CO_2} \times \frac{y_{H_2O}}{y_{CO_2}}\Big|_{T=T_{Cond}} \quad (2\text{-}5)$$

$$V_{H_2O} = V_{CO_2} \times \frac{y_{H_2O}}{y_{CO_2}}\Big|_{T=T_{Top}} \quad (2\text{-}6)$$

As the reflux liquid is almost pure water, D_{CO2} is assumed to be equal to V_{CO2}, as shown in Eq. (2-7):

$$D_{CO_2} \cong V_{CO_2} \quad (2\text{-}7)$$

Employing Eqs. (2-3) to (2-10), the reflux flow rate can be determined according to Eq. (2-11). The vapor fraction ratio ($y_{H2O}/y_{CO2)}$ increases under high temperature and low pressure conditions.

$$y_{H_2O} = \frac{P^{sat}(T)}{pstr} \quad (2\text{-}8)$$

$$y_{CO_2} = 1 - y_{H_2O}(T) \quad (2\text{-}9)$$

$$P^{sat}(\text{kPa}) = \exp[16.3872 - \frac{3885.7}{T(°C)+230.17}] \quad (2\text{-}10)$$

$$R_{H_2O} = V_{H_2O} - D_{H_2O} = D_{CO_2} \times \left[\frac{y_{H_2O}}{y_{CO_2}}\Big|_{T=T_{Top}} - \frac{y_{H_2O}}{y_{CO_2}}\Big|_{T=T_{Cond}}\right] \quad (2\text{-}11)$$

When the sensible heat is neglected in the condenser, the condenser cooling duty can be calculated by multiplying the condensation enthalpy and the reflux rate, as shown in Eq. (2-12). The value of the condenser cooling duty is comparable with the latent heat requirement, H_L. The condenser cooling duty

(or latent heat requirement) drops when the stripper top temperature is lowered. This is due to the reflux rate decreases under the low temperature.

$$Q_{Cond} \cong R_{H_2O} \times \Delta H_{Cond} \quad (2\text{-}12)$$

According to Eq. (2-11) and Antoine's equation (Eq. (2-10)), the condenser cooling duty is a function of the stripper top temperature and the condenser target temperature. When the distillate CO_2 flow rate (D_{CO2}), the condenser target temperature (T_{Cond}), and the stripper pressure (P^{str}) are fixed, the condenser cooling duty is simply a function of the stripper top temperature, which is determined by the inlet feed temperature and lean loading value at the stripper bottom.

Subsequently, the enthalpy change between the inlet and outlet streams is comparable with sum of the desorption reaction heat, (H_R), and sensible heat requirements, (H_S), as indicated in Eq. (2-13):

$$|\Delta H| \cong |H_R| + |H_S| \quad (2\text{-}13)$$

When the solvent lean/rich loading balance is determined, the reaction heat requirement, H_R, is constant, and so it can be reduced by improving the physical properties of the solvent.

The sensible heat requirement can be simply calculated by assuming the cold side heat capacity (flowrate x specific heat capacity) is comparable with hot side heat capacity according to Eq. (2-14). The 'H_{S0}' term indicates the

sensible heat requirement when the cross heat exchanger is absent, as indicated in Eq. (2-15). The supplying heat duty at the cross heat exchanger is calculated according to Eq. (2-16).

$$F \times C_{P,L\_Cold\ side} \cong B \times C_{P,L\_Hot\ side} \quad (2\text{-}14)$$

$$H_{S_0} = F \times C_{P,L} \times (T_{Hot-In} - T_{Cold-In}) \quad (2\text{-}15)$$

$$Q_{HX} = F \times C_{P,L} \times (T_{Hot-In} - T_{Hot-Out}) \quad (2\text{-}16)$$

By combining Eqs. (2-14) to (2-16), the net sensible heat requirement can be determined by the temperature approach, TA, at the cross heat exchanger, as indicated in Eq. (2-17).

$$H_S \cong H_{S_0} - Q_{HX} = F \times C_{P,L} \times (T_{Hot-In} - T_{Cold-Out}) \quad (2\text{-}17)$$

As a result, the reboiler heat requirement is a function of the temperature at the stripper top and the temperature approach at the cross heat exchanger when the CO_2 loading valance is fixed.

$$|Q_{Reb}| = |Q_{Cond}| + |H_S| + |H_R| \quad (2\text{-}18)$$

$$|Q_{Reb}| = \left|Q_{Cond}(T_{Top})\right| + F \times C_{P,L} \times TA + |H_R| \quad (2\text{-}19)$$

To reduce the reboiler heat requirement, the stripper top temperature or temperature approach should decrease according to Eqs. (2-18) and (2-19). However, there is unfortunately a trade-off between the stripper top temperature and the temperature approach in the conventional stripper

configuration. When the temperature approach decreases, the cold out temperature (T_{Cold_Out}) and the stripper top temperature (T_{Top}) rise. As the water vapor fraction at the stripper top increases with a rise in temperature, the reflux rate and the condenser cooling duty also increase. As indicated in Fig. 2-5, in the conventional MEA process, the condenser cooling duty increases with a decrease in the temperature approach. Although a decrease in the temperature approach is the preferred strategy for reducing the total reboiler heat requirement, it wastes a significant amount of heat energy for water vaporization in the reboiler. If the condenser cooling duty can be completely eliminated, the reboiler heat requirement will be reduced from the solid line to the dotted line, as depicted in Fig. 2-5. When the condenser cooling duty (or latent heat requirement) decreases to zero, the reboiler heat requirement is reduced by up to 25% as shown in Figs. 2-3 and 2-5. This trade-off is a significant limitation for the conventional stripper configuration of the MEA scrubbing process.

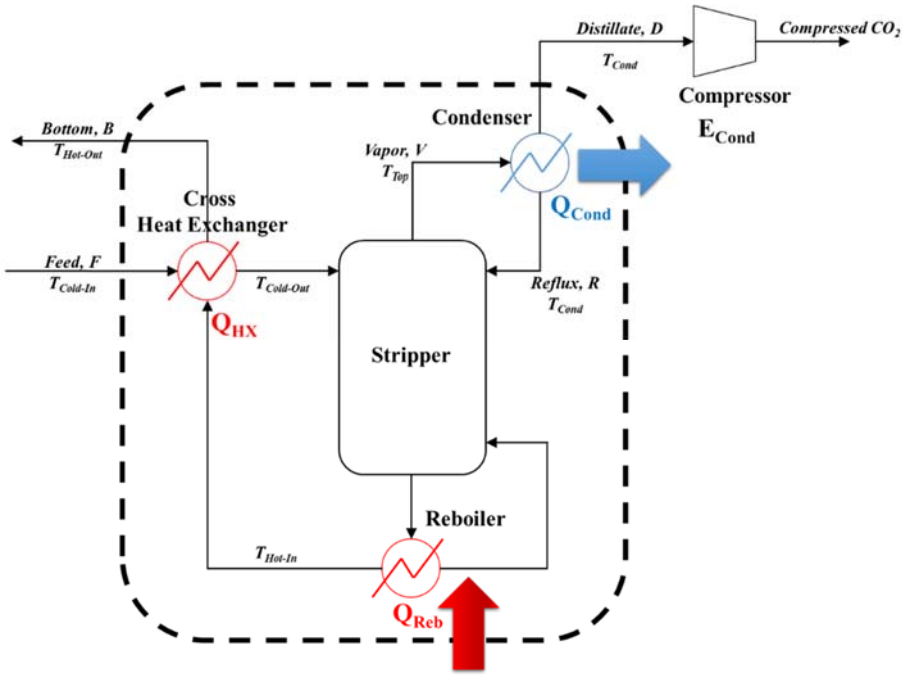

Fig. 2-4. Energy system of the stripper in the conventional MEA process

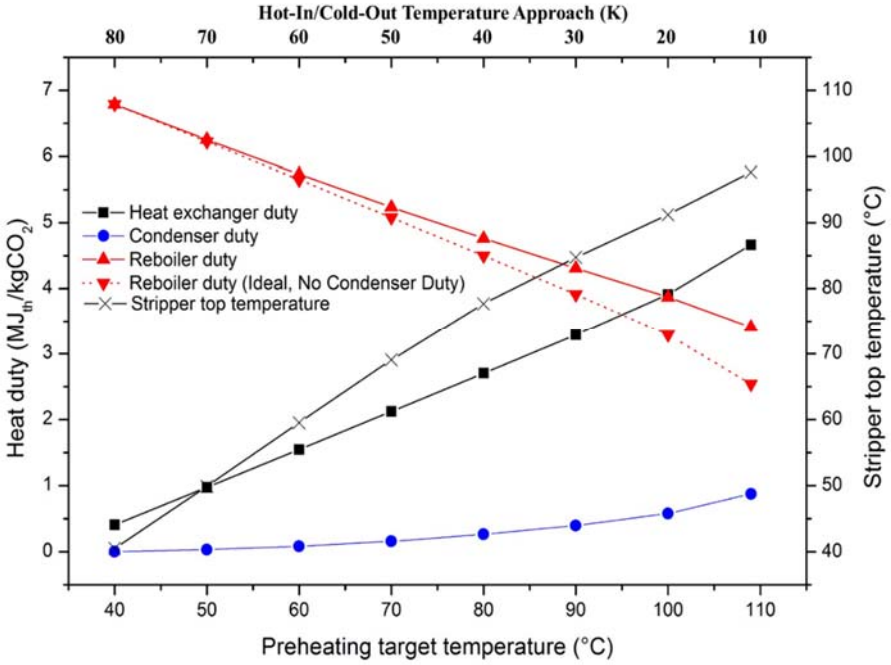

Fig. 2-5. Reboiler heat requirement change against temperature approach in the cross heat exchanger

2.2 Parametric study

The main design variables of the conventional MEA process are the operating pressure of the stripper, the cycling solvent flowrate, the temperature approach (or cross heat exchanger area), the absorber height, and the stripper height. These process design variables affect either the lean loading, the stripper inlet stream temperature, or the sensible heat recovery. Finally, these variables determined the latent heat requirement or sensible heat requirement at the reboiler. On the other hand, the desorption reaction heat remains constant value. It is because the desorption reaction heat is very slightly changed under the actual operation range although it is function of lean/rich loading. Table 2-2 indicates the results of the qualitative analysis under 90% CO_2 capture recovery conditions.

Initially, with an increase in stripper pressure, the latent heat requirement is reduced as mentioned in chapter 2.3. The water composition decreases in the vapor phase with the increase in pressure. For example, the water content in the vapor decreases from 0.62 to 0.31 mol/mol with a rise in pressure from 1.0 bar to 2.0 bar at 360 K. As the water content drops, the reflux ratio and condenser cooling duty decrease. In addition, the high operating pressure in the capture process is advantageous for the CO_2 compression process. As the initial pressure increases, the compression duty can be significantly reduced.

However, the operating pressure exhibits an upper limit due to issues with solvent thermal degradation.

Furthermore, when the cycling solvent flowrate increases, the latent heat requirement is reduced as the CO_2 loading balance changes according to the solvent flowrate. As the solvent flow rate increases, the CO_2 lean loading value increases at the stripper bottom. At high CO_2 loadings, the equilibrium CO_2 partial pressure also rises [16, 17], and as a result, less water vaporizes at the stripper bottom. Although the desorption reaction heat is a function of the CO_2 loading value, it is roughly comparable under the actual operating range [16, 18]. In addition, the sensible heat requirement increases slightly as the cycling solvent flowrate increases.

In addition, when the heat transfer area increases in the cross heat exchanger, the sensible heat requirement is reduced. Although the latent heat requirement increases through an increase in the stripper top temperature, the final reboiler heat requirement is reduced.

Also, when the absorber height increases, the latent heat requirement is reduced. This occurs because the CO_2 rich loading and lean loading values increase at the bottom of the absorber and bottom of stripper, respectively. As the lean loading increases, the quantity of vaporized water and the stripper top temperature both decrease.

Finally, with an increase in stripper height, the latent heat requirement is reduced. As the stripper height increases, the stripper top temperature moves closer to the feed stream temperature. In contrast, the stripper top temperature moves closer to the stripper bottom temperature with a decrease in stripper height.

Table 2-2. The qualitative parametric study of main variables in the conventional MEA process

Variable		Main Effect	H_R	H_L	H_S	E_C	LP Steam	Electricity
Operating Condition	Stripper Pressure↑	Water composition in vapor↓	-	↓	-	↓	↓	↓
	Solvent Flowrate↑	Lean Loading ↑	-	↓	↑	-	↑/↓	-
Equipment Size	HX Area↑	Sensible heat recovery ↑	-	↑	↓	-	↓	-
	Absorber Height↑	Lean Loading↑	-	↓	-	-	↓	-
	Stripper Height↑	Stripper top temp. ↓	-	↓	-	-	↓	-

Chapter 3: Modified MEA Scrubbing Process

3.1 Overview

As previously discussed, the reboiler heat requirement is the sum of the latent heat requirement, the sensible heat requirement, and the desorption reaction heat requirement. As the desorption reaction heat remains relatively constant under the actual operating conditions, various process alternatives have been developed to reduce the latent heat requirement and sensible heat requirement:

$$|Q_{Reb}| = |Q_{Cond}| + |H_S| + |H_R| \quad (2\text{-}18)$$

Initially, when the CO_2 rich loading increases at the absorber bottom, the CO_2 lean loading also increases at the stripper bottom. As the CO_2 lean loading increases, the quantity of water vaporization at the stripper bottom decreases. Thus, absorber intercooling, flue-gas splitting, flue-gas precooling, and semi-lean/semi-rich loop were incorporated in the modified configuration for increasing CO_2 lean loading at the stripper bottom. These modified configurations reduce the latent heat requirement as summarized in Table 3-1.

Secondly, with a decrease in the stripper inlet feed temperature, the stripper top temperature also decreases. The stripper interheating, staged feed of the stripper, lean vapor compression, and rich vapor compression are modified

configuration for decreasing the stripper inlet stream temperature, resulting in a reduction in the latent heat requirement, as summarized in Table 3-2.

Finally, with an increase in the wasting heat recovery, the sensible heat requirement reduces at the reboiler. The economizer reduces the minimum temperature approach at the cross heat exchanger, and the stripper overhead compression (or mechanical vapor recompression) recovers the heat generated from the CO_2 compression process. These modified configurations reduce the sensible heat requirement at the reboiler as summarized in Table 3-3. Furthermore, the heat integration with steam cycle reduces the power de-rate at the power plant [19].

3.2Modified configuration I: Increasing the CO_2 lean loading

3.1.1 Absorber intercooling

The absorber intercooling process cools the mid-bottom section of the absorber using an external coolant [6, 10, 20-23]. As CO_2 absorption is an exothermic reaction, the absorption capacity of the solvent increases at low temperatures, resulting in an increase in the CO_2 loading of the absorber outlet and a decrease in the solvent circulation flowrate. As the CO_2 loading increases, the latent heat requirement is reduced in the stripper, and as the circulation flowrate decreases, the sensible heat requirement is reduced slightly. The optimal intercooling position and temperature can be determined using the reaction rate and the reaction equilibrium. At low temperatures, the equilibrium CO_2 loading increases while the absorption reaction rate decreases. At the top of the absorber, the solvent exhibits a low CO_2 loading value, which is significantly lower than the equilibrium CO_2 loading value. Thus, the intercooling at the top of the absorber is generally not optimal. At the top of absorber, high temperature has advantage in the absorption reaction rate. At the bottom of the absorber, the solvent has a sufficiently high CO_2 loading value comparable to that of the equilibrium loading value. Therefore, the optimal intercooling position is at the mid-bottom of the absorber, which gives an increase in equilibrium loading value [24]. The configuration of the

absorber intercooling process also requires an additional heat exchanger and cooling utility. In addition, the absorber intercooling requires larger cross heat exchanger, due to the cold side temperature decrease.

3.1.2 Flue gas split

The flue gas split configuration cools the mid-bottom section of the absorber by splitting the flue gas [15]. Part of the flue gas is fed to the mid-bottom of the absorber, while the other part is fed to the absorber bottom. As the flue gas temperature is lower than that of the absorber middle section, the absorber operating temperature decreases. As the absorption capacity of the solvent increases at low temperatures, the CO_2 loading increases and the solvent circulation flowrate decreases. Therefore, with an increase in CO_2 loading, the latent heat requirement in the stripper drops. Although the cooling effect is lower than that of the absorber intercooling, this configuration cools the absorber bottom section without any additional heat exchanger or cooling utility. The configuration of the flue gas split therefore requires only a sufficient absorber height.

3.1.3 Flue gas precooling

The purpose of flue gas precooling is to cool the flue gas before it enters the absorber bottom [21]. By cooling the flue gas, the bottom of the absorber temperature is reduced. As the absorption capacity of the solvent increases at low temperatures, the CO_2 loading increases, while the solvent circulation flowrate decreases. Subsequently, as the CO_2 loading increases, the latent heat requirement is reduced in the stripper. Finally, the configuration of the flue-gas precooling requires both an additional heat exchanger and a cooling utility.

3.1.4 Semi-lean/semi-rich loop

The semi-lean/semi-rich configuration process consists of both semi-lean and semi-rich solvent loops [21, 22, 25-29]. The semi-lean/semi-rich loop improves the operating line at the stripper by changing the lean loading value and rich loading value. This variation in loading balance can break the bottleneck of the operating line at either the absorber or the stripper. In addition, the configuration of the semi-lean/semi-rich loop requires an additional heat exchanger.

Table 3-1. Process description for modified configurations I

Modified Configurations	Process Description
Absorber intercooling [6, 10, 20-23]	- Cooling the mid-bottom of the absorber using external coolant - Increasing the solvent's absorption capacity and CO_2 rich loading - Increasing the CO_2 lean loading at the stripper bottom - Requiring additional heat exchanger and utility
Flue gas Splitting [15]	- Cooling the mid-bottom of the absorber using split flue gas - Increasing the solvent's absorption capacity and CO_2 rich loading - Increasing the CO_2 lean loading at the stripper bottom - Requiring enough height of the absorber
Flue gas Precooling [21]	- Cooling the flue gas before it enters absorber bottom - Increasing the solvent's absorption capacity and CO_2 rich loading - Increasing the CO_2 lean loading at the stripper bottom - Requiring additional heat exchanger and utility
Semi-Lean/ Semi-Rich Loop [21, 22, 25-29]	- Composing additional semi-lean/semi-rich solvent loop - Improving the operating line in the stripper - Requiring additional heat exchanger

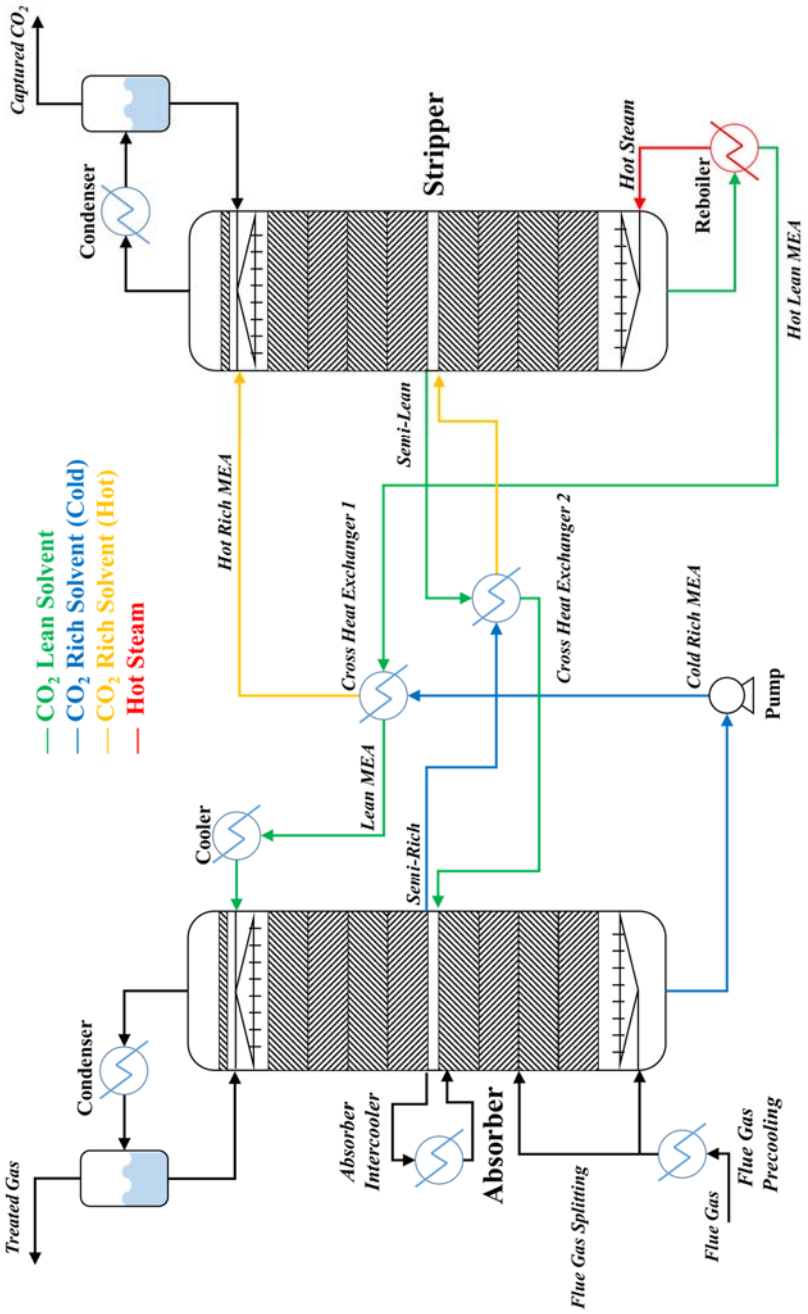

Fig. 3-1. Process flow diagram for absorber intercooling, flue gas splitting, flue gas precooling and semi-lean/semi-rich loop

3.2 Modified configuration II: Decreasing the stripper top temperature

3.2.1 Stripper interheating

The stripper interheating process heats the mid-bottom section of the stripper using the stripper bottom stream [30, 31]. This configuration recovers a part of the sensible heat at the stripper interheater in advance of the cross heat exchanger. However, the total sensible heat recovery remains constant because the sensible heat recovery is reduced at the cross heat exchanger, as is the heat recovery in the interheater. This configuration reduces the cold solvent outlet temperature at the cross heat exchanger and causes a temperature decrease at the top of the stripper. Therefore, the overall effect of stripper interheating is a decrease in the stripper top temperature rather than an increase sensible heat recovery. As the temperature of the stripper top decreases, the latent heat requirement is reduced. For this process, the configuration requires an additional heat exchanger, while the size of the cross heat exchanger can be reduced.

3.2.2 Staged feed of the stripper

The staged feed of the stripper (or cold solvent split) cools the stripper top using a split cold solvent [21, 32]. To cool the stripper top, ~15–20% of the cold inlet stream is split before passing through the cross heat exchanger. One split cold stream directly enters the stripper top, while the other enters the stripper middle after passing through the cross heat exchanger. As the cold solvent is fed to the stripper top, the temperature of the stripper top is lowered, resulting in a drop in both reflux ratio and condenser cooling duty. Thus, when the stripper top temperature reaches the condenser target temperature, the reflux ratio and condenser cooling duty drop to zero. This configuration reduces the majority of the latent heat requirement, although a significant amount of sensible heat recovery at the cross heat exchanger is lost. As the amount of cold side inlet flowrate decreases at the cross heat exchanger, the sensible heat recovery is reduced. As a result, the sensible heat requirement is increased, and the sum of the sensible heat requirement and latent heat requirement remains relatively constant.

3.2.3 Lean vapor compression

The lean vapor compression process vaporizes part of the stripper bottom stream in a flash drum at low pressure [21, 25, 27, 33, 34]. The vaporized steam is then pressurized once again and fed to the stripper bottom. This steam supplies the latent heat of the additional steam at the stripper bottom. However, a significant amount of sensible heat recovery is lost at the cross heat exchanger using this configuration. As the hot solvent temperature is lowered following solvent vaporization, the amount of sensible heat recovery is reduced along with any additional latent heat of steam. Although the total heat recovery holds, this configuration lowers the cold solvent outlet temperature at the cross heat exchanger, and causes a temperature decrease at the top of the stripper. Therefore, the overall effect of the lean vapor compression is to decrease the temperature of the stripper top. As this temperature decreases, the latent heat requirement is reduced. The key variable of this configuration is vaporization pressure, with a vaporization pressure of ~1.0 bar, and a stripper bottom pressure of ~1.8 bar, resulting in approximately 5% of the solvent vaporizing, and the lean solvent temperature being reduced by 20 ºC. The configuration of the lean vapor compression requires an additional valve, a flash drum, a compressor, and additional electricity costs. Finally, the size of the cross heat exchanger can be slightly reduced in this case.

3.2.4 Rich vapor compression

The rich vapor compression process vaporizes part of the rich solvent in the cross heat exchanger at low pressures [35]. The vapor (mixed steam and CO_2) is pressurized once again and then fed to either the stripper top or bottom. As the rich solvent begins to vaporize, the rich solvent outlet temperature decreases at the cross heat exchanger. As a result, this configuration reduces the temperature at the stripper top without any sensible heat recovery loss. As the temperature of the stripper top decreases, the latent heat requirement is reduced. The key variable of this configuration is the operating pressure of the cross heat exchanger. For the rich vapor compression, the cross heat exchanger operating pressure is 1.0–1.5 bar while for the conventional system, an operating pressure is higher than 5.0 bar. Approximately 5% of the solvent is vaporized, and the rich solvent temperature is reduced by 20 ºC. Finally, the configuration of the lean vapor compression requires a partial vaporizing heat exchanger, a compressor, and additional electricity costs.

Table 3-2. Process description for modified configurations II

Modified configuration.	for decreasing the stripper top temp Process Description
Stripper interheating [30, 31]	- Heating the middle of the stripper using hot lean solvent - Decreasing the stripper inlet stream temperature - Reducing the latent heat requirement by decreasing the stripper top temperature - Requiring additional heat exchanger
Staged feed of the Stripper (Cold Solvent Split) [21, 32]	- Cooling the stripper top using a split cold rich solvent - Reducing the latent heat requirement by decreasing the stripper top temperature - Requiring enough height of stripper
Lean vapor compression (Lean vapor recompression) [21, 25, 27, 33, 34]	- Vaporizing the hot lean solvent under the low pressure condition - Recompressing the generated steam to the stripper bottom - Decreasing the stripper inlet stream temperature - Reducing the latent heat requirement by decreasing stripper top temperature - Requiring additional compressor and flash vessel
Rich vapor compression (Rich vapor recompression) [35]	- Vaporizing the hot rich solvent under the low pressure condition - Recompressing the generated steam & CO_2 to the stripper bottom - Decreasing the stripper inlet stream temperature - Reducing the latent heat requirement by decreasing stripper top temperature - Requiring additional compressor and partial vaporizing heat exchanger

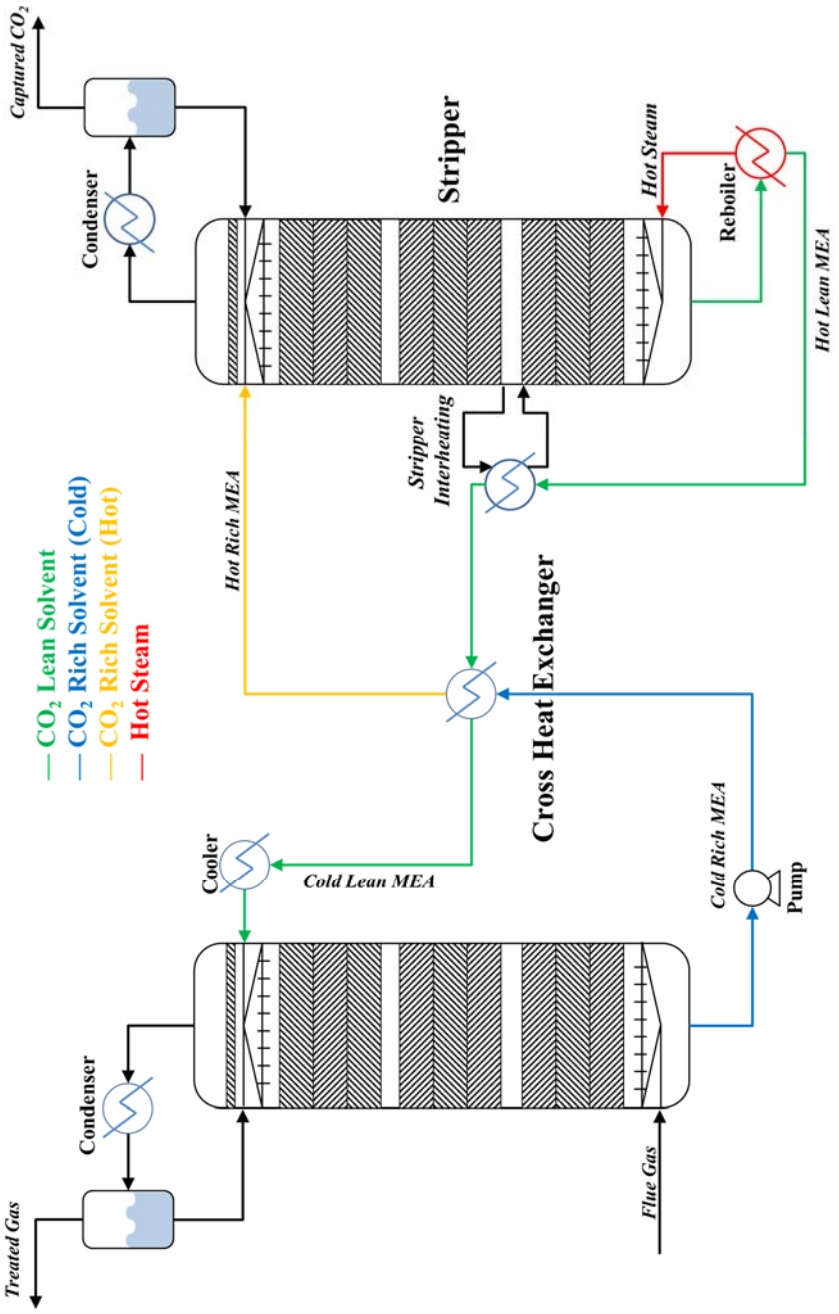

Fig. 3-2. Process flow diagram for stripper interheating

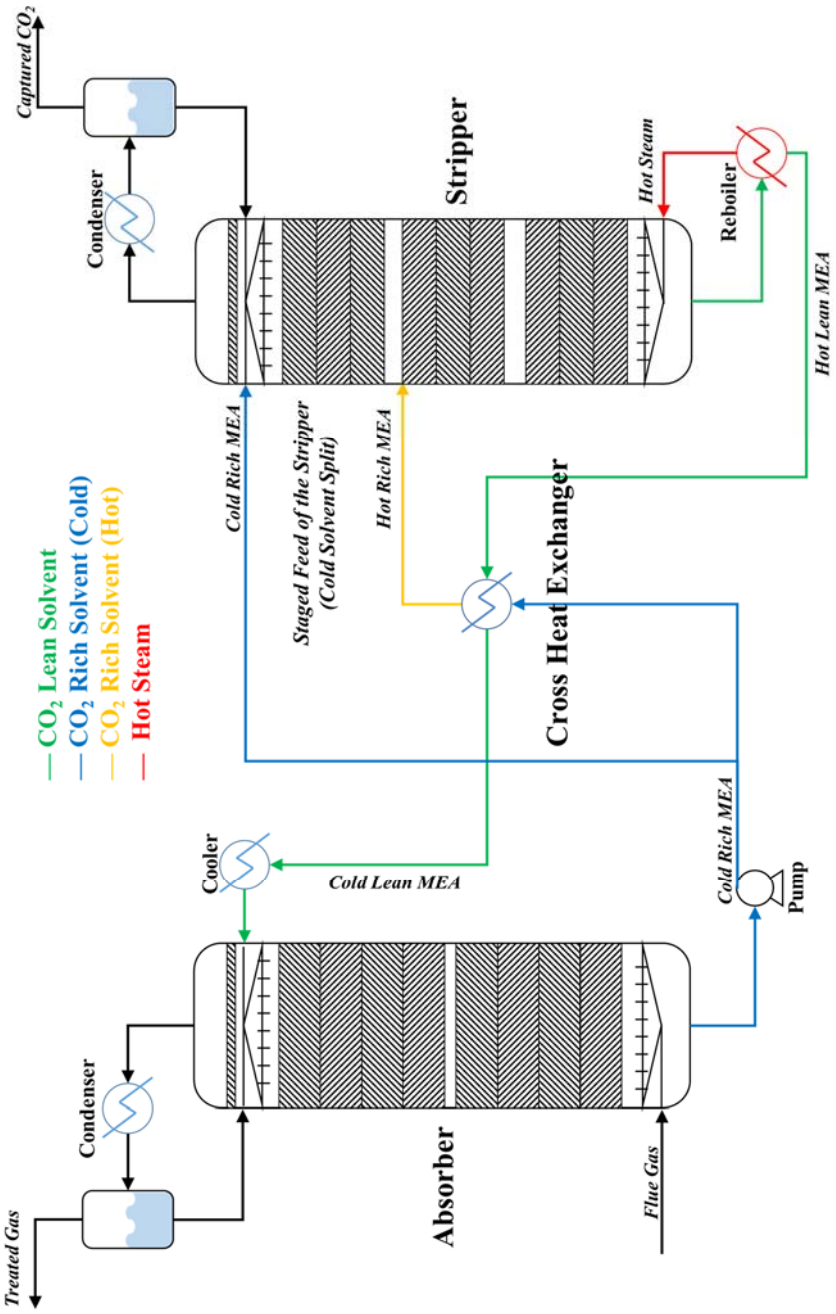

Fig. 3-3. Process flow diagram for staged feed of stripper (cold solvent split)

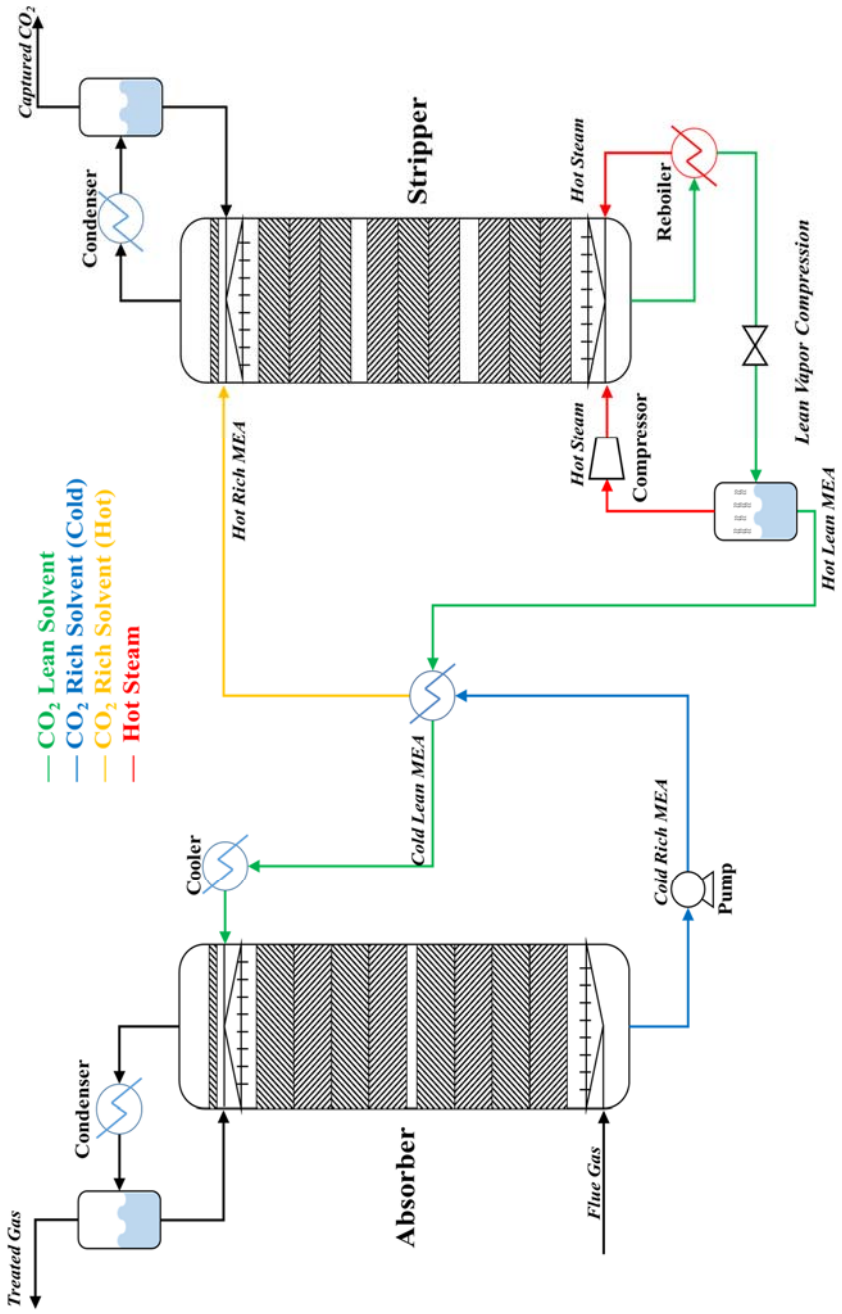

Fig. 3-4. Process flow diagram for lean vapor compression

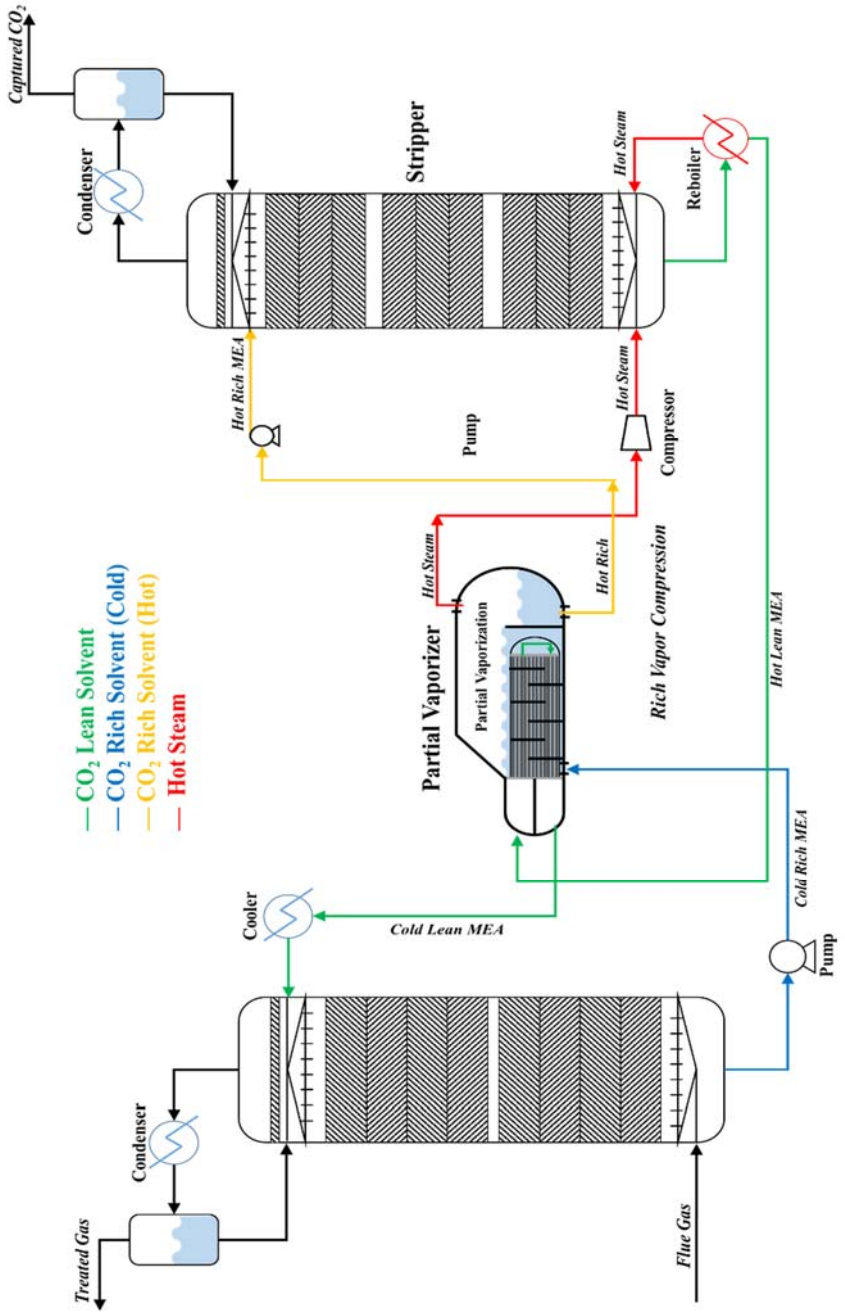

Fig. 3-5. Process flow diagram for rich vapor compression

3.3 Modified configuration III: Enhancing the waste heat recovery

3.3.1 Stripper overhead compression

The stripper overhead compression is based on a similar concept as the mechanical vapor compression [21, 36, 37]. The purpose of this configuration is compression of the distillate stream before the stripper condenser. As the distillate stream is compressed, the dew point of the distillate stream increases above the stripper bottom temperature, and the compressed distillate stream supplies latent heat by passing through the heat exchanger at the striper bottom. Although the temperature of the stripper top is not lowered, the latent heat requirement is reduced by recovering the latent heat at the stripper bottom. This stripper overhead compression configuration requires an additional heat exchanger, a compressor and additional electricity costs.

3.3.2 Economizer

Use of an economizer increases the sensible heat recovery at the cross heat exchanger by reducing the minimum temperature approach. A specially designed heat exchanger reduces the allowable minimum temperature approach below 5 ºC, while the conventional cross heat exchanger has a limit

of 10 ºC for the minimum temperature approach [21, 22]. As the sensible heat recovery increases, the sensible heat requirement is reduced at the reboiler.

3.3.3 Heat integration

The heat integration process combines the MEA process with either the steam cycle or CO_2 compression process [3, 19, 21, 27, 38-41]. As the processes are integrated, additional wasted sensible heat can be recovered from the system. This heat integration reduces the sensible heat requirement at the stripper by increasing the sensible heat recovery. This configuration of the heat integration requires an additional heat exchanger.

Table 3-3. Process description for modified configurations III

Modified configuration	Process Description
Stripper overhead compression (Mechanical vapor recompression) [21, 36, 37]	- Compressing the stripper top vapor before the condenser - Recovering the vapor's latent heat at the stripper bottom - Reducing the reboiler heat requirement by recovering the steam's latent heat - Requiring additional compressor and heat exchanger
Economizer [21, 22]	- Improving the minimum temperature approach of the cross heat exchanger - Increasing the sensible heat recovery in the cross heat exchanger - Reducing the sensible heat requirement - Requiring enough area of the cross heat exchanger
Heat Integrations [3, 21, 27, 38-41]	- Combining the capture process with steam cycle - Recovering the waste heat from the compression process - Requiring additional heat exchanger

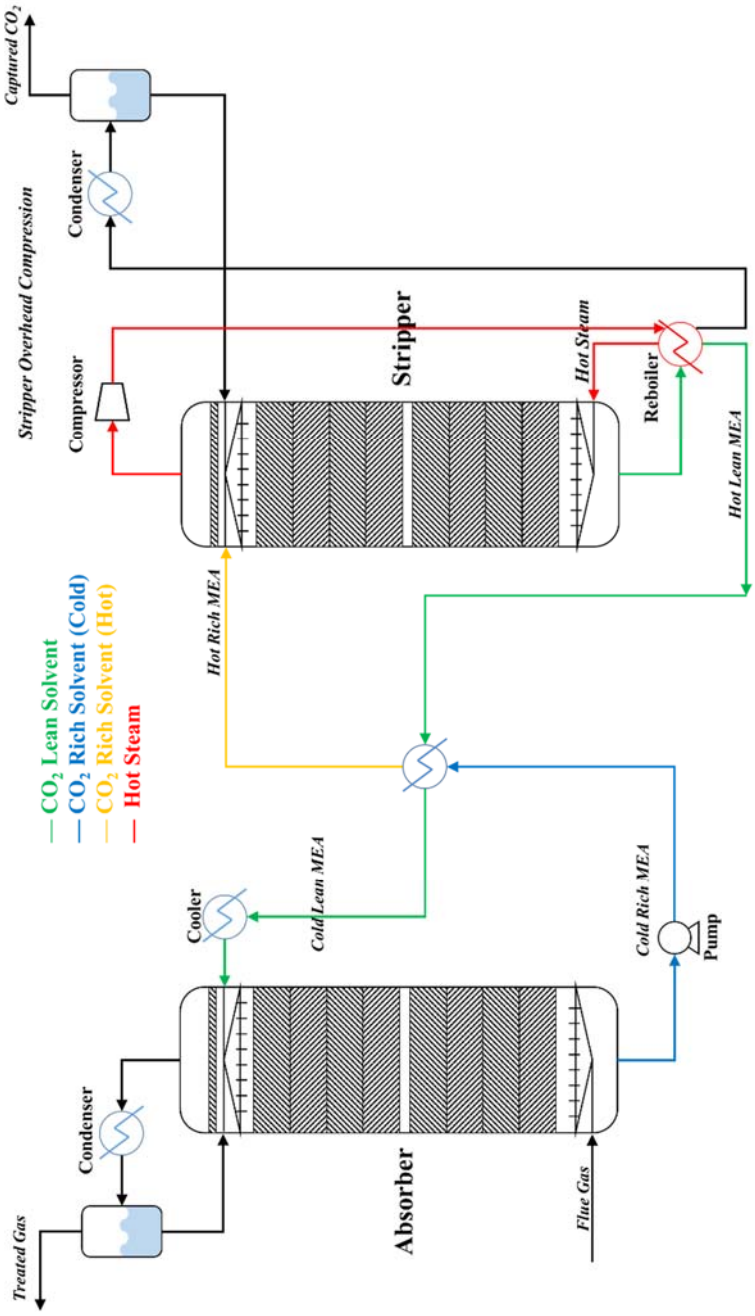

Fig. 3-6. Process flow diagram for stripper overhead compression (mechanical vapor compression)

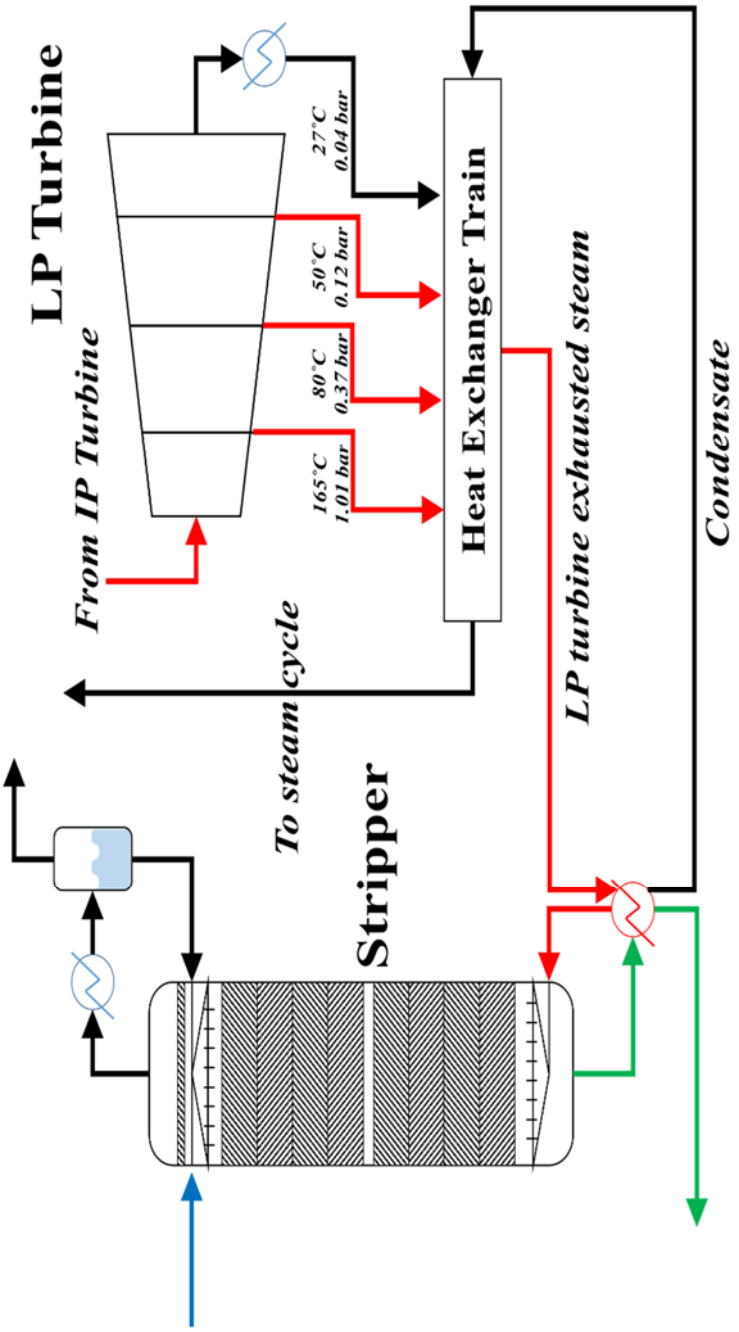

Fig. 3-7. Process flow diagram for heat integration (integration with steam cycle)

3.4 Parametric study

The modified configurations have additional design variables from absorber intercooling, semi-lean/semi-rich loop, staged feed of the stripper (cold solvent split), lean vapor compression, rich vapor compression, and heat integration with the compression process. With changes in the key variables, a qualitative effect was observed in terms of the energy requirements and equipment size requirements, as can be seen in Table 3-4, which also shows the results of qualitative analysis under 90% CO_2 capture recovery conditions.

Initially, the key variable of the absorber intercooling to be examined was the intercooling target temperature. As the cooling target temperature decreased, the rich loading and lean loading increased at the absorber bottom and the stripper bottom, respectively. In addition, as the lean loading increased, the latent heat requirement was reduced. Thus, a larger intercooler and cross heat exchanger, while the reboiler size can reduced.

The key variable of the semi-lean/semi-rich loop is the split fraction. As the configuration improves the CO_2 loading balance at the absorber and stripper, the latent heat requirement was reduced. This resulted in an increase in the cycling solvent flow rate and subsequent increase in the sensible heat requirement. For this process, an additional heat exchanger should be considered.

Furthermore, the split fraction of the absorber bottom stream was then examined as the key variable of the staged feed of the stripper. In this step, a portion of the cold solvent is split and fed to the stripper top. As the split fraction increases, the temperature of the stripper top decreases. The latent heat requirement is reduced with stripper top temperature decrease. Because the cold side inlet flowrate decreases at the cross heat exchanger, the sensible heat recovery is reduced. This results in an increase in the sensible heat requirement. As a result, the reboiler heat requirement remains relatively constant, even though the split fraction varies. In this case, the cross heat exchanger size can be reduced while the stripper size should be increased.

Vaporization pressure, the key variable of the lean vapor compression, was then investigated. When the vaporization pressure was lowered, a large amount of vapor was generated at the flash drum and the lean solvent temperature was reduced by water vaporization. As the lean solvent temperature decreased, the cold out temperature also decreased at the cross heat exchanger. Thus, the stripper top temperature and latent heat requirement were reduced. As the vaporized water should be compressed and fed to the stripper bottom, additional compression energy is required. Finally, the cross heat exchanger and reboiler size can be reduced while the compressor size and flash drum size should be increased.

The key variable of the rich vapor compression was then investigated. This was the operating pressure of the cross heat exchanger, which is not a liquid-liquid heat exchanger but a partial vaporizer. When the operating pressure was lowered, a large amount of vapor was generated at the partial vaporizer, and the rich solvent temperature was reduced by vaporization. Sensible heat recovery could also be enhanced through this phase change. In addition, the decrease in the rich solvent temperature was accompanied by a decrease in the temperature of the stripper top. The latent heat requirement was also reduced, while the compression energy increased. In this configuration, additional compressor, and vessel are required, while the reboiler size can be reduced.

Finally, the key variable of the heat integration is the preheating target temperature. The stripper top inlet stream was heating using the waste heat of the compression process. When the preheating target temperature increased, the sensible heat requirement was reduced, while the latent heat requirement was increased. Thus, the additional cross heat exchanger is required and stripper condenser should be larger, while the reboiler size can should be reduced.

Table 3-4. The qualitative parametric study of main variables in the modified MEA process

Modified Configuration	Key Variable	H_R	H_L	H_S	E_C	LS	EL	Equipment Size
1. Absorber Intercooling	Intercooling Temperature↓ (Lean loading↑)	-	↓	-	-	↓	-	Intercooler ↑ Cross HX ↑ Reboiler ↓
2. Semi Lean/Semi Rich Loop	Split fraction ↑ (Lean loading↑)	-	↓	↑	-	-	-	Cross HX-2 ↑
3. Staged Feed of the Stripper (Cold solvent split)	Split fraction↑ (Stripper Top T↓)	-	↓	↑	-	-	-	Cross HX ↓ Stripper ↑
4. Lean vapor compression	Vaporizing P↓ (Stripper Top T↓)	-	↓	-	↑	↓	↑	Cross HX ↓ Reboiler ↓ Compressor ↑ Flash drum ↑
5. Rich vapor compression	Vaporizing P↓ (Stripper Top T↓)	-	↓	↓	↑	↓	↑	Cross HX ↑ Reboiler ↓ Compressor ↑ Flash drum ↑
6. Heat Integration	Preheating T↑ (Stripper Top T↑)	-	↑	↓	-	↓	-	Cross HX-3 ↑ Stripper Cond ↑ Reboiler↓

LS: Low pressure steam, EL: Electricity

Chapter 4: Combination of the Modified MEA Scrubbing Process[†]

4.1 Overview

As previously discussed, numerous modified MEA processes have been introduced to reduce the heat requirement of the reboiler. These modified configurations can interact either positively or negatively with one another. For example, the absorber intercooling and cold solvent split strongly interact in a positive each other. As absorber intercooling reduces the rich cold solvent temperature, it enhances the effect of the cold solvent split. In contrast, the absorber intercooling and flue precooling interact in a negative interaction. As absorber intercooling already cools the mid-bottom of the absorber sufficiently, the flue gas precooling has no effect. In addition, the mechanical vapor recompression interacts negatively with stripper interheating, cold solvent split, lean vapor compression, and rich vapor compression. These configurations all lower the stripper top temperature, and so the water content is dramatically reduced. As a result, the amount of latent heat recovery is insignificant when the mechanical vapor recompression is combined with

[†]A part of this chapter is taken from the author's published paper in the journal, Jung, J.; Jeong, Y. S.; Lee, U.; Lim, Y.; Han, C., New Configuration of the CO2 Capture Process Using Aqueous Monoethanolamine for Coal-Fired Power Plants. *Industrial & Engineering Chemistry Research* **2015,** 54, (15), 3865-3878. http://pubs.acs.org/doi/abs/10.1021/ie504784p

such configurations. Furthermore, by combining the configurations that display positive interactions, a significant amount of reboiler duty could be reduced. The interaction map shown in Table 4-1 was prepared from the qualitative analysis of these modified MEA processes. A strong positive interaction (++) indicates that the combination always interacts positively and exhibits a significant synergetic effect. A positive interaction (+) indicates that the combination interacts positively under specific conditions and shows a slight synergetic effect. Finally, a negative interaction (-) indicates that the combination is incompatible, or that a negative effect was observed. As a result, the optimal combination of the modified configuration was integration of the absorber intercooling, cold solvent split, and rich vapor recompression. After calculating the energy reduction effect, the cost for additional equipment was then considered.

Table 4-1. Positive and negative interaction with each variable

	Configuration for increasing CO_2 lean loading					Configuration for decreasing stripper inlet stream temperature			Configuration for enhancing waste heat recovery		
	AI	FS	FC	SLSR	SI	**CSS**	LVR	**RVR**	MVR	EM	HI
AI	X	-	-	?	0	++	0	0	0	+	0
FS		X	+	?	0	0	0	0	0	0	0
FC			X	?	0	+	0	0	0	+	0
SLSR				X	?	?	?	?	?	?	?
SI					X	0	-	-	-	+	+
CSS						X	0	++	-	+	+
LVR							X	-	-	+	+
RVR								X	-	+	+
MVR									X	+	-
EM										X	+

(++): strong positive interaction (+): positive interaction, (-): negative interaction, (0): no interaction, (?): not clear

AI: absorber intercooling, FS: Flue gas splitting, FC: Flue gas precooling, SLSR: semi-lean/semi-rich looping, SI: stripper interheating, CSS: cold solvent split, LVR: lean vapor recompression, RVR: rich vapor recompression, MVR: mechanical vapor recompression, EM: economizer, HI: heat integration with compression process

4.2 Process description

The combination of the modified MEA process consist of the absorber intercooling (AI), cold solvent split (CSS) and a rich vapor recompression (RVR), as indicated in Fig. 4-1. The main concept behind this configuration is the minimization of the condenser cooling duty (latent heat requirement) and maximization of the heat exchanger preheating duty (sensible heat recovery), simultaneously. First, to eliminate the condenser cooling duty, this process cools the stripper top to prevent water vaporization. To cool the stripper top, about 15-20% of cold inlet stream (Cold Rich Inlet) is split before it passes through the heat exchanger. One of the split cold streams (Cold Rich to Top) directly enters the stripper top under low-temperature (33°C). The other stream (Cold Rich to HX) enters the heat exchanger for preheating. Because the stripper top is directly cooled to the condenser cooling target temperature, the reflux rate decreases to zero. As a result, this CSS configuration eliminates the reflux rate and the condenser cooling duty. Second, to maximize the heat exchanger preheating duty, it increases the thermal capacity of the cold stream by vaporizing the cold stream (Cold Rich to HX). In this paper, the thermal capacity means not the specific heat capacity [kJ/kg°C] but the mass x specific heat capacity [kJ/°C]. Because the cold stream is split, the thermal capacity of cold stream is reduced. In general, the allowable heat exchanger preheating duty decreases when the thermal capacity of cold stream is

reduced. To compensate the reduction of thermal capacity, the cold stream (Cold Rich to HX) is vaporized in a heat exchanger under low pressure conditions (1 atm). The liquid phase of the preheated cold stream (Hot Rich) enters the stripper middle (height for identical temperature) after passing it through the pump. The vapor phase of the preheated cold stream (RVR vapor, 77% of H_2O, 23% of CO_2, and 350 ppm of MEA, mole bases) enters the stripper bottom after passing it through the compressor. The ratio of vaporized MEA to liquid MEA is only 0.0001, which is 20% of that in the lean vapor recompression process. This RVR vapor supplies additional steam to the stripper bottom. As a result, this RVR configuration lost only 5% of preheating duty in the heat exchanger, even though 15-20% of the cold stream is split.

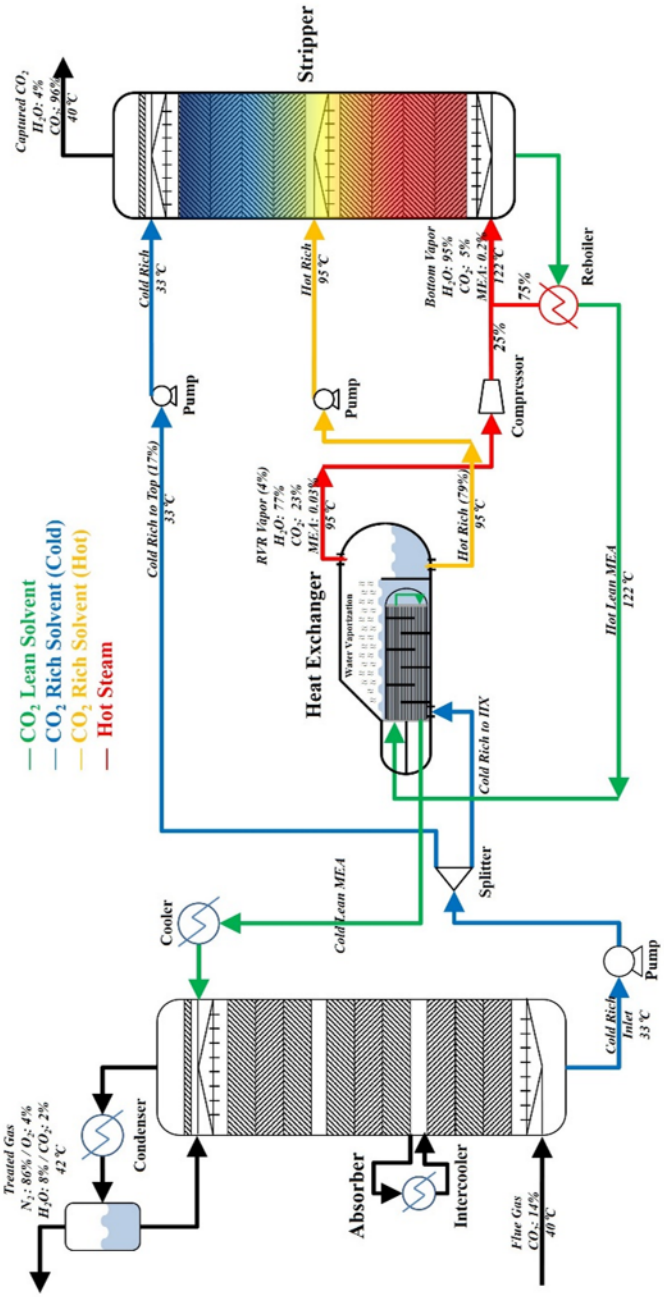

Fig. 4-1. Configuration of the rich vapor recompression combined with cold solvent split and absorber intercooling

4.3 Simulation specifications

Using the conventional simulator ASPEN PLUS v7.3 (ELECNRTL), the base model is established based on the data from a 0.1 MW CO_2 capture pilot plant (2 tons per day CO_2 capture capacity) in Boryeong, South Korea, as indicated in Fig. 4-2. The pilot plant is based on the conventional MEA process with absorber intercooling. The absorber and the stripper are simulated by a rate-based model that is a suitable unit for nonequilibrium reactive distillation [42-44]. The main process stream information and unit specification are shown in Table 4-2 and Table 4-3, respectively. To compare the effects of CSS and RVR separately, six different configurations were established as indicated in Fig. 4-3: Base process, Base process with cold solvent split (CSS), rich vapor recompression (RVR) process, RVR process with CSS, lean vapor recompression (LVR), and the LVR process with CSS. The combined configuration is compared with the LVR process, which is a well-known advanced configuration. In all six processes, the cold out temperature is determined by using a 10 °C minimum temperature approach (MTA) for internal temperature profile. In this work, we assumed all of compressor and turbine have constant efficiency as 0.75. The operating conditions for the six processes are summarized in Table 4-4.

Table 4-2. Process stream information for base process and alternative processes

Stream	Specification		Stream	Specification	
Flue gas	Temperature Pressure Flow rate CO_2 mole flow rate CO_2 mole frac.	40 °C 1.03 atm 353892 l/h 2.00 kmol/hr 0.141	Captured CO_2	Temperature Pressure Flow rate CO_2 recovery CO_2 mole flow rate CO_2 mole frac. H_2O mole frac.	40 °C 2.0 atm 81 kg/h 90% 1.80 kmol/hr 0.96 0.04
Cold Lean Solvent	Temperature Pressure Flow rate MEA Conc. CO_2 Loading L/G ratio	40 °C 2.5 atm 1370 kg/h 30 wt% 0.27 3.68 L/m^3	Cold Rich Solvent	Temperature Pressure Flow rate MEA Conc. CO_2 Loading	33 °C 1.01 atm 1456 kg/h 30 wt% 0.55

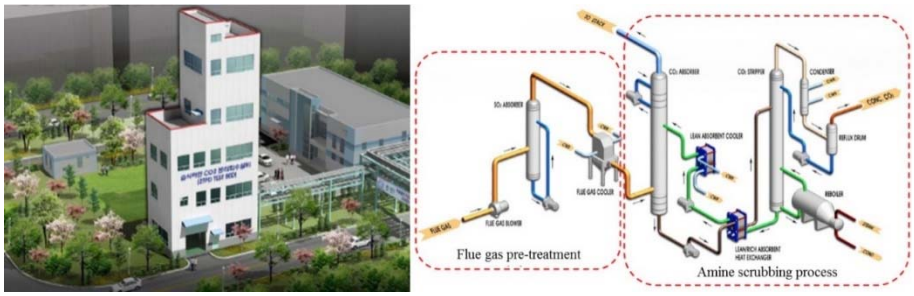

Fig. 4-2. Scheme of the 0.1 MW CO_2 capture pilot plant in Boryeong, South Korea

Table 4-3. Main unit specifications for Base process

Unit	Model	Specification[36]	
Absorber	Radfrac Rate-based model with ELECNRTL	Packing height	16.80 m
		Packing diameter	0.40 m
		Packing type	IMTP /1IN or 25MM
		Top pressure	1.0 atm
		Flow model	Mixed
		Mass transfer coefficient method	Onda et al.(1968)
		Interfacial area coefficient method	Onda et al.(1968)
		Interfacial area factor	2.0*
		Heat transfer coefficient method	Chilton and Colburn
		Heat transfer factor	1.0
		Hold up method	Stichlmair
		Film resistance	Discrxn for liquid film
		CO_2 recovery	Film for vapor film
		Top temperature	90 %
		Bottom temperature	40 °C
			33 °C
Stripper	Radfrac Rate-based model with ELECNRTL	Packing height	1.25 m** / 11.75 m
		Packing diameter	0.35 m
		Packing type	IMTP / 1IN or 25MM
		Top pressure	2.0 atm
		Flow model	Mixed
		Mass transfer coefficient method	Onda et al.(1968)
		Interfacial area coefficient method	Onda et al.(1968)
		Interfacial area factor	1.4*
		Heat transfer coefficient method	Chilton and Colburn
		Heat transfer factor	1.0
		Hold up method	Stichlmair
		Film resistance	Discrxn for liquid film
		Top temperature	Film for vapor film
			40 °C
Heat Exchanger	Heat Exchanger	Minimum temperature approach	10 °C
		Calculation mode	Design mode
Cooler	Heater	Cooling target temperature	40 °C

*Interfacial area factors are determined for fitting the plant data **1.25 m for water washing section

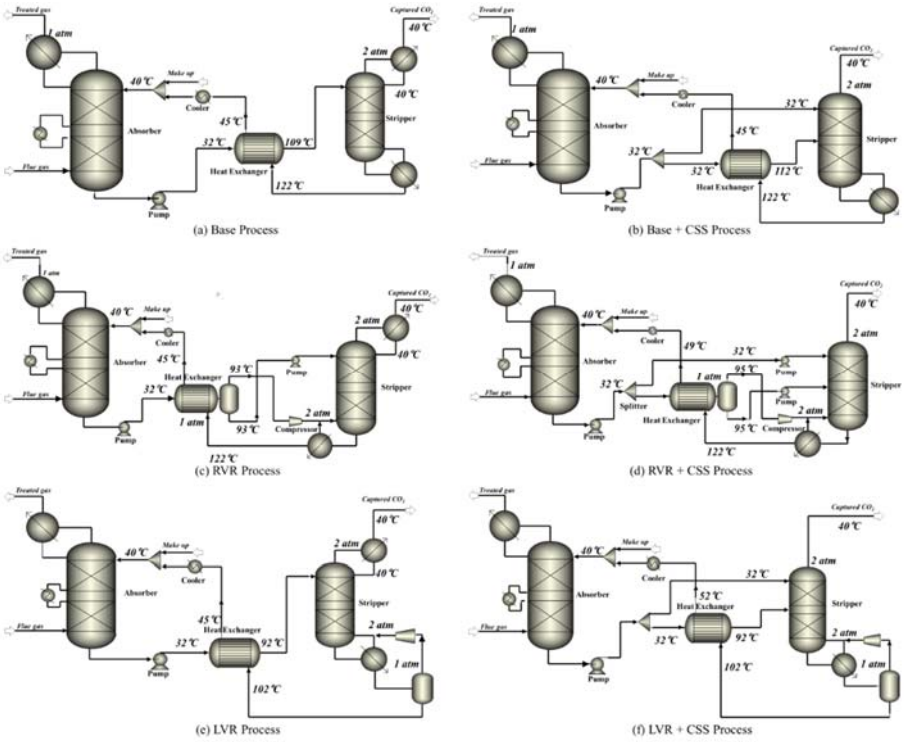

Fig. 4-3. Configuration of (a) Base process, (b) Base process with CSS, (c) RVR process, (d) RVR process with CSS, (e) LVR process, and (f) LVR process with CSS

Table 4-4. Main unit specifications for alternative processes

Process	Lean/Rich loading	Splitter	Heat Exchanger	Compressor** (Vapor Recompression)
Base (AI)*	0.27	-	Hot side temp.: 122 °C / 45 °C	-
Process	0.55		Cold side temp.: 33 °C / 109 °C	
Base + CSS	0.27	To Top: 0.21	Hot side temp.: 122 °C / 58 °C	
Process	0.55	To HX: 0.79	Cold side temp.: 33 °C / 112 °C	
RVR	0.27	-	Hot side temp.: 122 °C / 45 °C	Press.: 1.0 atm to 2.0 atm
Process	0.55		Cold side temp.: 33 °C / 93 °C	Temp. 93°C to 176°C
RVR + CSS	0.27	To Top: 0.17	Hot side temp.: 122 °C / 49 °C	Press.: 1.0 atm to 2.0 atm
Process	0.55	To HX: 0.83	Cold side temp.: 33 °C / 95 °C	Temp. 95°C to 180°C
LVR	0.27	-	Hot side temp.: 102 °C / 45 °C	Press.: 1.0 atm to 2.0 atm
Process	0.55		Cold side temp.: 33 °C / 92 °C	Temp. 102°C to 196°C
LVR + CSS	0.27	To Top: 0.13	Hot side temp.: 102 °C / 52 °C	Press.: 1.0 atm to 2.0 atm
Process	0.55	To HX: 0.87	Cold side temp.: 33 °C / 92 °C	Temp. 102°C to 196°C

*Absorber Intercooling **Compressor Efficiency = 0.75

4.4 Simulation results and discussions

4.4.1 Model validation

The base model, i.e., conventional process with absorber intercooling, is validated with the 0.1 MW pilot plant operating data, as indicated in Fig. 4-4. The validation data was generated by varying solvent flow rate (+10%, -10%), reboiler energy (-10%, -20%) and heat exchanger target temperature (from 99 °C to 67 °C) as indicated in Table 4-5. The model was calibrated to match experimental data by adjusting the interfacial area factor which is available to fit against plant data. The absorber interfacial area factor was determined by 2.0 for fitting CO_2 recovery percentage, which is slightly higher than that of previous study (1.8) based on no absorber intercooling system [45]. The stripper interfacial area factor is 1.4 for fitting stripper temperature profile as indicated in Fig. 4-4. The stripper temperature profile is compared with the simulation results and the operating data. In particular, the top stripper temperature (TE27) and the feed stage (TE26) are the most important variables for estimating the condenser cooling duty. In this model, the stripper top temperature (TE27) error is 2°C and 6 °C for average and maximum, respectively.

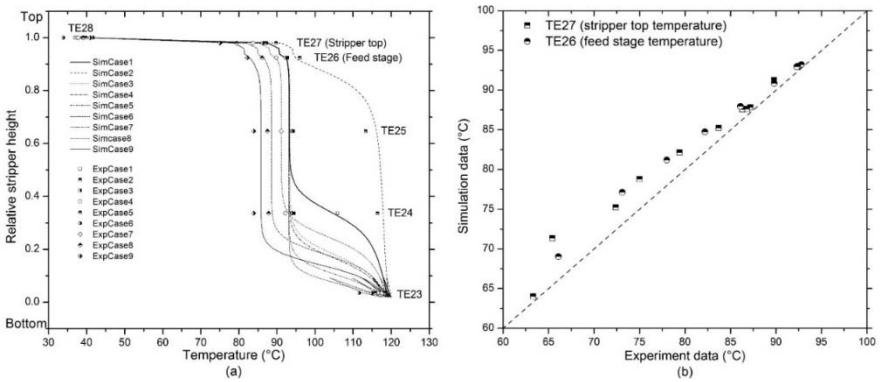

Fig. 4-4. Experimental data and simulation results of (a) the stripper overall temperature profile, and (b) the stripper top temperature

Table 4-5. The operating conditions of validation data set and result of model fitting

Case	Operating condition			Fitting result		
	Solvent flow rate [%]	Reboiler energy [%]	HX preheating target temp. [°C]	Stripper temp. average error (Top temp. error) [°C]	CO_2 Recovery plant data [%]	CO_2 Recovery Simulation [%]
Base case (Case 1)	100	100	99	± 1.6 (0.8)	88.3 ± 0.6	88.4
Case 2	90	100	99	± 1.4 (1.4)	80.5	80.8
Case 3	110	100	99	± 1.2 (0.6)	98.2	99.8
Case 4	100	90	99	± 1.3 (0.9)	76.8 ± 1.2	78.1
Case 5	100	80	99	± 1.0 (0.7)	66.7 ± 1.7	68.0
Case 6	100	70	99	± 2.1 (1.2)	54.7 ± 0.8	58.2
Case 7	100	100	95	± 1.2 (1.5)	-	-
Case 8	100	100	90	± 1.5 (2.7)	-	-
Case 9	100	100	85	± 1.9 (3.7)	-	-
Case 10	100	100	80	± 2.5 (2.8)	-	-
Case 11	100	100	75	± 2.8 (5.9)	-	-
Case 12	100	100	67	± 3.0 (0.7)	-	-

4.4.2 Effect of the cold solvent split

The main effect of the CSS is to cool the stripper top. To assess the stripper cooling by CSS, Fig. 4-5 shows the stripper temperature profile change when the CSS is combined with the Base process, the RVR process, and the LVR process. In all three processes, the stripper top is cooled up to the condenser target temperature, 40 °C. Because the stripper top is cooled to the condenser cooling target temperature, the amount of water vaporization is dramatically decreased at the stripper top. As a result, the reflux ratio and condenser cooling duty are reduced to almost zero in the combined CSS processes, as indicated in Table 4-6. This condenser cooling duty reduction causes the reboiler heat requirement reduction, according to Eq. (2-18). The CSS processes saved the condenser cooling duty: 0.85, 0.61, and 0.43 $MJ_{th}/kgCO_2$ for the Base process, RVR process, and LVR process, respectively. The stripper temperature profile change directly affects the stripper internal condition. The Fig. 4-6 indicates the CO_2 partial pressure profile and CO_2 loading profile against stripper height. The CO_2 partial pressure and loading profile show similar shape with the temperature profile. In the RVR with CSS process, the CO_2 loading value slightly increases at stripper top rather than it decreases. It is because the CO_2 partial pressure at stripper top (150 to 195 kPa) is much higher than that of the absorber bottom (14 to 15 kPa). Furthermore, the striper top maintains relatively low temperature (40 °C to

70 °C) compared with the Base process due to cold solvent split. It means the solvent absorbs additional CO_2 at stripper top, which corresponds with the experimental data. The equilibrium CO_2 loading value is reported by 0.60 under the 60 °C and 150kPa for CO_2 partial pressure [17].

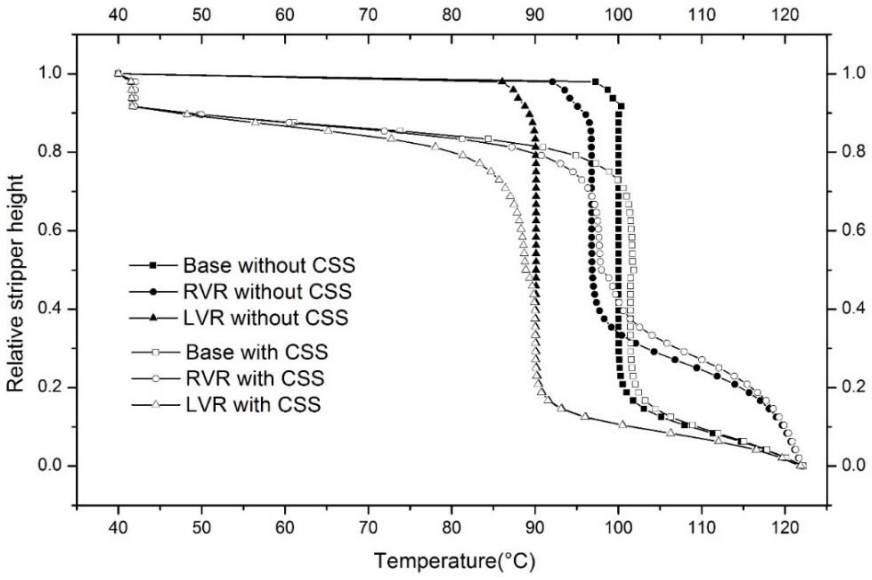

Fig. 4-5. The stripper temperature profile for the Base process and alternative processes

Table 4-6. Stripper simulation results for the Base process and alternative processes

Process	Split ratio To the top* *	Stripper top temp. [°C]	Condenser target temp. [°C]	Stripper reflux ratio	Condenser cooling duty [$MJ_{th}/kgCO_2$]	Condenser cooling duty save [$MJ_{th}/kgCO_2$]
Base (AI)*	0.00	97.3	40.0	0.75	0.85	-
Base + CSS	0.21	41.6	40.0	0.00	0.00	0.85
RVR	0.00	92.1	40.0	0.53	0.61	-
RVR + CSS	0.17	42.1	40.0	0.00	0.00	0.61
LVR	0.00	88.1	40.0	0.36	0.43	-
LVR + CSS	0.13	41.5	40.0	0.00	0.00	0.43

*Absorber Intercooling **Split ratio for satisfying that the stripper top temperature is below 42°C

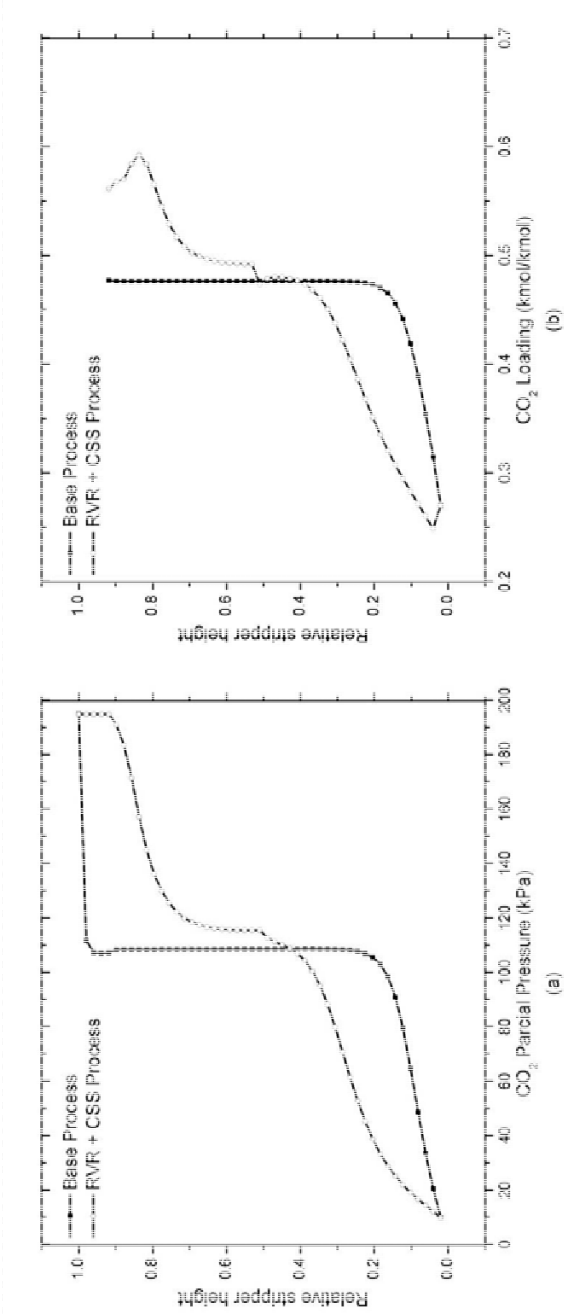

Fig. 4-6. (a) The CO_2 partial pressure profile and (b) CO_2 loading profile against the stripper height

4.4.3 Effect of rich vapor recompression

The CSS successfully eliminates the condenser cooling duty, as mentioned in the previous section. However, it also causes an unfortunate reduction in the heat exchanger preheating duty, because the thermal capacity of cold stream (mass x specific heat capacity, [kJ/°C]) is reduced. As indicated in Table 4-7, the heat exchanger preheating duty losses were 0.74, 0.24, and 0.43 $MJ_{th}/kgCO_2$ for the Base process, RVR process, and LVR process, respectively. This preheating loss causes an increase in the reboiler heat requirement, according to Eq. (1). To alleviate this preheating loss, the RVR process compensates the thermal capacity reduction by vaporizing the cold side stream. In other words, the main effect of the RVR is to increase the thermal capacity of cold stream using the latent heat of the cold stream. To clarify the changes in the thermal capacity of cold stream, Fig. 4-7 shows the heat exchanger composite curve for the six processes. In the RVR process, the thermal capacity of cold stream is increased as the cold side is vaporized (above 80°C). As indicated in Table 4-7, the cold out vapor fraction in the RVR process increases from 0.03 to 0.05. For this reason, the RVR process combined with CSS loses only 5% of the heat exchanger preheating duty, although 17% of the cold side is split; whereas, the thermal capacity of cold stream is almost constant against temperature in the Base process and the LVR process. The Base process combined with CSS loses about 16% of the

heat exchanger preheating duty, because 21% of the cold stream is split. In the case of the LVR process, adding CSS causes 13% of the heat exchanger preheating duty to be lost, as 13% of the cold solvent is split.

Table 4-7. Heat exchanger simulation results for the Base process and alternative processes

Process	Split ratio to HX	Cold side flow rate [kg/h]	Cold out temp. [°C]	Operating pressure [atm]	Cold out vapor fraction	Heat exchanger preheating duty [$MJ_{th}/kgCO_2$]	Preheating duty loss [$MJ_{th}/kgCO_2$]
Base (AI)*	1.00	1450	109	5.30	0.00	4.62	-
Base + CSS	0.79	1180	112	5.30	0.00	3.88	0.74
RVR	1.00	1450	93	1.00	0.03	4.61	-
RVR + CSS	0.83	1210	95	1.00	0.05	4.38	0.24
LVR	1.00	1460	92	5.30	0.00	3.41	-
LVR + CSS	0.87	1270	92	5.30	0.00	2.97	0.43

*Absorber intercooling

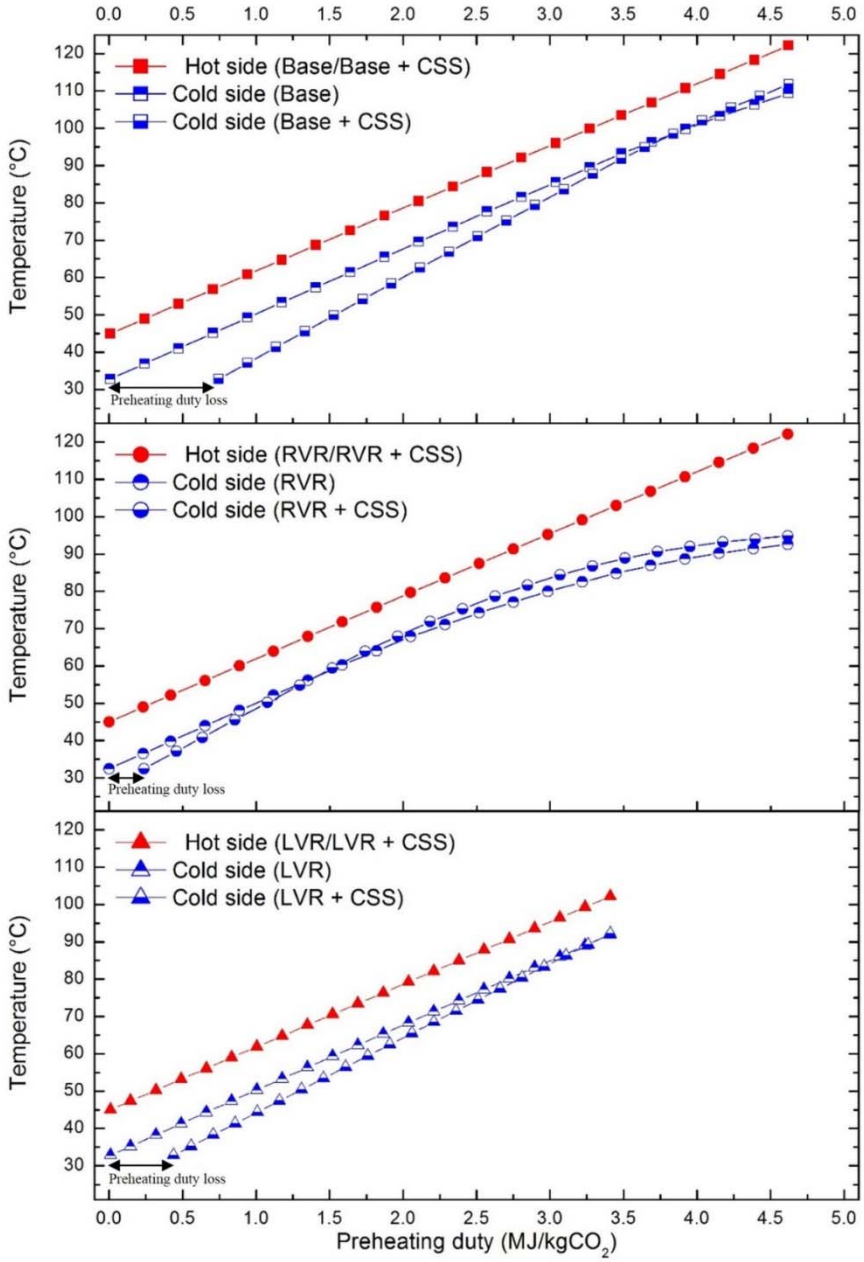

Fig. 4-7. Composite curves of the heat exchange for the Base process and alternative processes

4.4.4 Net equivalent energy reduction effect

Table 4-8 shows the net thermal reduction effect for the three processes with the CSS. When the Base process was combined with the CSS, it saved 0.85 $MJ_{th}/kgCO_2$ of the cooling duty, while it lost 0.74 $MJ_{th}/kgCO_2$ of the preheating duty. The net thermal energy reduction effect was 0.11 $MJ_{th}/kgCO_2$. The RVR showed a 0.38 $MJ_e/kgCO_2$ net reduction, while the LVR showed no reduction effect. Consequently, the RVR process with CSS showed the lowest reboiler duty, 2.75 $MJ_{th}/kgCO_2$, among the six processes. This is 20.0% lower than the reboiler energy requirement of the Base process. The result, 2.75 $MJ_{th}/kgCO_2$, is slightly lower than that in previous work (2.84 $MJ_{th}/kgCO_2$) [46] because the absorber intercooling is combined in this work. The total energy requirement for CO_2 capture and compression is the sum of the reboiler thermal energy and the compression electric energy. In the case of the RVR with the LVR process, the vapor recompression work is added to the total energy requirement. The total energy requirement is calculated by converting the thermal energy to equivalent electric energy as indicated in Eq. (4-1). The conversion factor, η, is calculated by Eq. (4-2) which is a function of steam source temperature, sink temperature and turbine efficiency. When the LP steam is supplied to reboiler for solvent regeneration, we assume that the source temperature is 438K and the sink temperature is 300K [21]. When the turbine efficiency, $\eta_{turbine}$, is 0.75, the conversion factor is 0.236 according to

Eq. (4-2). This value is almost same with the 'turbine power loss to reboiler duty ratio', α (0.23), from the study by Sanchez [33].

$$E_{total} = \eta \times Q_{Reb} + E_{Comp} \quad (4\text{-}1)$$

$$\eta = \eta_{turbine} \times \frac{T_{source}(K) - T_{sink}(K)}{T_{source}(K)} \quad (4\text{-}2)$$

Table 4-8 shows the total equivalent work (E_{total}) for the six processes from this work and reported process from other studies [33, 47]. The additional work indicates the sum of the Amine/water pumps, flue gas blower work, and vacuum pump work as described by Ahn et al. [47]. The compression process consists of four stage compressor (456 kPa/ 1,160 kPa/ 2,950 kPa/ 7,500 kPa) and one stage pump (15,270 kPa). In this work, the CO_2 compression work is recalculated by using 0.75 of compressor efficiency based on reported data [47]. As a result, the RVR with the CSS process requires 1.150 $MJ_e/kgCO_2$, which is 6.0% and 1.7-3.4% lower than that of the Base process and LVR process, respectively. This equivalent energy reduction effect is slightly higher than that of the LVR process reported by Sanchez et al. [33] and Ahn et al. [47] although this work use the lowest compressor efficiency.

Table 4-8. Total equivalent energy reductions effect for each process

Process	Equivalent reboiler duty* [$MJ_e/kgCO_2$]	Vapor compression work** [$MJ_e/kgCO_2$]	CO_2 Compression Work** (Ahn et al.) [$MJ_e/kgCO_2$]	Additional Work** (Ahn et al.) [$MJ_e/kgCO_2$]	Total energy consumption [$MJ_e/kgCO_2$]	Total equivalent energy reduction effect [%]
Base (AI)	0.813	-	0.342	0.068	1.224	-
Base + CSS	0.787	-	0.342	0.068	1.200	2.1
RVR	0.744	0.070	0.342	0.068	1.225	0.0
RVR + CSS	0.652	0.087	0.342	0.068	1.150	6.0
LVR (Optimal condition)	0.689 (0.680)	0.092 (0.080)	0.342 (0.342)	0.068 (0.068)	1.191 (1.170)	2.6 (4.3)
LVR + CSS	0.692	0.092	0.342	0.068	1.194	2.4
Base (No AI) (Sanchez et al.[33])	0.819	-	0.333	0.066	1.219	-
LVR (Sanchez et al.[33])	0.672	0.083	0.333	0.066	1.154	5.3
Base (AI) (Ahn et al. [47])	0.933	-	0.270	0.054	1.257	-
AI + LVR + CEE (Ahn et al. [47])	0.666	0.147	0.318	0.054	1.186	5.7

*Conversion factor: 0.236 (this work), 0.23 (Sanchez et al.), 0.30 (Ahn et al.). **Compressor and pump efficiency: 0.75 (this work), 0.77 (Sanchez et al.), 0.95 (Ahn et al.).

4.4.5 Net annual cost saving effect

As the LVR process, the RVR with CCS process requires additional compressor and flash vessel while the stripper condenser can be removed. To assure the economic feasibility of the alternative process, the table 4-9 indicates the equipment purchase cost which is calculated by based on CO_2 capture plant for 250MW_e power plant data [33]. The RVR with CSS process requires additional 1.64 M€ for purchasing compressor and flash vessel while the LVR process requires additional 1.07 M€. According to the Eq. (4-3), the annual depreciation change can be simply calculated by 4 for installation factor, 20 years for heat exchanger life time, 25 years for flash vessel life time and 10 years for compressor life time [33]. As a result, the RVR with CSS process requires additional 0.64 M€/yr while the LVR requires 0.50 M€/yr for annual deprecation.

$$Annual\ depreciation\ change = installation\ factor * \sum \frac{\Delta Purchance\ cost\ change}{Equipment\ lifetime} \qquad (4\text{-}3)$$

When we assume the 50 €/MWh for electricity cost and 7450 hour for annual operation time, the RVR with CSS saves 1.51 M€/yr while the LNR process saves 1.08 M€/yr. Consequently, the RVR process saves totally 0.87 M€/yr which is higher than that of the LVR process as indicated in Table 4-10. Although the literature work shows that the LVR process saves slightly high amount of total annual cost, the result clearly shows that the RVR with CSS process can be considered as one of the MEA process alternatives.

Table 4-1. Overview of main equipment purchase cost based on 250MW_e capture plant

Process	Reboiler [M€]	Flash vessel [M€]	Compressor [M€]	Heat exchanger [M€]	Condenser [M€]
Base (AI)	1.43	-	-	1.43	0.24
RVR + CSS	1.15	0.56	1.68	1.35	-
LVR (optimal condition)	1.20	0.52	1.54	0.79	0.12
Base (No AI) (Sanchez et al. [33])	1.30	-	-	1.11	0.31
LVR (1bar) (Sanchez et al. [33])	1.07	0.47	1.4	0.44	0.18

Table 4-2. Annual total cost saving based on 250MW_e capture plant

Process	Total equipment purchase cost change [M€]	Annual depreciation change* [M€/yr]	Annual energy cost saving** [M€//yr]	Annual total cost saving [M€/yr]
RVR + CSS	1.64	0.64	1.51	0.87
LVR (optimal condition)	1.07	0.50	1.08	0.58
LVR (Sanchez et al. [33])	0.20-0.86	0.15-0.44	1.19-1.24	0.80-1.04

*Installation factor = 4, Heat exchanger life time = 20 years, Flash vessel life time = 25 years, compressor life time = 10years **Electricity = 50 €/MWh

Chapter 5: Superstructure Modeling of the Modified MEA Scrubbing Process

5.1 Overview

As previously mentioned, a significant amount of equivalent energy can be reduced by combining configurations displaying positive interactions. However, combining the modified configurations is complicated, as the various process variables interact with one another. As the number of modified configuration rises, the complexity of the additional process variables and interactions increase. This will affect not only operating cost, but also capital cost. Although a parametric study or qualitative analysis can provide insight into the combination of these configurations, determination of the optimal combination of the modified MEA scrubbing processes is difficult. Thus, a flowsheet optimization of the superstructure model is one possible solution for determined optimal configuration to reduce the CO_2 capture cost.

The superstructure model is built to consider the various combinations of the modified configuration. The superstructure model contains the absorber intercooling, semi-lean/semi-rich loop, cold solvent split, lean vapor compression, rich vapor compression, economizer, heat integration with compression process, and various split flow configurations. This

superstructure model can propose an optimal combination of the modified configurations by quantitative calculations rather than qualitative analysis. As this superstructure involves the cost model, it can consider the OPEX and CAPEX terms simultaneously.

5.2 Target process

The target process is a post-combustion capture process from the Castor EU project [1]. The capture unit treats 90% of CO_2 emitted by a 630 MWe coal power plant. The captured CO_2 is compressed to 110 bar by a three-stage compression process, with a solvent regeneration energy of 3.7 GJ_{th}/ton CO_2 and a compression energy of 0.35 GJ_e/ton CO_2. The steam and electricity are obtained directly from the power plant. The heights of the absorber and stripper are 36 m and 30 m, respectively. In addition, the rich loading and lean loading are 0.48 and 0.24, respectively. Detailed process information and equipment specifications can be found in Fig. 5-1 and Table 5-1.

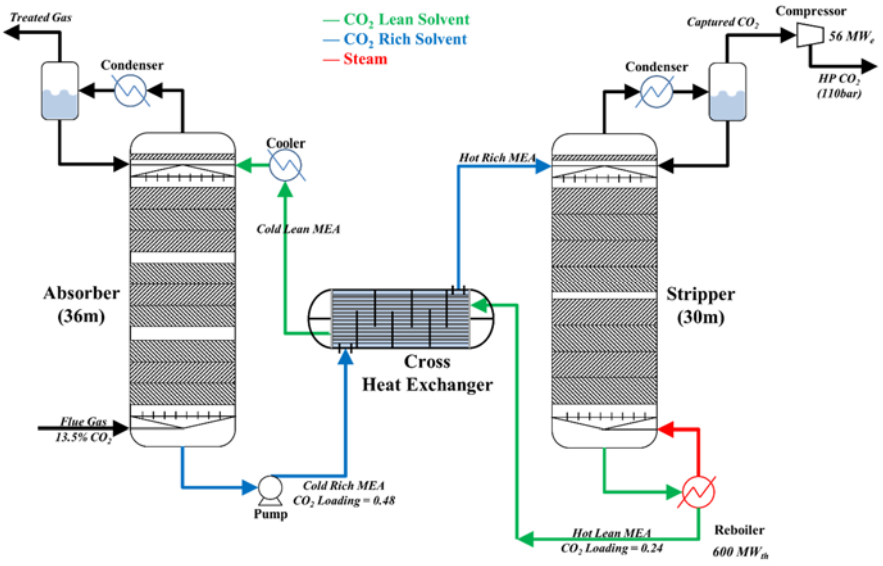

Fig. 5-1. Conventional MEA process from the Castor EU project

Table 5-1. Process specification of the target process from the Castor EU project [1]

Process variable	Specification
Power Plant Capacity	630 MWe
Flue gas Flow rate	104,840 kmol/h
Flue gas Temperature	45ºC
Flue gas Pressure	1 bar
Flue gas Composition	CO_2 13.5 vol%
CO_2 Capture	90 %
CO_2 Compression	110 bar
Solvent flow rate	30 wt% MEA
Lean / Rich loading	0.24 / 0.48
Solvent flow rate	10,800 m^3/h
Reboiler Energy	600 MW_{th} (3.7 GJ/tCO_2)
Compression Energy	56 MW_e (0.35 GJ/tCO_2)
Absorber	D = 9m / H = 36m (4 Columns)
Stripper	D = 9m / H = 30m (2 Columns)

5.3 Modeling procedure

To handle the various combinations of the modified configurations, the superstructure model was established on a gCCS simulation package, which is an equation-oriented environment. This equation-oriented simulation is suitable for complex recycling structures and multi-variable optimizations. In addition, the gCCS package is a gPROMS product, which is specialized for modeling the whole CCS chain (power section, capture section, compression and liquefaction section, and storage section).

5.3.1 Physical property model

The gCCS package provides a number of physical property models for each unit. The gSAFT, which is based on the SAFT (Statistical Associating Fluid Theory) equation of state, is given for a solvent-based CO_2 capture system. The SAFT is well known as an advanced molecular thermodynamics method that can accurately predict a wide range of thermodynamic properties of mixtures[48, 49]. Furthermore, the Peng Robinson equation is used for calculating the lean vapor compressor and rich vapor compressor sections as a cubic equation of states, while the RSK equation of state is utilized for modeling the CO_2 compression section as indicated in Table 5-2.

Table 5-2. Physical property model for capture unit, vapor compressor unit and CO_2 compression unit

Process	Physical Property package
CO_2 Capture unit	gSAFT (SAFT implemented by PSE*)
Lean vapor compressor Rich vapor compressor	Peng Robinson equation of state
CO_2 Compression unit	Soave Redlich-Kwong equation of state

*Process Systems Enterprise Limited

5.3.2 Superstructure model

The absorber and stripper are non-equilibrium models considering mass and heat transport between the bulk gas and liquid phases. The phase equilibrium is considered to be at the interface while the mass and heat transfer through the films can be modelled using Fick's law. In the superstructure, the absorber and stripper are divided into multiple sections to consider the various split flow configurations. The absorber is separated into the absorber top and absorber bottom, while the stripper is separated into the washing section, stripper top, and stripper bottom. The actual internal packing height is specified as 2/3 of the total column height. In addition, the superstructure model considers the partial vaporization of the solvent in the cross heat exchanger, while the conventional process considers it as a liquid-liquid heat

exchanger. The partial vaporizer unit was newly developed by the author, as the gCCS library provides only liquid-liquid heat exchanger information.

Furthermore, the superstructure model of the modified MEA process involves an additional absorber intercooler, second and third cross heat exchangers, a lean vapor compressor, a rich vapor compressor, and flow splitters, as depicted in Fig. 5-2. All additional equipment contains a bypass line with flow splitter. The splitter decides whether the final configuration involves the equipment or not. When the optimal configuration involves the use of the additional equipment, the splitter increases the split fraction to the additional equipment. When the additional equipment is not to be utilized, the splitter increases the split fraction to the bypass line. The operating conditions and sizing details of the main equipment are summarized in Table 5-3.

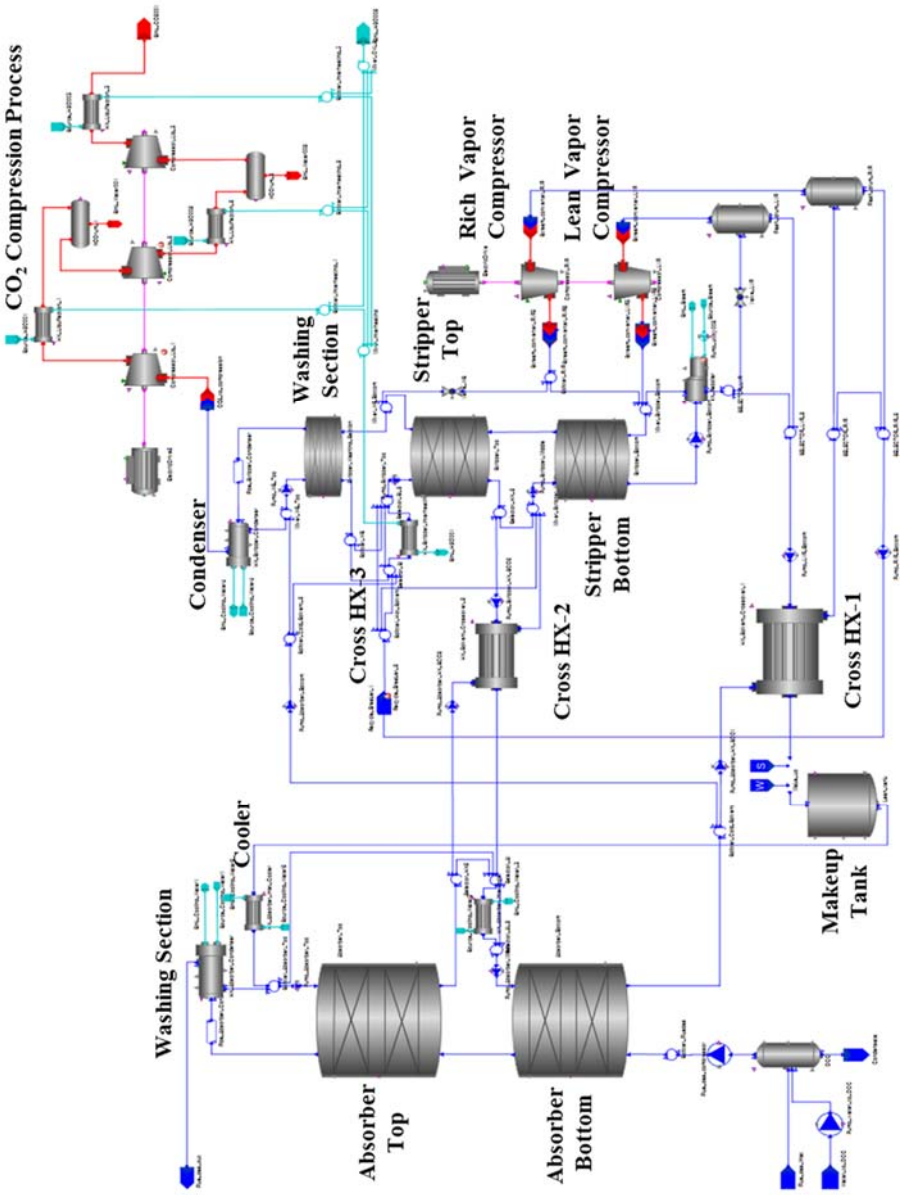

Fig. 5-2. Process configuration for the superstructure of the modified MEA processes on gCCS environment

Table 5-3. Main unit specifications for conventional model and modified model

Equipment	Conventional Model	Modified Model
Absorber Top (Absorber_chemical)	Height = 24 m Diameter = 18 m Internal = IMTP 50 / Steal	Height = 12 m Diameter = 18 m Internal = IMTP 50 / Steal
Absorber Bottom (Absorber_chemical)		Height = 12 m Diameter = 18 m Internal = IMTP 50 / Steal
Absorber Washing Cooler	Cooling T= 313.15 K	Cooling T = 313.15 K
Absorber Intercooler	-	Cooling T = 308.15 K
Washing Section (Stripper_chemical)	Height = 20 m Diameter = 12.7m Internal = IMTP 50 / Steal	Height = 2m Diameter = 12.7 m Internal = IMTP 50 / Steal
Stripper Top (Stripper_chemical)		Height = 9m Diameter = 12.7 m Internal = IMTP 50 / Steal
Stripper Bottom (Stripper_chemical)		Height = 9m Diameter = 12.7 m Internal = IMTP 50 / Steal
Stripper condenser	Cooling T= 313.15K	Cooling T= 313.15K
Cross heat exchanger-1 (Partial vaporizer)	HTC = 600 W/(m^2K) Hot out approach = 20K Pressure drop = 0.1bar	HTC = 600 W/(m^2K) Hot out approach = 24K Pressure drop = 0.1bar
Cross heat exchanger-2 (Liquid-Liquid HX)	-	HTC = 600 W/(m^2K) Hot out approach = 15K Pressure drop = 0.1bar
Cross heat exchanger-3 (Liquid-Liquid HX)	-	HTC = 600 W/(m^2K) Hot out approach = 10K Pressure drop = 0.1bar
CO_2 Compression Heat Exchanger-1	Outlet CO2 T = 313.15 K Pressure drop = 0.2 bar	HTA = 12000m^2 Pressure drop = 0.2 bar
CO_2 Compression Heat Exchanger-2	Outlet CO2 T = 313.15 K Pressure drop = 0.2 bar	HTA = 12000m^2 Pressure drop = 0.2 bar
CO_2 Compression Heat Exchanger-3	Outlet CO2 T = 313.15 K Pressure drop = 0.2 bar	HTA = 12000m^2 Pressure drop = 0.2 bar
CO_2 Compressor-1	Inlet P = 1.6 bar Outlet P = 6.8 bar	Inlet P = 1.7 bar Outlet P = 6.9 bar
CO_2 Compressor-2	Inlet P = 6.4 bar Outlet P = 26.7 bar	Inlet P = 6.5 bar Outlet P = 27.0 bar
CO_2 Compressor-3	Inlet P = 26.3 bar Outlet P = 110.0 bar	Inlet P = 26.6 bar Outlet P = 110.0 bar
Lean Vapor Compressor	-	Inlet P = 1.70 bar Outlet P = 1.79 bar
Rich Vapor Compressor	-	Inlet P = 1.40 bar Outlet P = 1.79 bar

5.3.3Cost model

The CAPEX and OPEX terms of the CASTOR project have been previously reported[1]. According to the literature, the cost data is calculated by IFPEN in-house software, which determines investment budgets with a ±30% precision. The main economic evaluation parameters are listed in Table 5-4 and the cost distribution is given in Table 5-5. The CAPEX term includes the cost of the main equipment (absorber, stripper, compressor, blower, reboiler, heat exchanger, vessel, pump, and solvent), while the OPEX term includes the cost of steam, electricity, and solvent makeup. To predict the change in the CAPEX term with variation in equipment size, the six-tenth rule is considered as shown in Eq. (5-1). This relationship has been found to give reasonable results for both individual equipment and entire plants [50]. When the equipment size is doubled, the cost increases by approximately 50%. The exponent, m, may vary from 0.48 to 0.87 for each piece of equipment. By combining literature CAPEX data and equipment size data from the conventional process model, the CF_E for the equipment is calculated as indicated in Eq. (5-3). Table 5-6 summarizes the key size variables and exponent values, along with cost factors for each piece of equipment. The new CAPEX, referred to as $CAPEX_{New}$, can be calculated by using the new equipment size, $Size_{new}$, and Cost Factor, CF_E according to Eq. (5-2). The CAPEX for the flue gas blower and solvent is assumed to be constant, as summarized in Table 5-6. In

contrast, the OPEX is calculated by the linear function of the utility usage as shown in Eq. (5-4). The reboiler heat duty represents the low pressure steam usage and the compressor duty represents the electricity usage. The amount of solvent makeup is assumed as a linear function of the cycling solvent flowrate. By combining OPEX data from the literature and utility usage data from the conventional process model, the cost factor, CF_U, can be calculated simply according to Eq. (5-5). The OPEX for the blower and pump is assumed to be constant, as summarized in Table 5-7. The total cost can be defined as the sum of the OPEX and CAPEX terms, as indicated in Eq. (5-6):

$$\frac{CAPEX_E[€/tonCO_2]}{CAPEX_{E\_Ref}[€/tonCO_2]} = \left(\frac{Size_E}{Size_{E\_Ref}}\right)^{m_E} \quad (5\text{-}1)$$

$$CAPEX_E\left[\frac{€}{tonCO_2}\right] = \frac{CF_E \times (Size_E)^{m_E}}{CO_2\ Capture[ton/yr]} \quad (5\text{-}2)$$

$$CF_E[€/yr] = \frac{CAPEX_{E\_Ref}[€/yr]}{(Size_{E\_Ref})^{\mathrm{m}}} \quad (5\text{-}3)$$

$$\frac{OPEX_U[€/tonCO_2]}{OPEX_{U\_Ref}[€/tonCO_2]} = \frac{Capacity_U}{Capacity_{U\_Ref}} \quad (5\text{-}4)$$

$$OPEX_U[€/tonCO_2] = CF_U[€/Unit] \times Capacity_U[Unit/tonCO_2] \quad (5\text{-}5)$$

$$Total\ Cost[€/tonCO_2] = \sum_E CAPEX_E + \sum_U OPEX_U \quad (5\text{-}6)$$

$$E = \{AB, ST, CM, RB, HX, VS, PM, BL, SV\},\ U = \{LS, EL, SV, PM, BL\}$$

Table 5-4. Economic evaluation parameters used in the cost model [1]

Economic evaluation parameters	Value
Reference year	2010
Capital allowances	25 yr
Depreciation	10 yr
Discount rate	10 %
Cost of debt	7 %
OSBL (storage, utilities, buildings, contingencies, etc.)	Percentage of ISBL
Times of construction	36 month
Project life years	25 yr
Tax rate	30 %
Coal price	87 (€/t) 3.4 (€/GJ)
CO_2 capture rate	156 (kg/sec) 4,428,000 (ton/yr)

Table 5-5. Cost distribution of the CAPEX and OPEX for the target process [1]

Items	Symbol	CAPEX €/ton CO_2	OPEX €/ton CO_2	Total Cost €/ton CO_2
Absorber	AB	9.1	-	9.1
Stripper	ST	2.4	-	2.4
CO_2 compressor	CM	5.0	7.3	12.3
Reboiler	RB	2.8	14.8	17.6
Heat Exchanger	HX	2.7	-	2.7
Vessel	VS	0.3	-	0.3
Pump	PM	1.2	0.9	2.1
Flue gas blower	BL	0.3	1.8	2.1
Solvent	SV	0.8	7.3	8.1
Sub Total (€/tonCO_2)		24.6	32.1	56.7
Sub Total (%)		43.3	56.7	100

Table 5-6. Cost index for the CAPEX items

Equipment	Symbol	Size Variable $Size_E$	Unit of Capacity	Cost Factor CF_E	Cost exponents m_E
Absorber	AB	Volume	[m^3]	215,000 [€/yr]	0.60
Stripper	ST	Volume	[m^3]	96,200 [€/yr]	0.60
Compressor	CM	Power	[W]	99.5 [€/yr]	0.67
Reboiler	RB	Heat duty	[W]	45.9 [€/yr]	0.62
Heat Exchanger	HX	Area	[m^2]	3,970 [€/yr]	0.62
Vessel	VS	Volume	[m^3]	61.4 [€/yr]	0.68
Pump	PM	Flowrate	[kg/s]	4,690 [€/yr]	0.70
Blower	BL	Assuming as constant value, 0.3 €/ton CO_2			
Solvent	SV	Assuming as constant value, 0.8 €/ton CO_2			

Table 5-7. Cost index for the OPEX items

Utility	Symbol	Capacity Variable	Unit of Capacity	Cost Factor CF_U
LP Steam	LS	Heat duty	[GJ/tonCO_2]	0.0040 [€/MJ]
Electricity	EL	Electricity	[GJ/tonCO_2]	0.0204 [€/MJ]
Solvent	SV	Mass	[ton/tonCO_2]	0.3788 [€/ton]
Pump	PM	Assuming as constant value, 0.9 €/ton CO_2		
Blower	BL	Assuming as constant value, 1.8 €/ton CO_2		

5.4 Parametric study

As previously discussed, the main design variables of the conventional MEA process are stripper operating pressure, cycling solvent flowrate, cross heat exchanger area (or temperature approach), absorber height, and stripper height. Table 5-8 shows the results of the quantitative cost effect in the conventional MEA process using the cost model. The stripper operating pressure appears to be the most effective variable for the total cost, while the cross heat exchanger temperature approach is the least effective variable. For each variable, the main items influencing costs are shown in Figs. 5-3 to 5-9.

Table 5-8. Cost effect of main control variables in conventional MEA process

Control Variable	Base	Lower Bound	Upper Bound	Unit	Cost Effect (%)
Stripper Pressure	1.79	1.00	2.00	bar	±6%
Cycling Solvent Flowrate	3000	2400	3600	kg/s	±5%
Cross HX Hot Temp. Approach	20	5	20	K	±1%
Absorber Height	24	12	30	m	±2%
Stripper Height	20	10	25	m	±2%
CO2 Recovery	90	85	98	%	±5% (OPEX only)
CO2 Mass Fraction	0.20	0.16	0.20	-	±5% (OPEX only)

As the stripper pressure increases, the reboiler heat requirement and compressor electricity requirement decrease, and at high pressures the latent heat requirement and compressing energy are reduced. As a result, the reboiler and compressor in the CAPEX and the LP steam and electricity in the OPEX. The total cost is therefore decreased with an increase in stripper pressure, and the upper bound of the stripper pressure is determined by the upper temperature limit to avoid solvent thermal degradation.

In addition, as the solvent flowrate increases, the latent heat requirement is reduced while the sensible heat requirement increases. As a result, the LP steam in the OPEX is optimal at base flowrate. The vessel and pump in the CAPEX and solvent makeup in the OPEX increase with a rise in solvent flowrate, and thus the total cost increases with a higher solvent flowrate.

As the temperature approach in the cross heat exchanger decreases, the sensible heat requirement is reduced. The reboiler in the CAPEX and the LP steam in the OPEX are reduced while the heat exchanger in the CAPEX is dramatically increased. In this case, the total cost remains relatively constant, with no significant difference observed.

Furthermore, as the absorber height decreases, the lean loading value decreases at the strip bottom. As the lean loading decreases, the latent heat requirement increases. Although the reboiler in the CAPEX and the LP steam

in the OPEX are increased, the absorber cost is significantly reduced, and so the total cost decreases slightly with a decrease in absorber height.

Finally, with a decrease in stripper height, the latent heat requirement is increased. Although the stripper cost is significantly reduced, the reboiler in the CAPEX and the LP steam in the OPEX increase, resulting in a slight increase in total cost with a decrease in stripper height.

Figs 5-8 and 5-9 show the steam and electricity costs per ton of CO_2 capture when the CO_2 target recovery and flue gas CO_2 fraction are varied. As the total amount of CO_2 capture changes according to the CO_2 recovery or CO_2 fraction, only the OPEX term was considered for comparison.

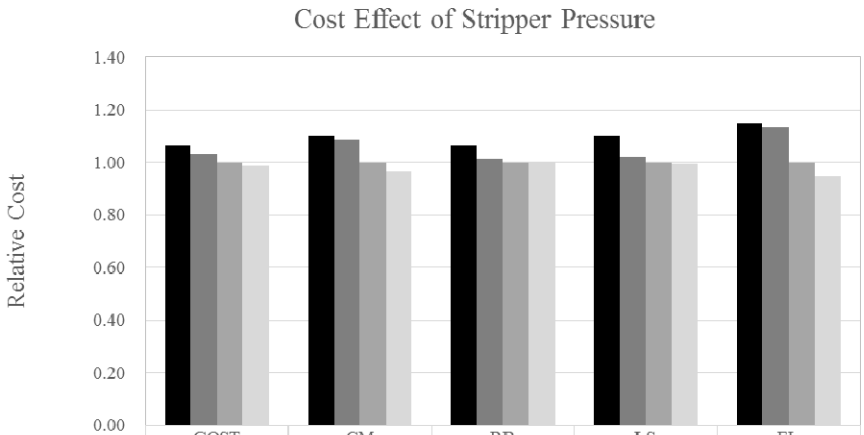

	COST	CM	RB	LS	EL
1.00 bar	1.06	1.10	1.06	1.10	1.15
1.40 bar	1.03	1.09	1.01	1.02	1.13
1.79 bar (base)	1.00	1.00	1.00	1.00	1.00
2.00 bar	0.99	0.97	1.00	1.00	0.95

Fig. 5-3. Cost effect against stripper operating pressure change

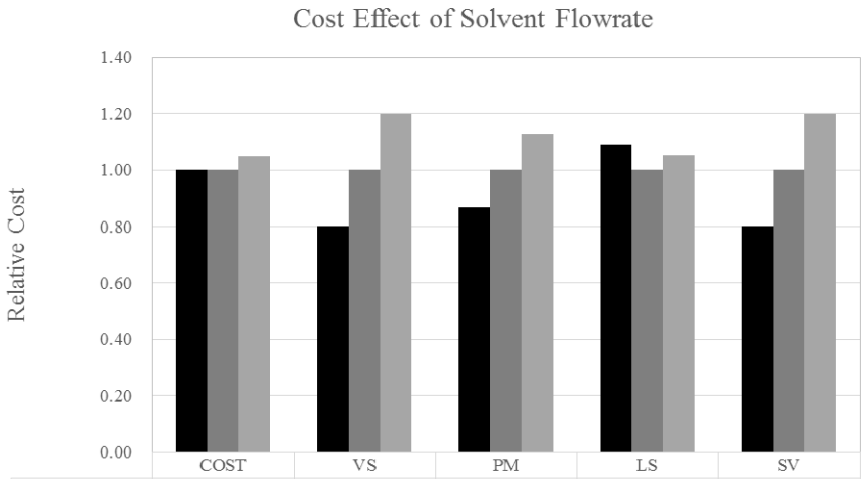

	COST	VS	PM	LS	SV
2400 kg/s	1.00	0.80	0.87	1.09	0.80
3000 kg/s(base)	1.00	1.00	1.00	1.00	1.00
3600 kg/s	1.05	1.20	1.13	1.05	1.20

Fig. 5-4. Cost effect against the cycling solvent flowrate change

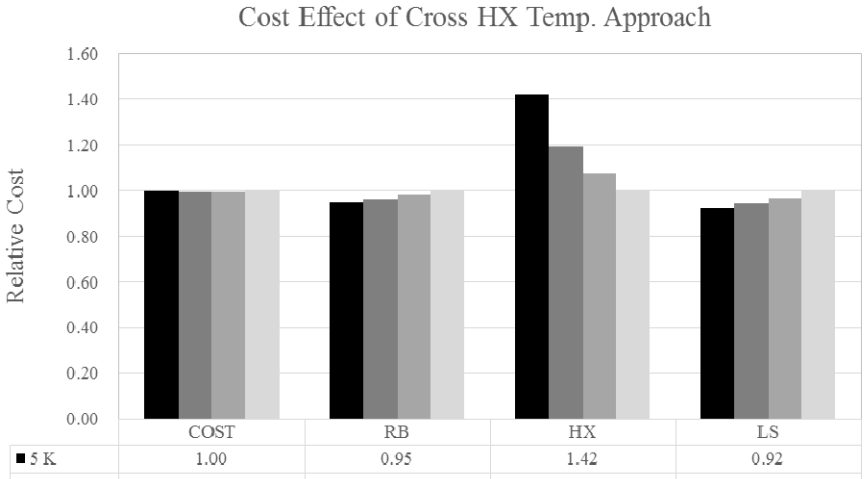

	COST	RB	HX	LS
5 K	1.00	0.95	1.42	0.92
10 K	0.99	0.96	1.19	0.94
15 K	0.99	0.98	1.08	0.97
20 K(Base)	1.00	1.00	1.00	1.00

Fig. 5-5. Cost effect against the temperature approach change in the cross heat exchanger

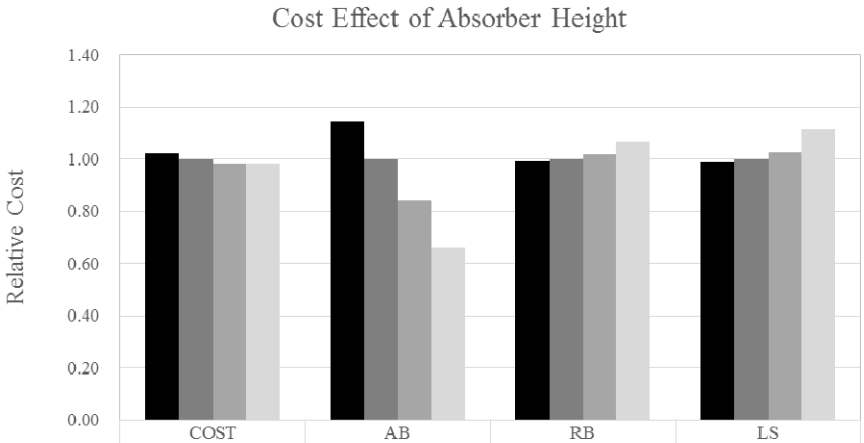

	COST	AB	RB	LS
30 m	1.02	1.14	0.99	0.99
24 m(Base)	1.00	1.00	1.00	1.00
18 m	0.98	0.84	1.02	1.03
12 m	0.98	0.66	1.07	1.11

Fig. 5-6. Cost effect against the absorber height change

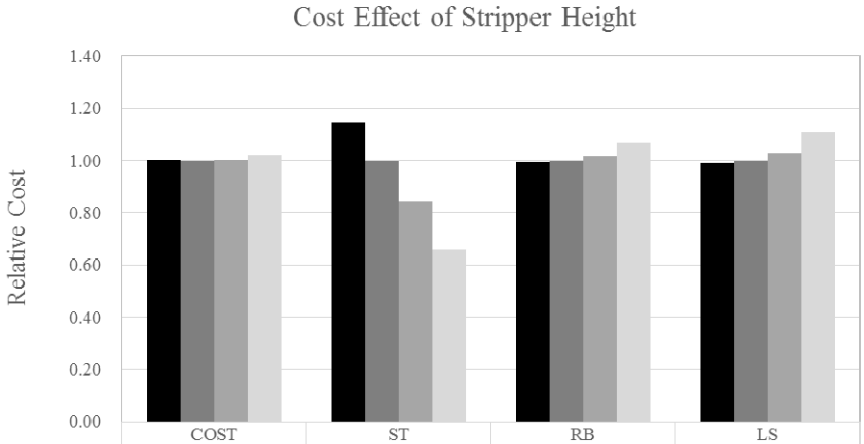

	COST	ST	RB	LS
25	1.00	1.14	0.99	0.99
20m (Base)	1.00	1.00	1.00	1.00
15m	1.00	0.84	1.02	1.03
10m	1.02	0.66	1.07	1.11

Fig. 5-7. Cost effect against the stripper height change

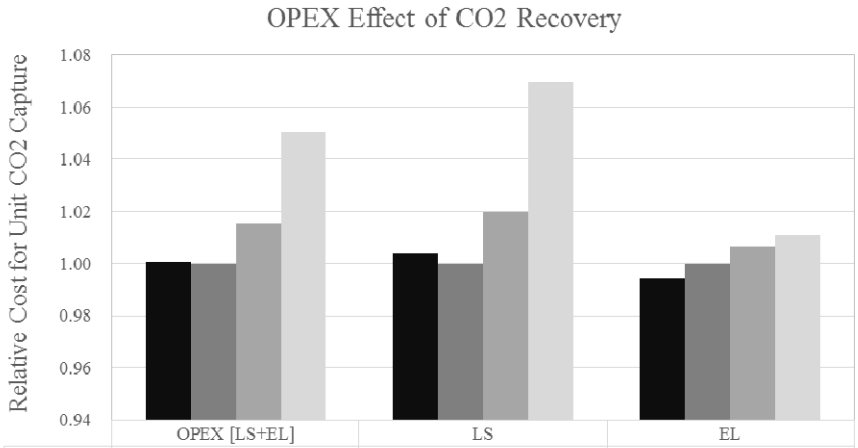

	OPEX [LS+EL]	LS	EL
85%	1.00	1.00	0.99
90% (base)	1.00	1.00	1.00
95%	1.02	1.02	1.01
98%	1.05	1.07	1.01

Fig. 5-8. OPEX effect against the CO_2 Recovery

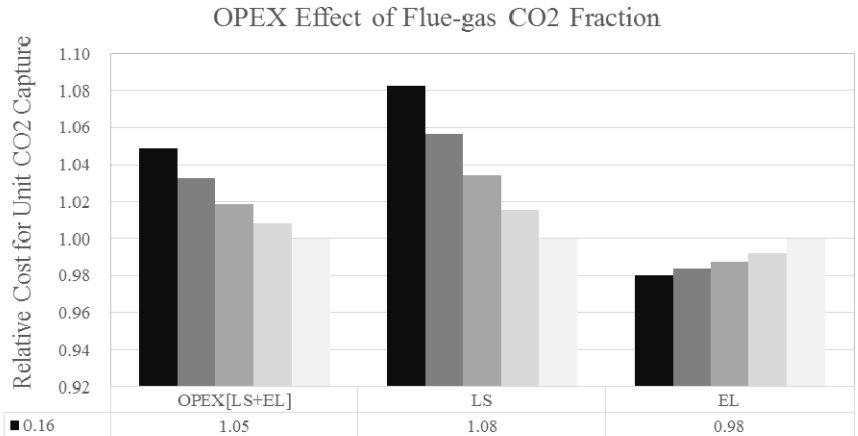

	OPEX[LS+EL]	LS	EL
0.16	1.05	1.08	0.98
0.17	1.03	1.06	0.98
0.18	1.02	1.03	0.99
0.19	1.01	1.02	0.99
0.20 (base)	1.00	1.00	1.00

Fig. 5-9. OPEX effect against the CO_2 mass fraction in the flue gas

The superstructure model consists of 35 design variables from 6 modified configurations (Absorber Intercooling, Semi-lean/Semi-rich loop, cold solvent split, lean vapor compression, rich vapor compression, heat integration, and split flow configurations). Table 5-9 indicates the total cost effect of each variable. The most effective variable is absorber top height, while the split flow fraction tends to have either no effect or a negative effect. The sum of the cost reduction effect is ~8.30% when the variables do not interact. A simplified configuration of the superstructure model is presented in Fig. 5-10.

Table 5-9. Cost effect of main control variables in modified MEA process

Variable	Control Variable	Symbol	Base	Lower Bound	Upper Bound	Unit	Cost Effect
Pressure	Stripper Operating Pressure (0)	P1	1.79	1.00	2.00	bar	-0.4%
	Lean Vapor Pressure (4)	P2	1.70	1.00	1.70	bar	-0.6%
	Rich Vapor Pressure (5)	P3	1.40	1.10	1.75	bar	-0.8%
Flowrate	Cycling Solvent (0)	F1	3000	2400	3600	kg/s	-0.3%
	1st Compressor HX CW (6)	F2	50.0	10.0	80.0	kg/s	-
	2nd Compressor HX CW (6)	F3	50.0	-	-	kg/s	-
	3rd Compressor HX CW (6)	F4	150	-	-	kg/s	-
Temp.	Absorber Intercooling Temp. (1)	T1	308	300	320	K	-
	Cross HX-1 Hot Out approach (0)	T2	24.0	10.0	30.0	K	-1.1%
	Cross HX-2 Hot Out approach (2)	T3	16.0	5.00	30.0	K	-0.1%
	Cross HX-3 Hot Out approach (6)	T4	10.0	5.00	20.0	K	-0.2%
Packing Height	Absorber Top Height (0)	H1	12.0	5.00	20.0	m	-1.3%
	Absorber Bottom Height (0)	H2	12.0	5.00	15.0	m	-0.6%
	Stripper Washing Section Height (0)	H3	2.00	1.00	6.00	m	-0.9%
	Stripper Top Height (0)	H4	9.00	1.00	20.0	m	-
	Stripper Bottom Height (0)	H5	9.00	1.00	20.0	m	-
Heat Transfer Area	1st Compressor HX (6)	A1	12000	6000	18000	m^2	-0.1%
	2nd Compressor HX (6)	A2	12000	-	-	m^2	
	3rd Compressor HX (6)	A3	12000	-	-	m^2	
Split Fraction	Absorber Top Split Fraction (7)	S1	1.00	0.95	1.00	-	-
	Cold Solvent Split Fraction-1 (3)	S2	0.30	0.10	0.60	-	-1.0%
	Cold Solvent Split Fraction-2 (3)	S3	0.00	0.00	1.00		-
	Washing Section Split Fraction (7)	S4	0.00	0.00	1.00	-	-
	Hot Solvent Split Fraction-1 (7)	S5	0.95	0.80	1.00	-	-0.4%
	Hot Solvent Split Fraction-2 (7)	S6	0.05	0.00	1.00		-0.2%
	Cross HX-3 Inlet-1 Split Fraction (7)	S7	1.00	0.00	1.00	-	
	Cross HX-3 Inlet-2 Split Fraction (7)	S8	1.00	-	-	-	
	Cross HX-3 Inlet-3 Split Fraction (7)	S9	1.00	-	-	-	
	Rich Vapor Split Fraction (5)	S10	0.70	0.00	1.00	-	-0.3%
Selector	Absorber Intercooling Selector (1)	S11	1.00	-	-	-	
	Cross HX-2 Cold Side Selector (2)	S12	0.05				
	Cross HX-2 Hot Side Selector (2)	S13	0.05				
	Lean Vapor Compression Selector (4)	S14	1.00	-	-	-	
	Rich Vapor Compression Selector (5)	S15	1.00	-	-	-	
	Cross HX-3 Selector (6)	S16	1.00	-	-	-	

Design variables from conventional process (0), absorber intercooling (1), semi-lean / semi-rich loop (2), cold solvent split (3), lean vapor compression (4), rich vapor compression (5), heat integration (6), split flow configurations (7).

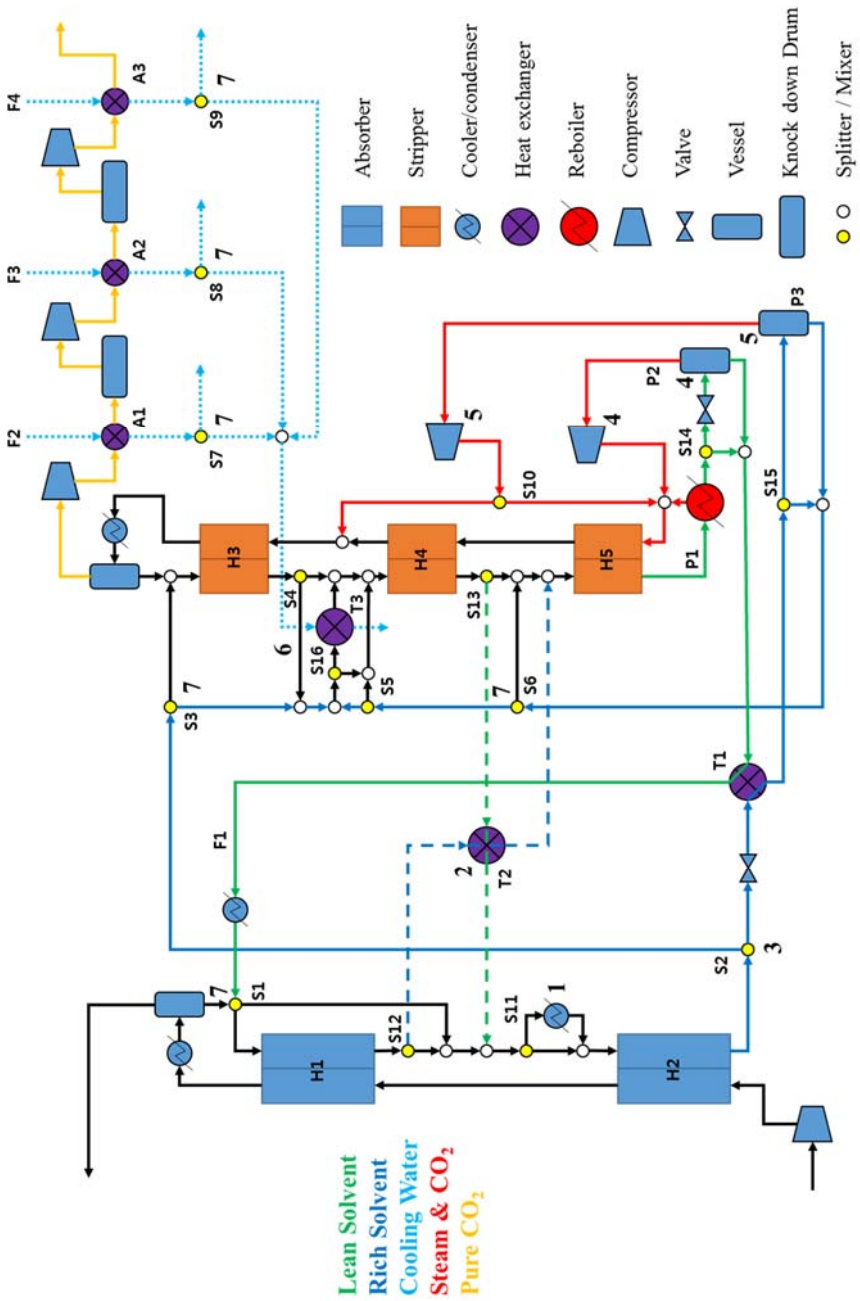

Fig. 5-10. Simplified process configuration for the superstructure of the modified MEA processes

Chapter 6: Superstructure Optimization of the Modified MEA Scrubbing Process

6.1 Overview

The superstructure model has numerous design variables, as discussed in the previous sections. These design variables can interact either positively or negatively with one another, thus affecting the OPEX and CAPEX terms. Although the parametric study provided a starting point to determine the optimal configurations, these cannot be determined using qualitative intuition. The multi-variable optimization method was therefore employed to find the optimal configuration and optimal variable sets of the superstructure model. As previously reported, the equation oriented approaches offer several advantages over more traditional sequential modular approaches for simulation [51]. As the equation oriented approach can easily calculate the first and second derivatives, the equation oriented environment is a fast and robust method for solving the multi-variable optimization problem, and is particularly suitable for calculating the recycle system. This method allows determination of all variables simultaneously rather than sequentially, as indicated in Fig. 6-1.

In this chapter, two case studies were conducted using the superstructure model of the modified MEA scrubbing process. The target process is from the

CASTOR project, which was mentioned previously in Chapter 5. The objective of scenario 1 is to minimize the equivalent energy requirements for the CO_2 capture and compression process for the existing plant, while the objective of scenario 2 is to minimize the total cost for the CO_2 capture and compression process using the utility provided from the integrated power plant.

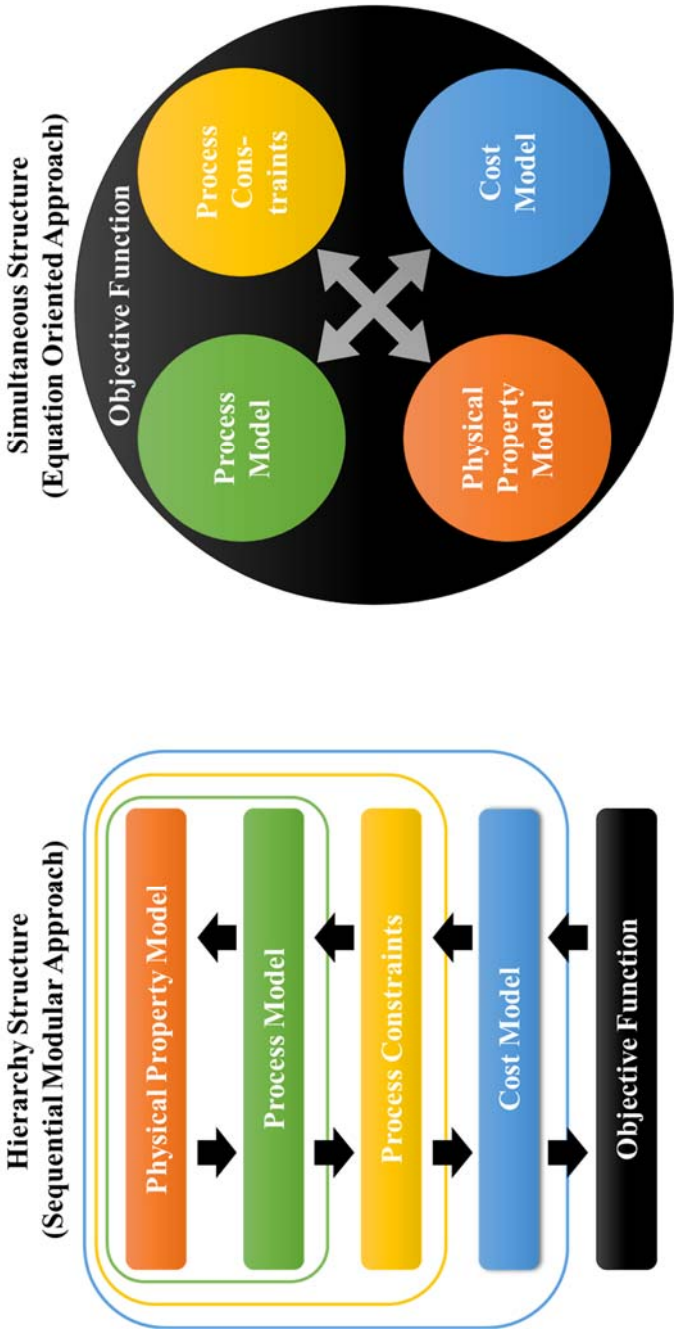

Fig. 6-1. Multivariable optimization based on equation oriented approach

6.2 Optimization scenario I

6.2.1 Optimization procedure

Using a current CO_2 capture and compression plant, the total equivalent energy consumption can be minimized by optimizing the operation variables. The equivalent energy can be minimized according to Eq. (6-1), which demonstrates that the equivalent energy is the sum of the thermal energy at the reboiler, Q_{Reb}, and the electric energy at the compressor, E_{Comp}. As mentioned in Chapter 4.4.4, the conversion factor, η, is 0.236 for this study. This superstructure model involves 6 modified configurations and 27 control variables. The minimum temperature approach was fixed at 10 K for all heat exchangers.

$$min\ Z = \eta \times Q_{Reb} + E_{Comp} \qquad (6\text{-}1)$$

6.2.2 Optimization results

As shown in Fig 6-2, the minimum equivalent energies are 1.18 GJ_e/ton CO_2 and 0.95 GJ_e/ton CO_2 for the conventional process and the modified process, respectively. The equivalent energy reduction effects are 3.3% and 22.1%, respectively.

For the conventional process, the stripper pressure increases to reduce the reboiler heat and CO_2 compression electricity terms, and the final pressure is determined because the reboiler temperature reaches the upper bound. In addition, the cycling solvent flowrate increases slightly, causing the lean loading to increase. As the cross heat exchanger temperature approach decreases, the reboiler heat requirement is reduced. Further details of the control variables and constraint variables are listed in Table 6-1.

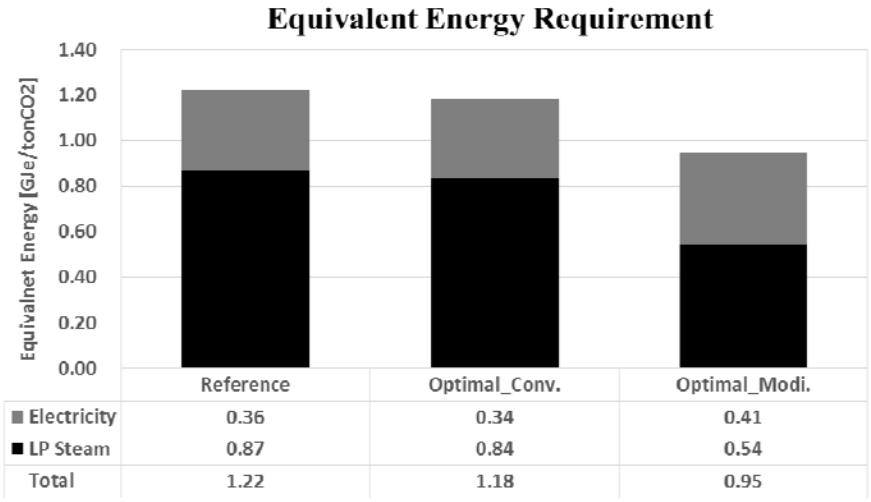

Fig. 6-2. Optimization result of conventional process and modified process

Table 6-1. Optimal control variable set and constraints variables of conventional process

Variable	Control Variables	Optimal value	Initial value	Lower Bound	Upper Bound	Unit
Pressure	Stripper Pressure	1.92	1.79	1.10	2.00	bar
Flowrate	Cycling Solvent	3180	3000	2400	3600	kg/s
Temp.	Cross HX Hot Out approach	10.7	20.0	10.0	100	K

Variable	Constraint Variables	Value	Lower Bound	Upper Bound	Unit
Temperature	Reboiler Temp	393	300	393	K
CO_2 Loading	Lean Loading	0.252	0.200	0.300	-
	Rich Loading	0.482	0.400	0.500	-

For the modified process, the lean vapor and rich vapor compressor significantly reduce the LP steam energy at the reboiler. Although additional electricity is required for vapor compression, the total equivalent energy is reduced. The optimal variable sets are listed in Table 6-2. Initially, the absorber intercooling temperature was set at the lower bound of 313 K. Since the absorber intercooling increases the rich loading value at the absorber bottom, the lean loading value increases at the stripper bottom despite a decrease in the solvent flowrate. In addition, the semi-lean/semi-rich loop is not considered because the absorber and stripper height are sufficiently high. As a result, the cross HX-2 temperature approach is not physically relevant. Furthermore, when 14% cold solvent is fed to the stripper top without passing through the cross heat exchanger, the split cold solvent directly cools the stripper top. Moreover, the lean vapor compression increases the amount of vapor generated through a decrease in the pressure, while the reboiler heat requirement is significantly reduced, and the electricity requirement is slightly increased. Finally, the rich vapor compression reduces the amount of vapor generated by increasing the pressure, and the generated rich vapor is fed to the stripper washing section rather than the stripper bottom. Further details of the control variables and constraint variables are given in Table 6-2.

To reduce the complexity of the configuration, the final split fraction was modified. With an optimal split fraction higher than 0.90 or lower than 0.10, the split fraction is fixed at (1.00) or (0.00), respectively. Following conversion

of these variables from control variables to fixed variables, the superstructure optimization is conceded again. The final configuration shows a simple structure with only slight increases in the objective function. The final configuration of the superstructure is shown in Fig. 6-3.

Table 6-2. Optimal control variable set and constraints variables of modified process

Variable	Control Variables	Symbol	Optimal value	Initial value	Lower Bound	Upper Bound	Unit
Pressure	Stripper Operating Pressure (0)	P1	1.88	1.79	1.10	2.00	bar
	Lean Vapor Pressure (4)	P2	1.05	1.70	0.35	1.85	bar
	Rich Vapor Pressure (5)	P3	1.50	1.40	1.05	5.00	bar
Flowrate	Cycling Solvent (0)	F1	2890	3000	2400	3600	kg/s
	1st Compressor HX CW (6)	F2	49.3	50.0	10.0	500	kg/s
	2nd Compressor HX CW (6)	F3	41.9	50.0	10.0	500	kg/s
	3rd Compressor HX CW (6)	F4	92.5	150	10.0	500	kg/s
Temp.	Absorber Intercooling Temp. (1)	T1	313	315	313	330	K
	Cross HX-1 Hot Out approach (0)	T2	13.1	24.0	10.0	100	K
	Cross HX-2 Hot Out approach (2)	T3	-	16.0	10.0	100	K
	Cross HX-3 Hot Out approach (6)	T4	10.0	10.0	10.0	100	K
Split Fraction	Absorber Top Split Fraction (7)	S1	0.00	0.05	0.00	1.00	-
	Cold Solvent Split Fraction-1 (3)	S2	0.14	0.30	0.00	1.00	-
	Cold Solvent Split Fraction-2 (3)	S3	0.00	0.00	0.00	1.00	-
	Washing Section Split Fraction (7)	S4	0.07 (0.00)	0.00	0.00	1.00	-
	Hot Solvent Split Fraction-1 (7)	S5	0.00	0.00	0.00	1.00	-
	Hot Solvent Split Fraction-2 (7)	S6	0.00	0.05	0.00	1.00	-
	Cross HX-3 Inlet-1 Split Fraction (7)	S7	1.00	1.00	0.00	1.00	-
	Cross HX-3 Inlet-2 Split Fraction (7)	S8	0.99 (1.00)	1.00	0.00	1.00	-
	Cross HX-3 Inlet-3 Split Fraction (7)	S9	1.00	1.00	0.00	1.00	-
	Rich Vapor Split Fraction (5)	S10	0.09 (0.00)	0.70	0.00	1.00	-
Selector	Absorber Intercooling Selector (1)	S11	1.00	1.00	1e-5	1.00	-
	Cross HX-2 Cold Side Selector (2)	S12	0.00	1.00	1e-5	1.00	-
	Cross HX-2 Hot Side Selector (2)	S13	0.00	1.00	1e-5	1.00	-
	Lean Vapor Compression Selector (4)	S14	1.00	1.00	1e-5	1.00	-
	Rich Vapor Compression Selector (5)	S15	0.99 (1.00)	1.00	1e-5	1.00	-
	Cross HX-3 Selector (6)	S16	0.29 (1.00)	1.00	1e-5	1.00	-

Variable	Constraint Variables	Value	Lower Bound	Upper Bound	Unit
Temperature	Reboiler Temp	393	300	393	K
	Cross HX-1 Temp Approach	10.1	10.0	100	K
	Cross HX-2 Temp Approach	-	10.0	100	K
	Liquefied CO_2 Temp	311	300	315	K
CO_2 Loading	Lean Loading	0.260	0.200	0.300	-
	Rich Loading	0.457	0.400	0.500	-

*Design variable from conventional process (0), absorber intercooling (1), semi-lean / semi-rich loop (2), cold solvent split (3), lean vapor compression (4), rich vapor compression (5), heat integration (6), split flow configurations (7).

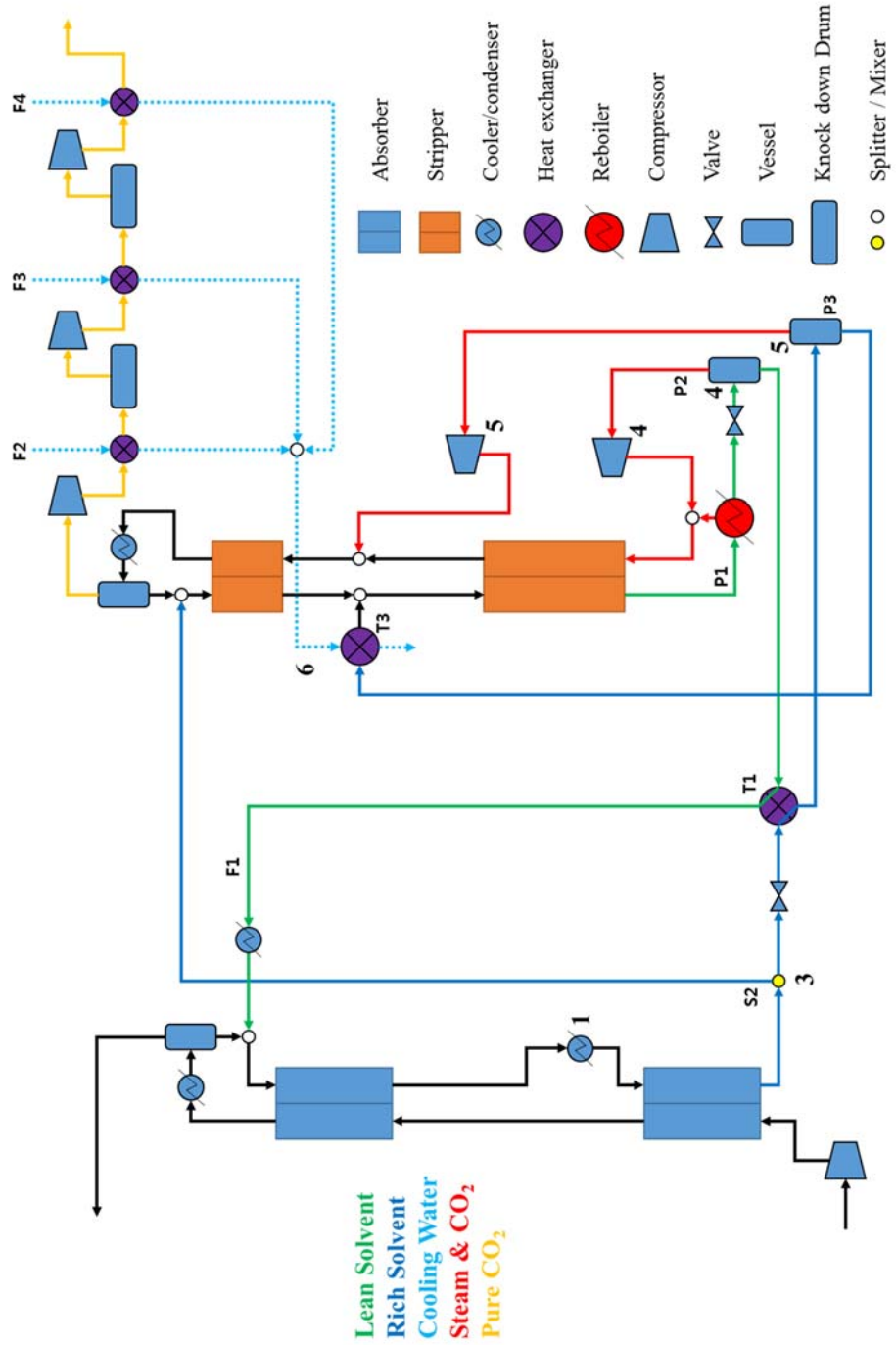

Fig. 6-3. Optimal configuration for minimizing equivalent energy

Table 6-3 shows a comparison of the equivalent energy requirements from this study and from previous literature studies based on the non-equilibrium column model, under 2 bar pressure, with 90% CO_2 capture [15, 33, 47, 52, 53]. The reboiler energy and compression energy are calculated again using the present energy conversion factor (0.236) and compressor efficiency (0.75). The equivalent reboiler energy can be converted to the equivalent energy using Eq. (6-1). The equivalent energy requirement in the conventional process for this study (1.23-1.30 GJ_e/ton CO_2) shows good agreement with the literature data (1.22-1.26 GJ_e/ton CO_2). From the literature, the equivalent energy indicates values of <1.10 GJ_e/ton CO_2 and <1.08 GJ_e/ton CO_2 for the single modified configuration and the multiple modified configuration, respectively. Through superstructure optimization, the equivalent energy was reduced up to 1.02 GJ_e/ton CO_2.

Table 6-3. Total equivalent energy reductions effect for each process

Process [15, 33, 47, 52, 53]	Reboiler Steam ($\eta = 0.236$)* [MJ_e/kg CO_2]	Vapour compression [MJ_e/kg CO_2]	Compression Energy ($E = 0.75$)* [MJ_e/kg CO_2]	Pump /Blower [MJ_e/kg CO_2]	Equivalent Energy [MJ_e/kg CO_2]
Conventional Process (This study)	0.81-0.87	-	0.35-0.36	(0.07)	1.23-1.30
Conventional Process (Literature)	0.81-0.84	-	0.34	0.05-0.08	1.22-1.26
Intercooling Process (Literature)	0.73-0.81	-	0.34	0.07-0.10	1.14-1.22
MVR Process (Literature)	0.46-0.54	0.38-0.55	0.11-0.15	0.08-0.10	1.17-1.22
LVR Process (Literature)	0.60-0.69	0.08-0.09	0.31-0.34	0.05-0.10	1.10-1.19
Combined Process (Literature)	0.39-0.69	0.00-0.15	0.34-0.68	0.05-0.10	1.08-1.18
Optimal modified process (This study)	0.54	0.06	0.35	(0.07)	1.02

6.3 Optimization scenario II

6.3.1 Optimization procedure

Upon the construction of a new CO_2 capture plant, the CAPEX and OPEX terms should be considered together. In this case, the aim is to minimize the total cost, i.e., the sum of the CAPEX and OPEX terms, as indicated in Eq. (6-2). The cost model uses the economic parameters and cost factors previously introduced in Chapter 5. It should be considered that both steam and electricity are supplied from the integrated power plant, as reported in the literature [1]. The superstructure involves 6 modified configurations and 35 control variables. At the cross heat exchanger, the minimum temperature approach is shifted from 10 K to 5 K, as the total cost model can consider the CAPEX and OPEX terms simultaneously.

$$min\ Z = \sum_E CAPEX_E + \sum_U OPEX_U \qquad (6\text{-}2)$$

$$E = \{AB, ST, CM, RB, HX, VS, PM, BL, SV\}, \qquad U = \{LS, EL, SV, PM, BL\}$$

6.3.2 Optimization results

As shown in Fig. 6-4 below, minimum costs of €54.7/ton CO_2 and €51.0/ton CO_2 were established for the conventional and modified processes, respectively, and the cost reduction effects were 3.7% and 10.2%, respectively. Thus, the annual cost reduction effects were €9.3 M/yr and €25.7 M/yr, respectively.

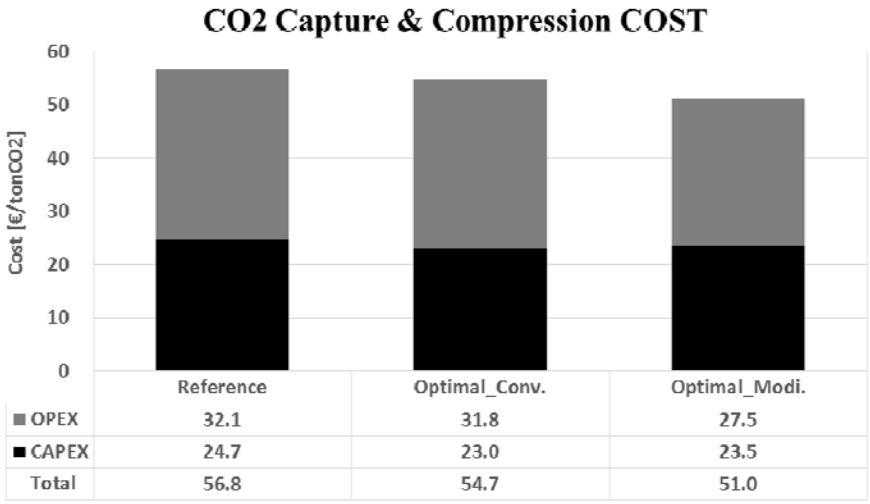

Fig. 6-4. Optimization result of conventional process and modified process

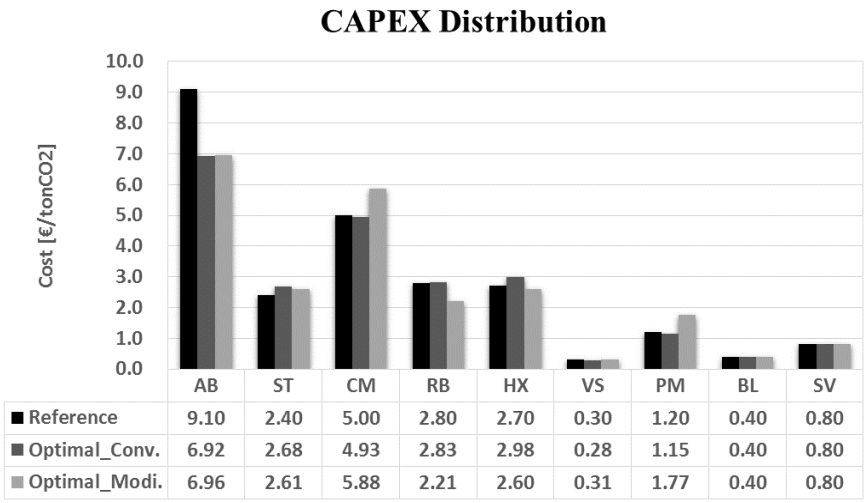

	AB	ST	CM	RB	HX	VS	PM	BL	SV
Reference	9.10	2.40	5.00	2.80	2.70	0.30	1.20	0.40	0.80
Optimal_Conv.	6.92	2.68	4.93	2.83	2.98	0.28	1.15	0.40	0.80
Optimal_Modi.	6.96	2.61	5.88	2.21	2.60	0.31	1.77	0.40	0.80

Fig. 6-5. CAPEX distribution of optimal conventional process and optimal modified process

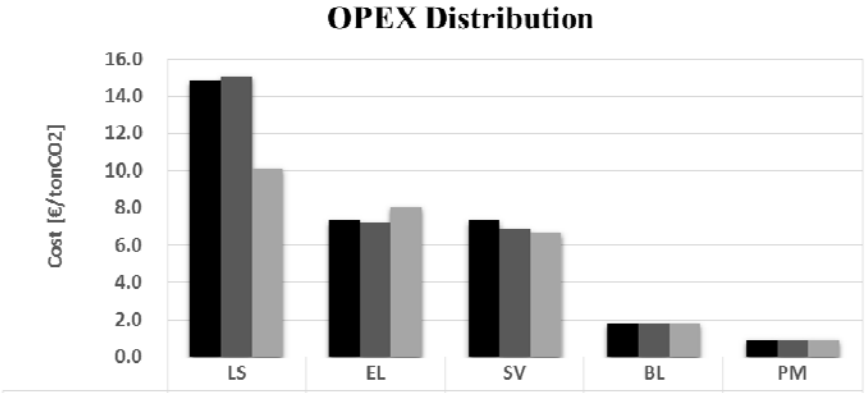

	LS	EL	SV	BL	PM
Reference	14.80	7.30	7.30	1.80	0.90
Optimal_Conv.	15.05	7.15	6.85	1.80	0.90
Optimal_Modi.	10.10	8.04	6.64	1.80	0.90

Fig. 6-6. OPEX distribution of optimal conventional process and optimal modified process

In the conventional process, the absorber height is significantly reduced while the stripper height is slightly increased. As the absorber height is lowered, the lean loading value is reduced from 0.24 to 0.21, accompanied by only a slight increase in the OPEX for LP steam. This is due to a decrease in the heat exchanger temperature approach. In contrast, the electricity OPEX factor reduces slightly as the stripper operating pressure increases. In addition, as the cross heat exchanger temperature approach decreases, the CAPEX term for the cross heat exchanger increases. The total cost reduction effect is €2.1/ton CO_2, which is a 3.7% reduction on the base process. Further details of the control variables and constraint variables are listed in Table 6-4.

Table 6-4. Optimal control variable set and constraints variables of conventional process

Variable	Control Variables	Optimal value	Initial value	Lower Bound	Upper Bound	Unit
Pressure	Stripper Pressure	1.87	1.79	1.10	2.00	Bar
Flowrate	Cycling Solvent	2820	3000	2400	3600	kg/s
Temp.	Cross HX Hot Out approach	14.4	20.0	5.00	100	K
Height	Absorber Height	15.2	24.0	1e-5	24.0	m
	Stripper Height	24.0	20.0	1e-5	24.0	m

Variable	Constraint Variables	Value	Lower Bound	Upper Bound	Unit
Temperature	Reboiler Temp.	393	300	393	K
CO_2 Loading	Lean Loading	0.212	0.200	0.300	-
	Rich Loading	0.472	0.400	0.500	-

For the modified process, the optimal configuration involves absorber intercooling, lean vapor compression, rich vapor compression, and heat integration with compression. The semi-lean/semi-rich loop can be ignored because the 1–2% split fraction has no effect on the total cost. As for the conventional process, the absorber height was significantly reduced. The lean loading value was larger than that of the conventional process because absorber intercooling increases the lean loading value. In addition, the lean vapor compressor and rich vapor compressor significantly reduce the LP steam cost, while the compression electricity cost increases. As a result, the CAPEX term for the reboiler is reduced and that of the compressor increases. The temperature approaches of the cross heat exchanger are 15.1 K and 7.25 K for exchangers 1 and 3, respectively. Although the temperature approach can be reduced up to 5.0 K, the optimal value is higher than the lower bound because the CAPEX for HX increases dramatically at low temperatures approach region. Finally, the total cost is reduced from €54.7 /ton CO_2 to €51.0/ton CO_2, which is a 6.8% reduction from the optimal conventional process cost. Details of the control variables and constraint variables are given in Tables 6-5 and 6-6, and the final configuration of the superstructure is shown in Fig. 6-7.

Table 6-5. Optimal control variable set of modified process

Variable	Control Variable	Symbol	Optimal value	Initial value	Lower Bound	Upper Bound	Unit
Pressure	Stripper Operating Pressure (0)	P1	1.84	1.79	1.10	2.00	bar
	Lean Vapor Pressure (4)	P2	1.02	1.70	0.35	1.85	bar
	Rich Vapor Pressure (5)	P3	1.60	1.40	1.05	5.00	bar
Flowrate	Cycling Solvent (0)	F1	2730	3000	2400	3600	kg/s
	1st Compressor HX CW (6)	F2	73.8	50.0	10.0	500	kg/s
	2nd Compressor HX CW (6)	F3	137	50.0	10.0	500	kg/s
	3rd Compressor HX CW (6)	F4	86.2	150	10.0	500	kg/s
Temp.	Absorber Intercooling Temp. (1)	T1	314	315	313	330	K
	Cross HX-1 Hot Out approach (0)	T2	15.1	24.0	5.00	100	K
	Cross HX-2 Hot Out approach (2)	T3	43.0	16.0	5.00	100	K
	Cross HX-3 Hot Out approach (6)	T4	7.25	10.0	5.00	100	K
Packing Height	Absorber Top Height (0)	H1	6.52	12.0	1e-5	24	m
	Absorber Bottom Height (0)	H2	8.87	12.0	1e-5	24	m
	Stripper Washing Section Height (0)	H3	3.29	1.00	1e-5	10	m
	Stripper Top Height (0)	H4	10.4	9.00	1e-5	20	m
	Stripper Bottom Height (0)	H5	9.30	9.00	1e-5	20	m
Heat Transfer Area	1st Compressor HX (6)	A1	14000	12000	1e-5	50000	m^2
	2nd Compressor HX (6)	A2	12900	12000	1e-5	50000	m^2
	3rd Compressor HX (6)	A3	11400	12000	1e-5	50000	m^2
Split Fraction	Absorber Top Split Fraction (7)	S1	0.01 (0.00)	0.05	0.00	1.00	-
	Cold Solvent Split Fraction-1 (3)	S2	0.27	0.30	0.00	1.00	-
	Cold Solvent Split Fraction-2 (3)	S3	0.00	0.00	0.00	1.00	
	Washing Section Split Fraction (7)	S4	0.76	0.00	0.00	1.00	-
	Hot Solvent Split Fraction-1 (7)	S5	0.14	0.00	0.00	1.00	-
	Hot Solvent Split Fraction-2 (7)	S6	0.01 (0.00)	0.05	0.00	1.00	-
	Cross HX-3 Inlet-1 Split Fraction (7)	S7	0.98 (1.00)	1.00	0.00	1.00	-
	Cross HX-3 Inlet-2 Split Fraction (7)	S8	0.15 (0.00)	1.00	0.00	1.00	-
	Cross HX-3 Inlet-3 Split Fraction (7)	S9	0.88 (1.00)	1.00	0.00	1.00	-
	Rich Vapor Split Fraction (5)	S10	0.09 (0.00)	0.70	0.00	1.00	-
Selector	Absorber Intercooling Selector (1)	S11	0.99 (1.00)	1.00	1e-5	1.00	-
	Cross HX-2 Cold Side Selector (2)	S12	0.01 (0.00)	0.05	1e-5	1.00	-
	Cross HX-2 Hot Side Selector (2)	S13	0.02 (0.00)	0.05	1e-5	1.00	
	Lean Vapor Compression Selector (4)	S14	1.00	1.00	1e-5	1.00	-
	Rich Vapor Compression Selector (5)	S15	0.99 (1.00)	1.00	1e-5	1.00	-
	Cross HX-3 Selector (6)	S16	1.00	1.00	1e-5	1.00	-

Table 6-6. Constraints variables of modified process

Variable	Constraint Variables	Value	Lower Bound	Upper Bound	Unit
Temperature	Reboiler Temp	393	300	393	K
	Cross HX-1 Temp Approach	6.70	5.00	100	K
	Cross HX-2 Temp Approach	5.86	5.00	100	K
	Liquefied CO_2 Temp	312	300	315	K
Height	Absorber Total Height	15.4	1e-5	24	m
	Stripper Total Height	23.0	1e-5	24	m
CO_2 Loading	Lean Loading	0.228	0.200	0.300	-
	Rich Loading	0.410	0.400	0.500	-

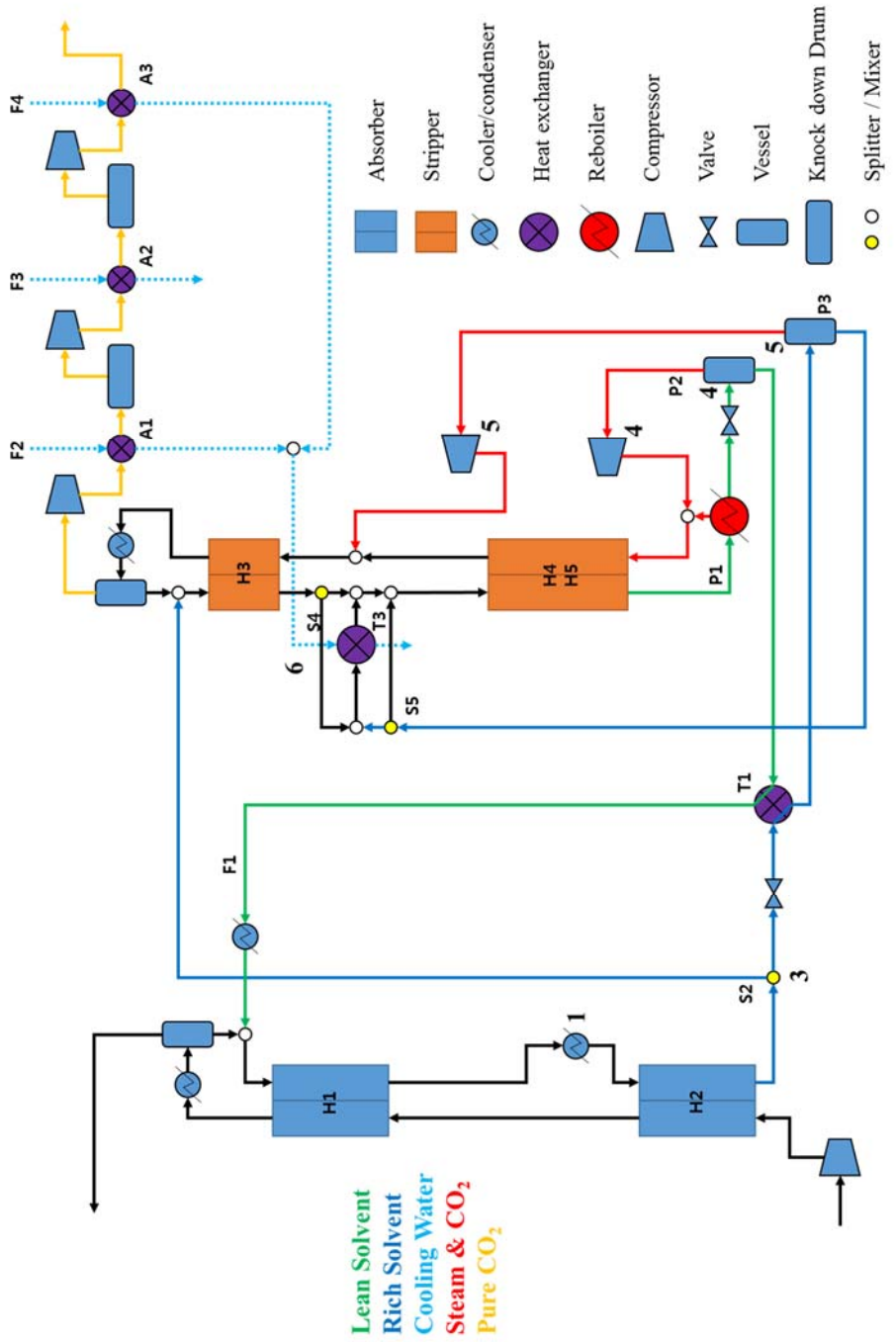

Fig. 6-7. Optimal configuration for minimizing total cost

To demonstrate the cost sensitivity of the optimal solution, the variation in cost indexes for steam and electricity were calculated, and were found to change from −20% to +20%. As indicated in Fig. 6-8 and Table 6-7, the heat exchanger temperature approach increases while the heat exchanger size decreases according to the decrease in the OPEX index.

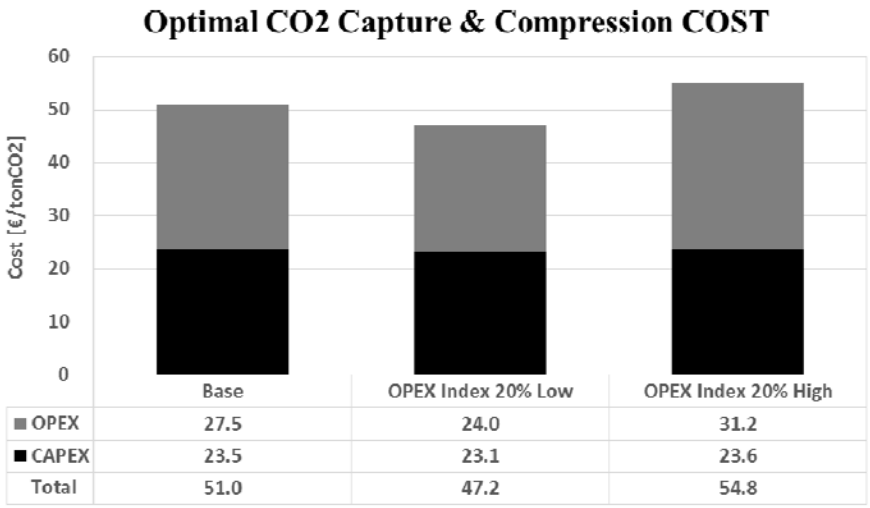

Fig. 6-8. Sensitivity analysis of the total cost with OPEX index change

Table 6-7. Optimal control variables for various OPEX index

Variable	Control Variable	Symbol	OPEX(LS, EL) Cost Index			Unit
			Base	-20%	+20%	
Pressure	Stripper Operating Pressure (0)	P1	1.84	1.83	1.85	bar
	Lean Vapor Pressure (4)	P2	1.02	1.20	1.03	bar
	Rich Vapor Pressure (5)	P3	1.60	1.67	1.78	bar
Flowrate	Cycling Solvent (0)	F1	2730	2730	2820	kg/s
	1st Compressor HX CW (6)	F2	73.8	100	59.2	kg/s
	2nd Compressor HX CW (6)	F3	137	131	133	kg/s
	3rd Compressor HX CW (6)	F4	86.2	88.2	88.8	kg/s
Temp.	Absorber Intercooling Temp. (1)	T1	314	315	314	K
	Cross HX-1 Hot Out approach (0)	T2	15.1	17.5	14.5	K
	Cross HX-2 Hot Out approach (2)	T3	-	-	-	K
	Cross HX-3 Hot Out approach (6)	T4	7.25	14.2	5.10	K
Packing Height	Absorber Top Height (0)	H1	6.52	5.96	6.35	m
	Absorber Bottom Height (0)	H2	8.87	8.12	8.54	m
	Stripper Washing Section Height (0)	H3	3.29	2.72	3.64	m
	Stripper Top Height (0)	H4	10.4	9.78	8.98	m
	Stripper Bottom Height (0)	H5	9.30	11.1	11.3	m
Heat Transfer Area	1st Compressor HX (6)	A1	14000	13200	17700	m^2
	2nd Compressor HX (6)	A2	12900	12900	13100	m^2
	3rd Compressor HX (6)	A3	11400	9650	22500	m^2
Split Fraction	Absorber Top Split Fraction (7)	S1	0.01 (0.00)	0.01 (0.00)	0.01 (0.00)	-
	Cold Solvent Split Fraction-1 (3)	S2	0.27	0.30	0.26	-
	Cold Solvent Split Fraction-2 (3)	S3	0.00	0.00	0.00	
	Washing Section Split Fraction (7)	S4	0.76	0.85	0.02 (0.00)	-
	Hot Solvent Split Fraction-1 (7)	S5	0.14	0.22	0.08 (0.00)	-
	Hot Solvent Split Fraction-2 (7)	S6	0.01 (0.00)	0.00	0.00	-
	Cross HX-3 Inlet-1 Split Fraction (7)	S7	0.98 (1.00)	0.46	1.00	-
	Cross HX-3 Inlet-2 Split Fraction (7)	S8	0.15 (0.00)	0.15 (0.00)	1.00	-
	Cross HX-3 Inlet-3 Split Fraction (7)	S9	0.88 (1.00)	0.99 (1.00)	1.00	-
	Rich Vapor Split Fraction (5)	S10	0.09 (0.00)	0.10 (0.00)	0.01 (0.00)	-
Selector	Absorber Intercooling Selector (1)	S11	0.99 (1.00)	1.00	0.99 (1.00)	-
	Cross HX-2 Cold Side Selector (2)	S12	0.01 (0.00)	0.01 (0.00)	0.00	-
	Cross HX-2 Hot Side Selector (2)	S13	0.02 (0.00)	0.01 (0.00)	0.00	
	Lean Vapor Compression Selector (4)	S14	1.00	1.00	0.99 (1.00)	-
	Rich Vapor Compression Selector (5)	S15	0.99 (1.00)	0.98 (1.00)	1.00	-
	Cross HX-3 Selector (6)	S16	1.00	0.83 (1.00)	1.00	-

Chapter 7: Conclusions and Remark

7.1 Conclusions

For the past decade, reducing energy consumption in the MEA scrubbing process for post-combustion CO_2 capture has become increasingly important and has received a large amount of attention. Numerous modified configurations have therefore been introduced to reduce the solvent regeneration energy of this process. A number of these modified configurations exhibit positive interactions, while others have either no interaction or display negative interactions. When configurations of positive interactions are combined, the energy requirements can be reduced significantly. However, the combination of modified configuration becomes complex as the number of modified configurations increases. Moreover, additional capital costs should also be considered when combining modified configurations. Although the quantitative analysis of each modified configuration provides an insight into possible combination strategies, it is not a suitable method to determine optimal combinations and variable sets.

The main objective of this thesis was to reduce the total cost of the MEA scrubbing process for post-combustion CO_2 capture. The author therefore suggested and built a superstructure model for the modified MEA scrubbing processes. This superstructure model involves multiple modified

configurations based on the results of qualitative analysis, while incorporating the total cost model, i.e., the sum of the OPEX and CAPEX terms. This superstructure model can simultaneously consider the multiple modified configurations and total cost. It also considers the hidden positive interactive variables, which can be difficult to detect through qualitative analysis. As a result, the suggested superstructure model significantly reduced either the energy requirement or the total cost by combining a range of modified configurations.

7.2 Future work

It is possible to expand or modify the proposed superstructure by a variety of means. Firstly, various solvents or solvent mixtures can be utilized, including methyldiethanolamine (MDEA), diethanolamine (DEA), and piperazine. Moreover, the mixing composition of the solvents can be considered as another control variable of the superstructure. The optimal configuration may differ significantly according to the mixed solvent composition. When considering solvent mixing, the physical properties should be for the mixed solvent system. In addition, the superstructure can be integrated with a steam cycle. As the suggested superstructure model is isolated with a steam cycle, the steam cost and equivalent energy conversion factor remain constant. When the steam cycle is integrated with the capture process, the extracted

steam conditions from the steam cycle may vary. Therefore, as the steam condition determines the reboiler temperature and reboiler size, the optimal conditions may also vary. Furthermore, the cost model can be modified using precise equations or vendor data instead of six-tenth rule. The optimal solution will exhibits greater reliability in the accurate cost model. Finally, process complexity can also be considered. The suggested optimal configuration is suitable only for minimizing cost without any consideration of the process operationality or controllability. Following quantification of the process complexity, this can be added to the objective function as a penalty term.

Nomenclature

B : Stripper bottom flow rate [kmol/kg CO_2]

D : Stripper distillate feed flow rate [kmol/kg CO_2]

D_{CO2} : CO_2 flow rate in the stripper distillate [kmol/kg CO_2]

D_{H2O} : H_2O flow rate in the stripper distillate [kmol/kg CO_2]

E_{Comp} : Electricity requirement for the compressor [MJ/kg CO_2]

E_{Total} : Total equivalent energy for capture and compression [MJ/kg CO_2]

F : Stripper inlet flow rate [kmol/kg CO_2]

h_B : Molar enthalpy of the stripper bottom [MJ/kmol]

h_D : Molar enthalpy of the stripper distillate [MJ/kmol]

h_F : Molar enthalpy of the stripper inlet [MJ/kmol]

ΔH : Enthalpy change between the stripper outlet and the inlet [MJ/kg CO_2]

ΔH_{Cond} : Heat of water condensation [MJ/kmol]

$P^{Sat}_{H2O(T)}$: Saturated water partial pressure at temperature [atm]

P^{str} : Stripper operating pressure [atm]

Q_{Reb} : Heat requirement for the reboiler [MJ/kg CO_2]

Q_{Cond} : Condenser cooling duty [MJ/kg CO_2]

Q_{HX} : Heat exchanger preheating duty [MJ/kg CO_2]

R : Stripper reflux feed flow rate [kmol/kg CO_2]

R_{H2O} : H_2O flow rate in the stripper reflux [kmol/kg CO_2]

$T_{Cold\text{-}In}$: Cold-side inlet temperature in the cross heat exchanger [°C]

$T_{Cold\text{-}Out}$: Cold-side outlet temperature in the cross heat exchanger [°C]

$T_{Hot\text{-}In}$: Hot-side inlet temperature in the cross heat exchanger [°C]

$T_{Hot\text{-}Out}$: Hot-side outlet temperature in the cross heat exchanger [°C]

T_{Top} : Temperature at the stripper top [°C]

T_{Cond} : Temperature at the condenser of the stripper [°C]

V : Stripper vapor flow rate [kmol/kg CO_2]

V_{CO2} : CO_2 flow rate in the stripper vapor [kmol/kg CO_2]

V_{H2O} : H_2O flow rate in the stripper vapor [kmol/kg CO_2]

y_{CO2} : CO_2 vapor fraction

y_{H2O} : H_2O vapor fraction

Abbreviations

AB	Absorber
AI	Absorber intercooling
BL	Blower
CAPEX	Capital expenditures
CEE	Condensate evaporation and evaporation
COE	Cost of electricity
CSS	Cold solvent split
CM	Compressor
EL	Electricity
EM	Economizer
FC	Flue gas precooling
FS	Flue gas splitting
HI	Heat integration
HX	Heat exchanger
LS	Low pressure steam
LVR	Lean vapor recompression
MEA	Monoethanolamine
MTA	Minimum temperature approach
MVR	Mechanical vapor recompression
OPEX	Operating expenses
PM	Pump

PR	Peng-Robinsion equation of state
RB	Reboiler
RVR	Rich vapor recompression
SI	Stripper interheating
SLSR	Semi-lean/semi-rich loop
SRK	Soave-Redlich-Kwong equation of state
ST	Stripper
SV	Solvent
VS	Vessel

Literature cited

(1) Raynal, L.; Gomez, A.; Caillat, B.; Haroun, Y., CO2 Capture Cost Reduction: Use of a Multiscale Simulations Strategy for a Multiscale Issue. *Oil and Gas Science and Technology* **2013,** 68, (6), 1093-1108.

(2) Raynal, L.; Bouillon, P.-A.; Gomez, A.; Broutin, P., From MEA to demixing solvents and future steps, a roadmap for lowering the cost of post-combustion carbon capture. *Chemical Engineering Journal* **2011,** 171, (3), 742-752.

(3) Alabdulkarem, A.; Hwang, Y.; Radermacher, R., Energy consumption reduction in CO_2 capturing and sequestration of an LNG plant through process integration and waste heat utilization. *International journal of greenhouse gas control* **2012,** 10, 215-228.

(4) Cousins, A.; Wardhaugh, L. T.; Feron, P. H. M., A survey of process flow sheet modifications for energy efficient CO_2 capture from flue gases using chemical absorption. *International journal of greenhouse gas control* **2011,** 5, (4), 605-619.

(5) Strube, R.; Manfrida, G., CO_2 capture in coal-fired power plants—Impact on plant performance. *International journal of greenhouse gas control* **2011,** 5, (4), 710-726.

(6) NETL, D., NETL Advanced Carbon Dioxide Capture R&D Program: Technology Update 3/2011. In 2011.

(7) Benson, S. M.; Orr Jr, F. M., Carbon dioxide capture and storage. *MRS bulletin* **2008,** 33, (4).

(8) Notz, R.; Mangalapally, H. P.; Hasse, H., Post combustion CO_2 capture by reactive absorption: Pilot plant description and results of systematic studies with MEA. *International journal of greenhouse gas control* **2012,** 6, 84-112.

(9) Kwak, N.-S.; Lee, J. H.; Lee, I. Y.; Jang, K. R.; Shim, J.-G., A study of the CO_2 capture pilot plant by amine absorption. *Energy* **2012**.

(10) Moser, P.; Schmidt, S.; Sieder, G.; Garcia, H.; Stoffregen, T., Performance of MEA in a long-term test at the post-combustion capture pilot plant in Niederaussem. *International journal of greenhouse gas control* **2011,** 5, (4), 620-627.

(11) Endo, T.; Kajiya, Y.; Nagayasu, H.; Iijima, M.; Ohishi, T.; Tanaka, H.; Mitchell, R., Current status of MHI CO_2 capture plant technology, large scale demonstration

project and road map to commercialization for coal fired flue gas application. *Energy Procedia* **2011,** 4, 1513-1519.
(12) Abu-Zahra, M. R. M.; Schneiders, L. H. J.; Niederer, J. P. M.; Feron, P. H. M.; Versteeg, G. F., CO_2 capture from power plants. *International journal of greenhouse gas control* **2007,** 1, (1), 37-46.
(13) Knudsen, J. N.; Jensen, J. N.; Vilhelmsen, P.-J.; Biede, O., Experience with CO_2 capture from coal flue gas in pilot-scale: Testing of different amine solvents. *Energy Procedia* **2009,** 1, (1), 783-790.
(14) Gao, H.; Zhou, L.; Liang, Z.; Idem, R. O.; Fu, K.; Sema, T.; Tontiwachwuthikul, P., Comparative studies of heat duty and total equivalent work of a new heat pump distillation with split flow process, conventional split flow process, and conventional baseline process for CO2 capture using monoethanolamine. *International journal of greenhouse gas control* **2014,** 24, (0), 87-97.
(15) Jung, J.; Jeong, Y. S.; Lim, Y.; Lee, C. S.; Han, C., Advanced CO 2 Capture Process Using MEA Scrubbing: Configuration of a Split Flow and Phase Separation Heat Exchanger. *Energy Procedia* **2013,** 37, 1778-1784.
(16) Zhang, Y.; Que, H.; Chen, C.-C., Thermodynamic modeling for CO 2 absorption in aqueous MEA solution with electrolyte NRTL model. *Fluid Phase Equilibria* **2011,** 311, 67-75.
(17) Dang, H.; Rochelle, G. T., CO2 absorption rate and solubility in monoethanolamine/piperazine/water. *Separation science and technology* **2003,** 38, (2), 337-357.
(18) Kim, I.; Svendsen, H. F., Heat of absorption of carbon dioxide (CO2) in monoethanolamine (MEA) and 2-(aminoethyl) ethanolamine (AEEA) solutions. *Industrial & engineering chemistry research* **2007,** 46, (17), 5803-5809.
(19) An, J.; Lee, U.; Jung, J.; Han, C., Parametric optimization for power de-rate reduction in the integrated coal-fired power plant with CCS. *Industrial & Engineering Chemistry Research* **2015**.
(20) Biliyok, C.; Lawal, A.; Wang, M.; Seibert, F., Dynamic modelling, validation and analysis of post-combustion chemical absorption CO_2 capture plant. *International journal of greenhouse gas control* **2012,** 9, 428-445.

(21) Le Moullec, Y.; Kanniche, M., Screening of flowsheet modifications for an efficient monoethanolamine (MEA) based post-combustion CO_2 capture. *International journal of greenhouse gas control* **2011,** 5, (4), 727-740.
(22) Chang, H.; Shih, C. M., Simulation and Optimization for Power Plant Flue Gas CO_2 Absorption & Stripping Systems. *Separation science and technology* **2005,** 40, (4), 877-909.
(23) Plaza, J. M.; Van Wagener, D.; Rochelle, G. T., Modeling CO_2 capture with aqueous monoethanolamine. *International journal of greenhouse gas control* **2010,** 4, (2), 161-166.
(24) de Sousa Gomes, M. R. F., Modelling and validation of CO2 capture processes with piperazine. **2015**.
(25) Karimi, M.; Hillestad, M.; Svendsen, H. F., Investigation of the dynamic behavior of different stripper configurations for post-combustion CO_2 capture. *International journal of greenhouse gas control* **2012,** 7, 230-239.
(26) Øi, L.; Vozniuk, I., Optimizing CO_2 absorption using split-stream configuration. In *Process and Technologies for a Sustainable Energy*, Ischia, 2010.
(27) Karimi, M.; Hillestad, M.; Svendsen, H. F., Capital costs and energy considerations of different alternative stripper configurations for post combustion CO_2 capture. *Chemical Engineering Research and Design* **2011,** 89, (8), 1229.
(28) Aroonwilas, A.; Veawab, A., Integration of CO_2 capture unit using single- and blended-amines into supercritical coal-fired power plants: Implications for emission and energy management. *International journal of greenhouse gas control* **2007,** 1, (2), 143-150.
(29) Oyenekan, B. A.; Rochelle, G. T., Alternative stripper configurations for CO_2 capture by aqueous amines. *AIChE Journal* **2007,** 53, (12), 3144-3154.
(30) Van Wagener, D. H.; Rochelle, G. T., Stripper configurations for CO_2 capture by aqueous monoethanolamine. *Chemical Engineering Research and Design* **2011,** 89, (9), 1639-1646.
(31) Karimi, M.; Hillestad, M.; Svendsen, H. F., Positive and Negative Effects on Energy Consumption by Inter–heating of Stripper in CO_2 Capture Plant. *Energy Procedia* **2012,** 23, 15-22.

(32) Soave, G.; Feliu, J. A., Saving energy in distillation towers by feed splitting. *Applied Thermal Engineering* **2002,** 22, (8), 889-896.
(33) Fernandez, E. S.; Bergsma, E. J.; de Miguel Mercader, F.; Goetheer, E. L.; Vlugt, T. J., Optimisation of lean vapour compression (LVC) as an option for post-combustion CO 2 capture: Net present value maximisation. *International Journal of Greenhouse Gas Control* **2012,** 11, S114-S121.
(34) Jassim, M. S.; Gary, T., Innovative absorber/stripper configurations for CO_2 capture by aqueous monoethanolamine. *Industrial & Engineering Chemistry Research* **2006,** 45, (8), 2465-2472.
(35) Jung, J.; Jeong, Y. S.; Lee, U.; Lim, Y.; Han, C., New Configuration of the CO2 Capture Process Using Aqueous Monoethanolamine for Coal-Fired Power Plants. *Industrial & Engineering Chemistry Research* **2015,** 54, (15), 3865-3878.
(36) Jeong, Y. S.; Jung, J.; Lee, U.; Yang, C.; Han, C., Techno-economic analysis of mechanical vapor recompression for process integration of post-combustion CO 2 capture with downstream compression. *Chemical Engineering Research and Design* **2015,** 104, 247-255.
(37) Jassim, M. S.; Rochelle, G. T., Innovative absorber/stripper configurations for CO2 capture by aqueous monoethanolamine. *Industrial & Engineering Chemistry Research* **2006,** 45, (8), 2465-2472.
(38) Johansson, D.; Sjöblom, J.; Berntsson, T., Heat supply alternatives for CO_2 capture in the process industry. *International journal of greenhouse gas control* **2012,** 8, 217-232.
(39) Khalilpour, R.; Abbas, A., HEN optimization for efficient retrofitting of coal-fired power plants with post-combustion carbon capture. *International journal of greenhouse gas control* **2011,** 5, (2), 189-199.
(40) Liang, H.; Xu, Z.; Si, F., Economic analysis of amine based carbon dioxide capture system with bi-pressure stripper in supercritical coal-fired power plant. *International journal of greenhouse gas control* **2011,** 5, (4), 702-709.
(41) Romeo, L. M.; Bolea, I.; Escosa, J. M., Integration of power plant and amine scrubbing to reduce CO_2 capture costs. *Applied Thermal Engineering* **2008,** 28, (8-9), 1039-1046.

(42) Mores, P.; Scenna, N.; Mussati, S., A rate based model of a packed column for CO_2 absorption using aqueous monoethanolamine solution. *International journal of greenhouse gas control* **2012,** 6, 21-36.
(43) Zhang, Y.; Chen, H.; Chen, C. C.; Plaza, J. M.; Dugas, R.; Rochelle, G. T., Rate-Based Process Modeling Study of CO_2 Capture with Aqueous Monoethanolamine Solution. *Industrial & Engineering Chemistry Research* **2009,** 48, (20), 9233-9246.
(44) Asprion, N., Nonequilibrium rate-based simulation of reactive systems: Simulation model, heat transfer, and influence of film discretization. *Industrial & Engineering Chemistry Research* **2006,** 45, (6), 2054-2069.
(45) Lim, Y.; Kim, J.; Jung, J.; Lee, C. S.; Han, C., Modeling and Simulation of CO 2 Capture Process for Coal-based Power Plant Using Amine Solvent in South Korea. *Energy Procedia* **2013,** 37, 1855-1862.
(46) Jung, J.; Jeong, Y. S.; Lim, Y.; Lee, C. S.; Han, C., Advanced CO_2 Capture Process Using MEA Scrubbing: Configuration of a Split Flow and Phase Separation Heat Exchanger. *Energy Procedia* **2013,** 37, 1778-1784.
(47) Ahn, H.; Luberti, M.; Liu, Z.; Brandani, S., Process configuration studies of the amine capture process for coal-fired power plants. *International journal of greenhouse gas control* **2013,** 16, 29-40.
(48) Dufal, S.; Lafitte, T.; Haslam, A. J.; Galindo, A.; Clark, G. N.; Vega, C.; Jackson, G., The A in SAFT: developing the contribution of association to the Helmholtz free energy within a Wertheim TPT1 treatment of generic Mie fluids. *Molecular Physics* **2015,** 113, (9-10), 948-984.
(49) Papaioannou, V.; Lafitte, T.; Avendaño, C.; Adjiman, C. S.; Jackson, G.; Müller, E. A.; Galindo, A., Group contribution methodology based on the statistical associating fluid theory for heteronuclear molecules formed from Mie segments. *The Journal of chemical physics* **2014,** 140, (5), 054107.
(50) Seider, W. D.; Seader, J. D.; Lewin, D. R., *PRODUCT & PROCESS DESIGN PRINCIPLES: SYNTHESIS, ANALYSIS AND EVALUATION, (With CD)*. John Wiley & Sons: 2009.
(51) Dowling, A. W.; Biegler, L. T., A framework for efficient large scale equation-oriented flowsheet optimization. *Computers & Chemical Engineering* **2015,** 72, 3-20.

(52) Le Moullec, Y.; Kanniche, M., Screening of flowsheet modifications for an efficient monoethanolamine (MEA) based post-combustion CO 2 capture. *International journal of greenhouse gas control* **2011,** 5, (4), 727-740.
(53) Gao, H.; Zhou, L.; Liang, Z.; Idem, R. O.; Fu, K.; Sema, T.; Tontiwachwuthikul, P., Comparative studies of heat duty and total equivalent work of a new heat pump distillation with split flow process, conventional split flow process, and conventional baseline process for CO 2 capture using monoethanolamine. *International journal of greenhouse gas control* **2014,** 24, 87-97.

Abstract in Korean (요약)

모노에탄올아민(MEA)으로 대표되는 습식 아민 흡수제를 이용한 연소 후 이산화탄소 포집 공정은 기술적 신뢰도가 높고 기존 발전 설비와의 연계가 용이하여 중-단기적 탄소 포집 및 저장 (Carbon Capture and Storage) 시장을 주도하고 있다. 다만 흡수제를 이용한 이산화탄소 포집 공정은 흡수제 재생 시 에너지 소비가 많아 포집 비용이 높아지는 단점을 지적받고 있다. 이러한 이유로 흡수제 재생 에너지 절감을 위한 다양한 공정 개선안이 연구되어 왔으며 상호 보완적인 공정 개선안을 조합하면 더 큰 에너지 절감 효과를 기대할 수 있다. 이에 따라 최근에는 각 공정 개선안의 정성적인 분석 또는 조합에 대한 결과 분석을 통해 최적의 공정 개선안 조합을 제안하고 있다. 하지만 공정 개선안 수가 많아짐에 따라 고려해야할 공정 변수가 늘어날 뿐만 아니라 변수들 간에 복잡한 상관관계가 발생하게 된다. 때문에 다수의 공정 개선안에 대한 정성적인 분석은 한계가 있으며 모든 조합을 고려하기에는 경우의 수가 과도하게 많아지는 문제점이 발생한다. 동시에 대부분의 공정 개선안의 경우 추가적인 장치 비용이 발생하기 때문에 이에 대한 정량적인 평가도 함께 수행되어야 한다.

본 연구에서는 MEA 흡수제를 이용한 이산화탄소 포집 공정의 비용 절감을 위해 일련의 순서에 따른 공정 분석을 수행한다. 첫째, 일반적인 MEA 공정의 에너지 시스템을 분석하고 에너지 소비량을 결정하는 공정 변수를 파악한다. 둘째, MEA 공정 개선안의 에너지 절감 효과를 분석하고 그 기작에 따라 공정 개선안을 분류한다. 셋째, MEA 공정 개선안의 정성적 분석을 통해 상호 보완적인 공정 개선안 조합을 제시하고 이에 대한 에너지 절감 효과와 추가 장치 비용을 분석한다. 넷째, 다수의 공정 개선안을 하나의 초구조 모델로 구성하고 운전비용과 장치비용을 포함하는 비용 모델을 함께 구성한다. 마지막으로 공정 개선안 초구조 모델의 최적화를 통해 에너지 소비를 최소화 하거나 전체 비용을 최소화 하는 공정 개선안 조합을 도출하고 그 효과를 분석한다. 에너지 소비 최적화 결과 이산화탄소 포집 및 압축에 필요한 등가 에너지(Equivalent Energy)가 1.02 GJ/ton CO_2 로 기준 공정 대비 22.1% 감소하였다. 전체 비용 최적화 결과 이산화탄소 포집 및 압축에 필요한 비용이 51.0 €/ ton CO_2 로 기준 공정 대비 10.2% 감소하였다. 대상 공정인 630MWe 급 발전 설비에 적용 시 산술적으로 연간 25.7 Milion €의 비용 절감효과를 기대할 수 있다..

주요어: 연소 후 이산화탄소 포집, 연소 후 포집 공정 개선안, 포집 공정 최적화

학번: 2010-21014

성명: 정재흠